The Hidden Conformal Symmetry and Quasinormal Modes of the Four Dimensional Kerr Black Hole

by

Blake Jordan

Dissertation presented in fulfillment of the requirements for the degree of

Master of Science in Physics

at the University of the Witwatersrand

School of Physics,
University of the Witwatersrand,
Johannesburg, South Africa

Supervisors: Dr Alan S. Cornell and Dr Kevin Goldstein

March 2012

Abstract

This dissertation has two areas of interest with regard to the four dimensional Kerr black hole; the first being its conformal nature in its near region and second it characteristic frequencies.

With it now known that the scalar solution space of the four dimensional Kerr black hole has a two dimensional conformal symmetry in its near region, it was the first focus of this dissertation to see if this conformal symmetry is unique to the near region scalar solution space or if it is also present in the spin-half solution space.

The second focus of this dissertation was to explore techniques which can be used to calculate these quasinormal mode (characteristic) frequencies, such as the WKB(J) approximation which has been improved from third order to sixth order recently and applied to the perturbations of a Schwarzschild black hole. The additional correction terms show a significant increase of accuracy when comparing to numerical methods. This dissertation shall use the sixth order WKB(J) method to calculate the quasinormal mode frequencies for both the scalar and spin-half perturbations of a four dimensional Kerr black hole.

An additional method used was the asymptotic iteration method, a relatively new technique being used to calculate the quasinormal mode frequencies of black holes that have been perturbed. Prior to this dissertation it had only been used on a variety of Schwarzschild black holes and their possible perturbations. For this dissertation the asymptotic iteration method has been used to calculate the quasinormal frequencies for both the scalar and spin-half perturbations of the four dimensional Kerr black hole.

The quasinormal mode frequencies calculated using both the sixth order WKB(J) method and the asymptotic iteration method were compared to previously published values and each other. For the most part, they both compare favourably with the numerical values, with differences that are near negligible. The differences did become more apparent when the mode number (or angular momentum per unit mass increased), but less so when the angular number increased. The only factor that separates these two methods significantly, was that the computational time for the sixth order WKB(J) method is less than than that of the asymptotic iteration method.

Acknowledgements

I would like to thank the National Institute for Theoretical Physics (NITheP) for providing the funding necessary to undertake this dissertation.

I offer my sincerest gratitude to my supervisors Dr Kevin Goldstein and Dr Alan S. Cornell for providing both direction and assistance throughout my work on this dissertation.

And finally, I would like to mention Dr Jason Doukas and Prof. Roman A. Konoplya for their help with the numerical aspects of this dissertation.

Declaration

I, the undersigned, hereby declare that the work contained in this thesis is my own original work and that I have not previously in its entirety or in part submitted it at any university for a degree.

Signature: . . . . . .

Date: March 2012

Contents

List of Tables

List of Figures

Chapter 1

Introduction

The black holes of nature are the most perfect macroscopic objects there are in the universe: the only elements in their construction are our concepts of space and time. Since the general theory of relativity provides only a single unique family of solutions for their descriptions, they are the simplest objects as well.

The unique two-parameter family of solutions which describes the space-time around black holes is the Kerr family discovered by Roy Patrick Kerr in July 1963 [1]. The two parameters are the mass of the black hole and the angular momentum of the black hole, where the static solution, with zero angular momentum, was discovered earlier by Karl Schwarzschild in December 1915 [2]. A study of the black holes of nature is then a study of these solutions.

Two areas of interest, which are focused on in this dissertation, when it comes to studying black holes (specifically those of the Kerr variety), are their conformal nature, which is of significance in string theory (a potential unification theory) and their characteristic properties, which can be determined from their quasinormal modes (QNMs) and corresponding frequencies.

1.1 Hidden Conformal Symmetry

One of the deepest discoveries in modern theoretical physics is that of holographic dualities, which relate a quantum theory of gravity to a quantum field theory without gravity in fewer dimensions and these dualities come to prominence in the construct of string theory [3]. It is an occasional misconception, however, that the existence of holographic dualities is exclusive to string theory. This is not the case. For example, the demonstration that any consistent theory of quantum gravity on three-dimensional anti-de Sitter (AdS_3) space appears to be holographically dual to a two-dimensional conformal field theory (CFT) did not invoke string theory. When holographic duality was used to find the microscopic origin of the Berkenstein-Hawking entropy for a class of black holes, the construction at first appeared to depend heavily on details of string theory [4]. However, it was later convincingly extended [5] to essentially any consistent, unitary quantum theory of gravity containing black holes as

classical solutions.

Oddly, the rich ideas surrounding holographic dualities so far have not been successfully applied to the enigmatic objects which largely inspired their original discovery - the Schwarzschild or Kerr black holes we actually observe.

1.2 Quasinormal Modes

For a number of years the QNMs of oscillation of black holes have been of great interest both to gravitational theorists and to gravitational wave experimentalists [6]. These modes are the resonant, non-radial perturbations of black holes. They are characterized by a spectrum of discrete, complex frequencies, whose real parts determine the oscillation frequency, and whose imaginary parts determine the rate at which each mode is damped as a result of the emission of radiation. For a given kind of physical perturbation the complex frequencies are uniquely determined by the mass and angular momentum of the black hole, the angular harmonic indices (l, m) of the deformation, and the degree of the harmonic of the mode (n).

To the gravitational wave astronomer black hole QNMs may be an important source of gravitational waves emitted at discrete frequencies by a deformed black hole left over following a supernova collapse. Recent numerical calculations of rotating collapse have found that for some collapse scenarios in which a black hole is formed, the bulk of gravitational radiation emitted via QNM oscillations of the black hole that continue after the matter has crossed the horizon [6]. The identification of the frequencies and damping times of such waves could aid in estimating the parameters of the black hole. Studies of perturbations of black holes by passing particles have also shown excitations of QNMs [7]. QNMs are important in analyzing the stability of black holes against external perturbations. Although the non-rotating Schwarzschild black hole is known to be rigorously stable, the situation is not so certain in the case of the rotating Kerr black hole [8], and a systematic study of QNMs could contribute to a resolution of this question.

Although the fundamental equations describing the perturbations of black holes reduce to a single second-order ordinary differential equation that is similar to the one-dimensional Schrödinger equation for a particle encountering a potential barrier on the infinite line; the nature of the potential precludes an exact, closed-form solution in terms of known functions. Mathematically, a QNM is a solution to the differential equation with a complex frequency, satisfying the boundary condition of purely outgoing waves, that is, waves propagating away from the barrier at both $+\infty$ and $-\infty$, the latter boundary condition corresponding to waves traveling across the horizon to the interior of the black hole. The quantum mechanical analogue of this is a scattering resonance with a complex energy. Because such a boundary condition cannot actually correspond to a stationary state, the energy or squared frequency must be complex, leading to a characteristic damping with time of wave packets constructed from the modes.

Studying black hole QNMs numerically requires selecting a value for the complex frequency, integrating the differential equation, and checking whether the boundary conditions are satisfied. Since those conditions are not satisfied in general, the complex frequency plane

must be surveyed for discrete values that lead to QNMs. This technique is time consuming and therefore costly, and it makes it difficult to systematically survey the QNMs for a wide range of parameter values. Following early work by Vishveshwara [8], Chandrasekhar and Detweiler [9] pioneered this method for the study of QNMs.

A few semi-analytic analyses have also been attempted. In one approach, employed by Mashoon *et al.* [10], the potential barrier in the effective one-dimensional Schrödinger equation is replaced by a parameterized analytic potential barrier function for which simple exact solutions are known. The overall shape approximates that of the true black hole barrier, and the parameters of the barrier function are adjusted to fit the height and curvature of the true barrier at the peak. The resulting estimates for the QNM frequencies have been applied to the Schwarzschild, Reissner-Nordstrom and Kerr black holes, with agreement within a few percent with the numerical results of Chandrasekhar and Detweiler in the Schwarzschild case [9], and with Gunter [11] in the Reissner-Nordstrom case. However, as this method relies upon a specialized barrier function, there is no systematic way to estimate the errors or to improve the accuracy.

The method by Leaver [12], which is a hybrid of the analytic and the numerical, successfully generates QNM frequencies by making use of an analytic infinite-series representation of the solutions, together with a numerical solution of an equation for the QNM frequencies which involves continued fractions. This technique is known as the Continued Fraction Method (CFM).

The third-order WKB approximation is another technique, which we shall consider in this dissertation [13]. Even though it is based on an approximation, this approach is powerful as: (a) the WKB approximation is known in many cases to be more accurate than one may expect; (b) because the method can be carried to higher orders, either as a means to improve accuracy or as a means to estimate the errors explicitly and (c) because it will allow a more systematic study of QNMs than has been possible using outright numerical methods. The WKB approximation was later extended to sixth-order by Konoplya [14].

Finally, we shall also use the Asymptotic Iteration Method (AIM), which was previously used to solve eigenvalue problems [15] as a semi-analytic technique for solving second-order homogeneous linear differential equations. It has also been successfully shown that the AIM is an efficient and accurate technique for calculating QNMs of different types of Schwarzschild black holes [16].

1.3 Quasinormal Modes and Conformal Field Theory

While the statistical origin of black hole entropy remains a subject of active research, one may wonder if the celebrated analogy [17] between the laws of black hole mechanics and the laws of thermodynamics can be generalized to non-equilibrium processes. Holographic AdS / CFT correspondences (reviewed by [18]) provides a suitable arena for such generalizations. The AdS / CFT conjecture asserts that string theories on certain asymptotically anti de Sitter space-times are dual to quantum field theories in lower dimensions. Since the low-energy limit of string theory is described by the appropriate supergravity, problems in general

relativity can be mapped to problems in the dual field theory. According to the duality, asymptotically AdS background space-times with event horizons are interpreted as thermal states in dual field theories. Correspondingly, small perturbations of a black hole or a black brane background are interpreted as small deviations from thermodynamic equilibrium in a dual theory. This particular entry in the holographic dictionary can be made precise by considering quasinormal spectra of asymptotically AdS space-times.

QNMs (reviewed by [19]) are solutions to linearized equations obeyed by classical fluctuations of a gravitational background subject to specific boundary conditions. The choice of the boundary condition at the (future) horizon is dictated by the fact that classically horizons do not emit radiation. Thus out of two local solutions near the horizon typically representing waves incoming to the horizon and outgoing from it, one chooses the incoming waves only. This choice of the boundary condition has profound consequences, making the boundary value problem non-Hermitian, and the associated eigen-frequencies complex. This, however, is exactly what one expects in a holographically dual theory, where small deviations from thermal equilibrium are described by dispersion relations which correspond to non-zero damping [20]. Mathematically, these dispersion relations appear as singularities of the retarded Greens functions in the complex frequency plane. The connection between quasinormal spectrum of AdS black holes and singularities of thermal correlators in dual quantum field theories was first noted and explored for $2+1$ dimensional BTZ black holes in [21].

1.4 Outline for This Dissertation

The main part of this dissertation is divided into four chapters, starting with chapter 2, which reviews the mathematics and physics necessary for the study of Kerr black holes. Chapter 3 studies the conformal nature of both the scalar and spin-half solution spaces in the near region of the Kerr black hole. Chapter 4 reviews the background techniques involved in the study of QNMs, whilst chapter 5 presents the QNM frequencies calculated as part of this dissertation and compares them to accepted values in previous publications for both scalar and spin-half particle cases using two techniques; the WKB method and the AIM.

The final chapter (6) presents the conclusions for this dissertation, along with a discussion of the possible future research directions.

For this dissertation, $c = G = 1$ and additionally $M = 1$ for the calculated QNM frequencies.

Chapter 2

Mathematics and Physics Background

2.1 Kerr Space-time

The Kerr space-time was discovered in 1963 through an intellectually intensive method and it continues to provide nontrivial mathematical and physical problems to this day [1].

The final form of Albert Einstein's general theory of relativity was developed in 1915, and within two months Schwarzschild had already solved the field equations that determine the exact space-time geometry of a non-rotating point particle. It was relatively quickly realized that the space-time geometry in the vacuum region outside any localized spherically symmetric source is equivalent, up to a possible coordinate transformation, to a portion of the Schwarzschild geometry - and so of direct physical interest to modeling the space-time geometry surrounding and exterior to idealized non-rotating spherical stars and planets.

Considerably more slowly and only after intense debate was it realized that the inward analytic extension of Schwarzschild's exterior solution represents a non-rotating black hole, the endpoint of stellar collapse. In the most common form, which is not always the most useful form for understanding the physics, the Schwarzschild geometry is described by the line element [22]

$$ds^2 = -\left(1-\frac{2M}{r}\right)dt^2 + \left(1-\frac{2M}{r}\right)^{-1}dr^2 + r^2\left(d\theta^2+\sin^2\theta d\phi^2\right), \tag{2.1}$$

where the parameter M is the physical mass of the central object.

But in connection with astrophysics we know that stars, planets, etcetera rotate, and from the weak-field approximation to the Einstein equations we even know the approximate form of the metric at large distance from a stationary isolated body of mass M and angular momentum J. In suitable coordinates [22]

$$\begin{aligned} ds^2 = & - \left(1-\frac{2M}{r}+O\left(\frac{1}{r^2}\right)\right)dt^2 - \left(\frac{4J\sin^2\theta}{r}+O\left(\frac{1}{r^2}\right)\right)d\phi dt \\ & + \left(1+\frac{2M}{r}+O\left(\frac{1}{r^2}\right)\right)dr^2 + r^2\left(d\theta^2+\left(1+O\left(\frac{1}{r^2}\right)\right)\sin^2\theta d\phi^2\right). \end{aligned} \tag{2.2}$$

This approximate metric is perfectly adequate for almost all solar system tests of general relativity, but there certainly are well-known astrophysical situations for which this approximation is inadequate - and so a strong field solution is physically called for. Furthermore, if a rotating star were to undergo gravitational collapse, then the resulting black hole would be expected to retain at least some fraction of its initial angular momentum - thus suggesting, on physical grounds, that somehow there should be an extension of the Schwarzschild geometry to the situation where the central body carries angular momentum.

Physicists and mathematicians looked for such a solution for many years, and had almost given up hope, until the Kerr solution was discovered almost fifty years after the Einstein field equations were first developed. From the weak-field asymptotic result we can already see that angular momentum destroys spherical symmetry, and this lack of spherical symmetry makes the calculations much more difficult. It is not that the basic principles are all that different, but simply that the algebraic complexity of the computations is so high that relatively few physicists or mathematicians have the fortitude to carry them through to completion.

The very first version of the Kerr space-time geometry to be explicitly written down in the literature [1] had the line element given as

$$\begin{aligned} ds^2 = & - \left(1 - \frac{2Mr}{r^2 + a^2\cos^2\theta}\right)\left(du + a\sin^2\theta d\phi\right)^2 \\ & + 2\left(du + a\sin^2\theta d\phi\right)\left(dr + a\sin^2\theta d\phi\right) \\ & + \left(r^2 + a^2\cos^2\theta\right)\left(d\theta^2 + \sin^2\theta d\phi^2\right), \end{aligned} \tag{2.3}$$

where M and a are the mass and angular momentum per unit mass of the rotating black hole, respectively.

2.1.1 Boyer-Lindquist Coordinates

The original coordinates that were used, see equation (2.3), are not always the best choice to study Kerr black holes, so we change to Boyer-Lindquist coordinates.

These coordinates are best motivated in two stages: First, consider a slightly different but completely equivalent form of the metric which follows Kerr's original, equation (2.3), via the coordinate substitution

$$u = t + r, \tag{2.4}$$

in which case

$$\begin{aligned} ds^2 = & - dt^2 \\ & + dr^2 + 2a\sin^2\theta dr d\phi + \left(r^2 + a^2\cos^2\theta\right)d\theta^2 + \left(r^2 + a^2\right)\sin^2\theta d\phi^2 \\ & + \frac{2Mr}{r^2 + a^2\cos^2\theta}\left(dt + dr + a\sin^2\theta d\phi\right)^2. \end{aligned} \tag{2.5}$$

Here the second line is again simply flat three-space in disguise. An advantage of this coordinate system is that t can naturally be thought of as a time coordinate - at least at large distances near spatial infinity. There are, however, still three off-diagonal terms in

the metric, so this is not yet any great advance on the original form (2.3). One can easily consider the limits $M \to 0$, $a \to 0$, etcetera, but there are no real surprises.

Second, it is now extremely useful to perform a further M-dependent coordinate transformation, which will put the line element into Boyer-Lindquist form

$$\begin{aligned} t &= t_{BL} + 2M \int \frac{r}{r^2 - 2Mr + a^2} dr, \\ \phi &= -\phi_{BL} - a \int \frac{1}{r^2 - 2Mr + a^2} dr, \qquad (2.6) \\ r &= r_{BL}, \\ \theta &= \theta_{BL}. \qquad (2.7) \end{aligned}$$

Making the transformation, and dropping the BL subscript, the Kerr line element now takes the form

$$\begin{aligned} ds^2 = & - \left(1 - \frac{2Mr}{\rho^2}\right) dt^2 - \left(\frac{4Mra\sin^2\theta}{\rho^2}\right) dt d\phi + \left(\frac{\rho^2}{\Delta}\right) dr^2 \\ & + \left(\rho^2\right) d\theta^2 + \left(r^2 + a^2 + \frac{2Mra^2\sin^2\theta}{\rho^2}\right) \sin^2\theta d\phi^2, \qquad (2.8) \end{aligned}$$

where

$$\rho^2 = r^2 + a^2\cos^2\theta \text{ and } \Delta = r^2 + a^2 - 2Mr. \qquad (2.9)$$

The properties apparent from expressing the Kerr space-time in Boyer-Lindquist coordinates are

- These Boyer-Lindquist coordinates are particularly useful in that they minimize the number of off-diagonal components in the metric - there is now only one off-diagonal component. We shall subsequently see that this helps in analyzing the asymptotic behaviour, and in trying to understand the key differences between the event horizon and an ergosphere.

- Another particularly useful feature is that the asymptotic ($r \to \infty$) behaviour in Boyer-Lindquist coordinates is

$$\begin{aligned} ds^2 = & - \left(1 - \frac{2M}{r} + O\left(\frac{1}{r^2}\right)\right) dt^2 - \left(\frac{4Ma\sin^2\theta}{r} + O\left(\frac{1}{r^2}\right)\right) d\phi dt \\ & + \left(1 + \frac{2M}{r} + O\left(\frac{1}{r^2}\right)\right) dr^2 + r^2 \left(d\theta^2 + \left(1 + O\left(\frac{1}{r^2}\right)\right) \sin^2\theta d\phi^2\right) \qquad (2.10) \end{aligned}$$

  From this we conclude that M is indeed the mass and $J = Ma$ is indeed the angular momentum.

- If $a \to 0$ the Boyer-Lindquist line element reproduces the Schwarzschild line element in standard Schwarzschild curvature coordinates.

- If $M \to 0$ the Boyer-Lindquist line element reduces to

$$ds^2 \to -dt^2 + \left(\frac{\rho^2}{r^2+a^2}\right) dr^2 + \left(\rho^2\right) d\theta^2 + \left(r^2+a^2\right) \sin^2\theta d\phi^2. \tag{2.11}$$

This is flat Minkowski space in so-called oblate spheroidal coordinates.

2.1.2 Killing Vectors

The symmetries of a space-time, in a particular coordinate system, are useful for calculations and can be summarized using quantities called Killing vectors. The general properties of a Killing vector and the Kerr Killing vectors are given in this subsection.

A Killing vector X^μ generates an isometry of the metric, and satisfies Killing's equation [23]

$$X_{\mu;\nu} + X_{\nu;\mu} = 0. \tag{2.12}$$

A Killing vector corresponds to a symmetry of the space-time. By Noether's theorem, symmetries lead to conserved quantities. If X_μ is a Killing vector then it follows that

$$u^\nu \nabla_\nu (u^\mu X_\mu) = u^\nu u^\mu X_{\mu:\nu} = \frac{1}{2} u^\nu u^\mu (X_{\mu;\nu} + X_{\nu;\mu}) = 0, \tag{2.13}$$

by symmetry. In other words, the contraction of the tangent vector with a Killing vector, $X_\mu u^\mu$, gives a constant of motion on a geodesic. It is straightforward to see that if the metric does not depend on a particular coordinate, x^1 say, then $X^\mu = \delta^\mu_1$ is a Killing vector.

In Boyer-Lindquist coordinates, the time-translation and azimuthal (rotational) Killing vectors are

$$K^\mu = (1,0,0,0) \text{ and } R^\mu = (0,0,0,1). \tag{2.14}$$

2.1.3 Horizons and the Ergosphere

To briefly survey the key properties of the horizons and ergospheres occurring in the Kerr space-time, let us concentrate on using the Boyer-Lindquist coordinates. First, consider the components of the metric in these coordinates. The metric components have singularities when either [22]

$$\rho^2 = 0, \text{ that is , } r = 0 \text{ and } \theta = \frac{\pi}{2}, \tag{2.15}$$

or

$$\Delta = 0, \text{ that is , } r = r_\pm \equiv M \pm \sqrt{M^2 - a^2}. \tag{2.16}$$

The first of these possibilities corresponds to what we have already seen is a real physical curvature singularity, while the second pair of singularities is an artifact of the Boyer-Lindquist coordinate system.

In fact the second option above ($r = r_\pm$) corresponds to all orthonormal curvature components and all curvature invariants being finite. Furthermore, as $a \to 0$ we have the smooth

limit that $r_\pm \to 2M$, the location of the horizon in the Schwarzschild geometry. We will tentatively identify $r_\pm$ as the locations of the inner and outer horizons.

Since the divergence at $r = 0$ occurs only for $\theta = \frac{\pi}{2}$, it is clear that its nature cannot be the same as the singularity at $r = 0$ of the Schwarzschild and the Reissner-Nordstrom space-times [24]. To understand the real nature of the singularity of the Kerr space-time, we must first eliminate the inherent ambiguity in the coordinate system, (r, θ, ϕ), at $r = 0$. This ambiguity is abolished by choosing the 'Cartesian' coordinate system (x, y, z), such that

$$(x^2 + y^2) = (r^2 + a^2) \sin^2 \theta. \tag{2.17}$$

The surfaces of constant r are confocal ellipsoids whose principal axes coincide with the coordinate axes. These ellipsoids degenerate, for $r = 0$, to the disc,

$$x^2 + y^2 \leq a^2, z = 0. \tag{2.18}$$

The point $(r = 0, \theta = \frac{\pi}{2})$ corresponds then to the ring,

$$x^2 + y^2 = a^2, \tag{2.19}$$

and the singularity along this ring is the only singularity of the Kerr space-time.

This is a new concept for rotating black holes, the ergosphere, that does not arise for non-rotating black holes. Suppose we have a rocket ship and turn on its engines, and move so as to try to remain in a fixed position in the coordinate system - that is, suppose we try to follow the world line [22]

$$X(t) = (t, r(t), \theta(t), \phi(t)) = (t, r_0, \theta_0, \phi_0)\,. \tag{2.20}$$

Are there locations in the space-time for which it is impossible to remain fixed? Now the tangent vector to the world line of an observer who is fixed is

$$T^a = \frac{dX^a(t)}{dt} = (1, 0, 0, 0)\,, \tag{2.21}$$

and a necessary condition for a physical observer to be fixed is that his trajectory should be time-like. That is, we need

$$g\,(T, T) < 0. \tag{2.22}$$

But

$$g\,(T, T) = g_{ab} T^a T^b = g_{tt}, \tag{2.23}$$

so in the specific case of the Kerr geometry

$$g\,(T, T) = -\left(1 - \frac{2Mr}{r^2 + a^2 \cos^2 \theta}\right). \tag{2.24}$$

However, the right hand side becomes positive once

$$r^2 + a^2 \cos^2 \theta < 0. \tag{2.25}$$

That is, defining

$$r_E^{\pm} \equiv M \pm \sqrt{M^2 - a^2 \cos^2\theta}, \tag{2.26}$$

the right hand side becomes positive once

$$r_E^- < r < r_E^+. \tag{2.27}$$

The surfaces $r = r_E^{\pm}$, between which it is impossible to stand still, are known as the stationary limit surfaces.

Compare this with the location of the event horizons

$$r_{\pm} \equiv M \pm \sqrt{M^2 - a^2}, \tag{2.28}$$

and we see that

$$r_E^- \leq r_- \leq r_+ \leq r_E^+. \tag{2.29}$$

In fact $r_E^+ \geq r_+$ with equality only at $\theta = 0$ and $\theta = \pi$, which corresponds to the axis of rotation. Similarly $r_E^- \leq r_-$ with equality only at the axis of rotation.

Restricting attention to the outer region: There is a region between the outer stationary limit surface and the outer event horizon in which it is impossible to remain fixed, but it is still possible to escape to infinity. This region is known as the ergosphere. Physically it is extremely important to realize that you should trust in the existence of the ergo-surface and event horizon, and the region immediately below the event horizon [25]. Figure 2.1 shows the key features of the Kerr geometry. However you should not physically trust in the inner horizon or the inner ergo-surface. Although they are certainly there as mathematical solutions of the exact vacuum Einstein equations, there are good physics reasons to suspect that the region at and inside the inner horizon, which can be shown to be unstable and unlikely to form in any real astrophysical collapse.

The starting point for the work of this dissertation is the equations of motion for both the scalar and spin-half particles in the Kerr space-time. The following two sections show the derivation of these equations of motion for both types of particles in a curved space-time and then their specific forms in the Kerr space-time.

2.2 Scalar Particle

2.2.1 Klein-Gordon Equation

The evolution of a scalar field Ψ may be determined from an action principle [26]. Let us assume the field is real, and implicitly take the real part of the expressions wherever necessary. The minimally-coupled action is

$$S = \int \mathrm{d}^4x \mathcal{L}(\Psi, \partial_\mu; \Psi g_{\mu\nu}), \tag{2.30}$$

with

$$\mathcal{L} = \frac{1}{2}\sqrt{-\mathbf{g}}(g^{\mu\nu}\partial_\mu\Psi\partial_\nu\Psi), \tag{2.31}$$

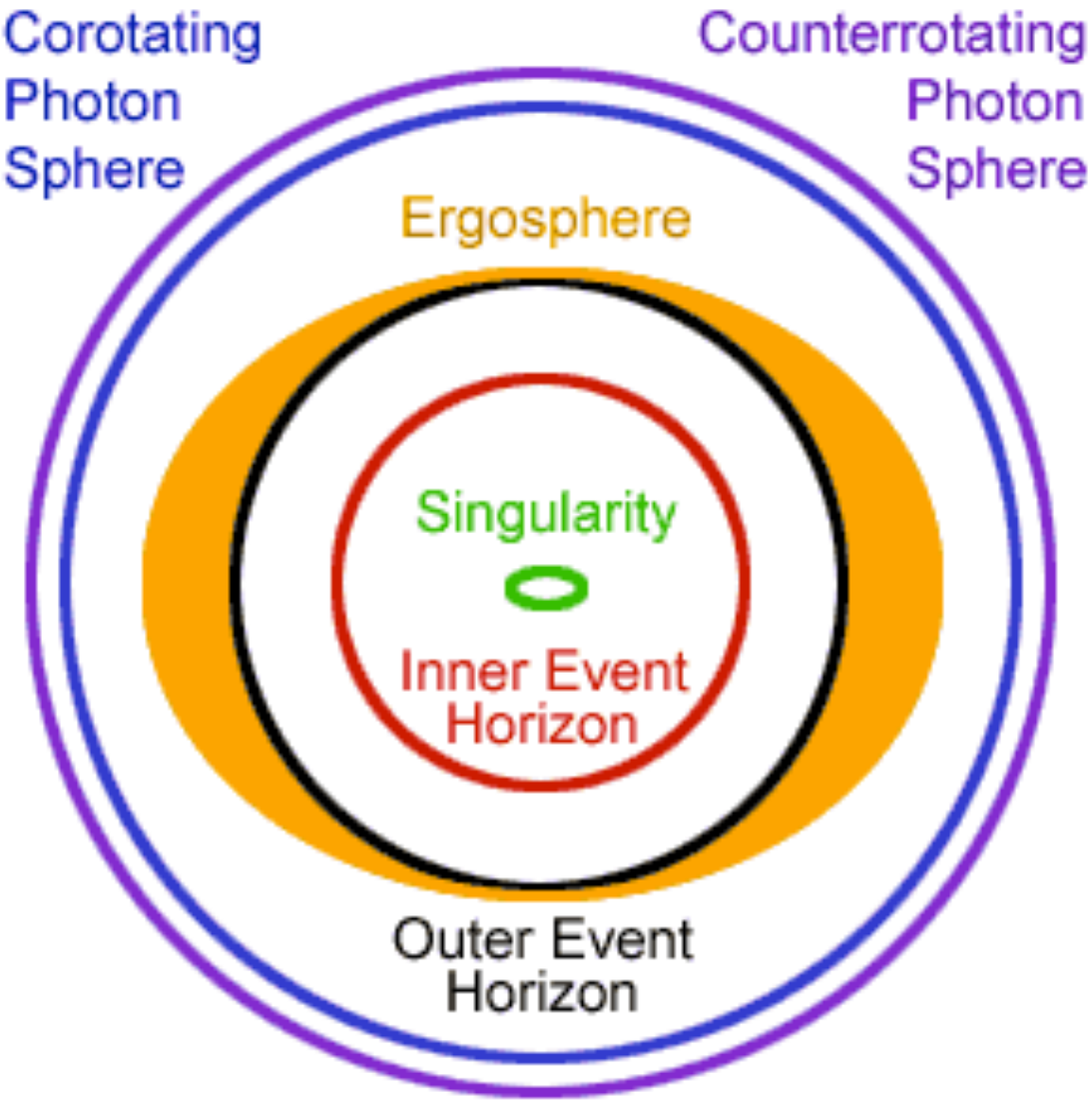

Figure 2.1: *Schematic location of the horizons, ergo-surfaces, and curvature singularity in the Kerr space-time.*

where partial differentiation is denoted by $\partial_\mu \Psi = \frac{\partial}{\partial x^\mu}\Psi$ and the summation convention is assumed. In this expression $\mathbf{g}$ is the determinant of the metric tensor. We extremise the action by employing the Euler-Lagrange equation

$$\frac{\partial \mathcal{L}}{\partial \Psi} = \frac{\partial}{\partial x^\mu}\left(\frac{\partial \mathcal{L}}{\partial(\partial_\mu \Psi)}\right). \tag{2.32}$$

This leads to the massless generalized scalar wave equation, i.e.,

$$\frac{1}{\sqrt{-\mathbf{g}}}\partial_\mu(\sqrt{-\mathbf{g}}g^{\mu\nu}\partial_\nu \Psi) = 0. \tag{2.33}$$

2.2.2 In the Kerr Space-time

Because the Kerr space-time metric is independent of t and ϕ, it is possible to expand (2.33) in eigenmodes, i.e.,

$$\Psi(t, r, \theta, \phi) = e^{-i\omega t + im\phi}\psi(r, \theta), \tag{2.34}$$

where $\omega > 0$ and m are the angular frequency and azimuthal quantum number respectively. Using (2.8) with the above, equation (2.33) becomes

$$\begin{aligned} 0 \;=\; & \frac{1}{\psi}\frac{\partial}{\partial r}\left(\Delta\frac{\partial}{\partial r}\psi\right) + \frac{1}{\Delta}(\omega^2(r^2+a^2)^2 - 4Mam\omega r + m^2a^2) \\ & + \frac{1}{\psi}\frac{1}{\sin\theta}\frac{\partial}{\partial\theta}\left(\sin\theta\frac{\partial}{\partial\theta}\psi\right) + \left(\omega^2a^2\sin^2\theta - \frac{m^2}{\sin^2\theta}\right). \end{aligned} \tag{2.35}$$

Equation (2.35) is in the form that allows it to be separated into individual equations for r and θ, so by writing

$$\psi(r, \theta) = R(r)S(\theta), \tag{2.36}$$

equation (2.35) separates into a angular equation

$$\frac{1}{\sin\theta}\frac{\mathrm{d}}{\mathrm{d}\theta}\left(\sin\theta\frac{\mathrm{d}}{\mathrm{d}\theta}\psi\right) + \left(\omega^2a^2\sin^2\theta - \frac{m^2}{\sin^2\theta}\right)S = -A_{l,m}S, \tag{2.37}$$

and an radial equation

$$\frac{\mathrm{d}}{\mathrm{d}r}\left(\Delta\frac{\mathrm{d}}{\mathrm{d}r}R\right) + \frac{1}{\Delta}(\omega^2(r^2+a^2)^2 - 4Mam\omega r + m^2a^2)R = A_{l,m}R, \tag{2.38}$$

where the $A_{l,m}$'s are the separation constants for each combination of l and m.

In appendix A, it is shown how it is possible for a scalar particle to extract rotational energy from a Kerr black hole and what condition is necessary for it to do so.

2.3 Spin-Half Particle

Unlike in the case of the scalar particle, where the theory necessary for the derivation of the equations of motion was already known, the theory behind the derivation of the spin half particle equation of motion was learnt specifically for the work necessary in this dissertation and therefore a review of it is given below.

2.3.1 The Tetrad Formalism

The standard practice in general relativity is to express a problem in a particular basis (local coordinate basis), however, it has proven to be more useful for spin-half particles to express the problem in a tetrad basis. But in recent years, it has appeared advantageous, in some contexts, to proceed somewhat differently by choosing a suitable tetrad basis of four linearly independent vector-fields, projecting the relevant quantities on to the chosen basis, and considering the equations satisfied by them. This is the tetrad formalism.

In the applications of the tetrad formalism, the choice of the tetrad basis depends on the underlying symmetries of the space-time we wish to grasp and is, to some extent, a part of the problem. Besides, it is not always clear what the relevant equations are and what the relations among them may be. On these accounts, we shall present the basic ideas of the theory without any prior commitments and derive the various equations which will later appear as the relevant ones of the formalism for the applications we have in view.

The Tetrad Representation

We set up at each point of space-time a basis of four contravariant vectors,

$$e_{(a)}{}^{j}(a = 1, 2, 3, 4), \tag{2.39}$$

where enclosure in parentheses distinguishes the tetrad indices from tensor indices (which are not enclosed). Also, we shall reserve the earlier letters of the Latin alphabet $(a, b, ...)$ for the tetrad indices and the later letters $(j, k, ...)$ for tensor indices. Associated with the contravariant vectors (2.39) we have the covariant vectors,

$$e_{(a)j} = g_{jk} e_{(a)}{}^{k}, \tag{2.40}$$

where g_{jk} denotes the metric tensor. In addition, we also define the inverse, $e^{(b)}{}_{j}$ of the matrix $[e_{(a)}{}^{j}]$ (with the tetrad index labeling the rows and the tensor index labeling the columns) so that

$$e_{(a)}{}^{j} e^{(b)}{}_{j} = \delta^{(b)}{}_{(a)} \text{ and } e_{(a)}{}^{j} e^{(a)}{}_{k} = \delta^{(j)}{}_{(k)}, \tag{2.41}$$

where the summation convention with respect to the indices of the two sorts, independently, is assumed (here and elsewhere). Further, as a part of the definitions, we shall also assume that

$$e_{(a)}{}^{j} e_{(b)j} = \eta_{(a)(b)}, \tag{2.42}$$

where $\eta_{(a)(b)}$ is a constant symmetric invertible matrix.

One most often supposes that the basis vectors, $e_{(a)}{}^{j}$, are orthonormal in which case $\eta_{(a)(b)}$ represents a diagonal matrix with the diagonal elements, $(+1, -1, -1, -1)$. We shall not make this assumption though it should be stated that a formalism, more general than the one we shall describe in detail, can be developed in which the $\eta_{(a)(b)}$'s are allowed to be functions on the manifold. In some contexts this further generalizations may commend itself. We consider it briefly below; but, for the present, we shall proceed on the assumption that $\eta_{(a)(b)}$'s are constants.

Returning to equation (2.42), let $\eta^{(a)(b)}$ be the inverse of the matrix $[\eta_{(a)(b)}]$; then

$$\eta^{(a)(b)}\eta_{(a)(c)} = \delta^{(a)}{}_{(c)}. \tag{2.43}$$

As a consequence of the various definitions,

$$\eta_{(a)(b)}e^{(a)}{}_{j} = e_{(b)j}\ ,\ \eta^{(a)(b)}e_{(a)j} = e^{(b)}{}_{j}, \tag{2.44}$$

and most importantly,

$$e_{(a)j}e^{(a)}{}_{k} = g_{jk}. \tag{2.45}$$

Given any vector or tensor field, we project it onto the tetrad frame to obtain its tetrad components. Thus,

$$\begin{aligned} A_{(a)} &= e_{(a)j}A^{j} = e_{(a)}{}^{j}A_{j}, \\ A^{(a)} &= \eta^{(a)(b)}A_{(b)} = e^{(a)}{}_{j}A^{j} = e^{(a)j}A_{j}, \end{aligned} \tag{2.46}$$

and

$$A^{j} = e_{(a)}{}^{j}A^{(a)} = e^{(a)j}A_{(a)}, \tag{2.47}$$

and more generally,

$$\begin{aligned} T_{(a)(b)} &= e_{(a)}{}^{j}e_{(b)}{}^{k}T_{jk} = e_{(a)}{}^{j}T_{j(a)}, \\ T_{jk} &= e^{(a)}{}_{j}e^{(b)}{}_{k}T_{(a)(b)} = e^{(a)}{}_{j}T_{(a)j} \end{aligned} \tag{2.48}$$

It is clear from the above formulae that (a) we can pass freely from the tensor indices to tetrad indices and vice vera; (b) raise and lower the tetrad indices with $\eta^{(a)(b)}$ and $\eta_{(a)(b)}$ even as we can raise and lower the tensor indices with the metric tensor; (c) there is not ambiguity in having quantities in which the indices of both sorts occur; and (d) the result of contracting a tensor is the same whether it is carried out with respect to its tensor or tetrad indices.

Directional Derivatives and the Ricci Rotation-coefficients

Now that the basic properties of the quantities within the tetrad formalism have been established, it is instructive to study these properties in order to determine the structure of the space-time being described by the formalism.

The contravariant vectors $\mathbf{e}_{(a)}$, considered as tangent vectors, define the directional derivatives

$$\mathbf{e}_{(a)} = e_{(a)}{}^{j}\frac{\partial}{\partial x^{j}}, \tag{2.49}$$

and we shall write

$$\phi_{,(a)} = e_{(a)}{}^{j}\frac{\partial\phi}{\partial x^{j}} = e_{(a)}{}^{j}\phi_{,j}, \tag{2.50}$$

where ϕ is any scalar field. More generally, we define

$$\begin{aligned} A_{(a),(b)} &= e_{(b)}{}^{j}\frac{\partial}{\partial x^{j}}A_{(a)} = e_{(b)}{}^{j}\frac{\partial}{\partial x^{j}}e_{(a)}{}^{k}A_{k} \\ &= e_{(b)}{}^{j}[e_{(a)}{}^{k}A_{k;j} + A_{p}e_{(a)}{}^{p}{}_{;j}] = e_{(b)}{}^{j}\nabla_{j}[A_{k}e_{(a)}{}^{k}], \end{aligned} \tag{2.51}$$

where

$$\nabla_{j}[A_{k}e_{(a)}{}^{k}] = e_{(a)}{}^{k}A_{k;j} + A_{p}e_{(a)}{}^{p}{}_{;j}, \tag{2.52}$$

is how the covariant derivative is defined in the tetrad formalism and

$$A_{k;j} = \partial_{j}A_{k} - \Gamma^{p}{}_{kj}A_{p}. \tag{2.53}$$

We thus obtain

$$A_{(a),(b)} = e_{(a)}{}^{k}A_{k;j}e_{(b)}{}^{j} + e_{(a)p;j}e_{(b)}{}^{j}e_{(c)}{}^{p}A^{(c)}, \tag{2.54}$$

making use of the various rules enunciated at the end of the preceding subsection and of the fact that the raising and the lowering of tensor indices permutes with the operation of covariant differentiation.

With the definition

$$\gamma_{(c)(a)(b)} = e_{(c)}{}^{p}e_{(a)p;j}e_{(b)}{}^{j}, \tag{2.55}$$

we can rewrite equation (2.54) in the form

$$A_{(a),(b)} = e_{(a)}{}^{k}A_{k;j}e_{(b)}{}^{j} + \gamma_{(c)(a)(b)}A^{(c)}. \tag{2.56}$$

The quantities, $\gamma_{(c)(a)(b)}$, which we have defined in equation (2.55) are called the Ricci rotation-coefficients. An equivalent definition of these coefficients is

$$e_{(a)p;j} = e^{(c)}{}_{p}\gamma_{(c)(a)(b)}e^{(b)}{}_{j}. \tag{2.57}$$

The Ricci rotation-coefficients are antisymmetric in the first pair of indices:

$$\gamma_{(c)(a)(b)} = -\gamma_{(c)(c)(b)}, \tag{2.58}$$

a fact which follows from expanding the identity

$$0 = \eta_{(a)(b),j} = [e_{(a)p} e_{(b)}{}^{p}]_{;j}. \tag{2.59}$$

By virtue of this antisymmetry, equation (2.57) can also be written in the form

$$e_{(a)}{}^{p}{}_{;j} = -\gamma_{(a)}{}^{p}{}_{j}. \tag{2.60}$$

Returning to equation (2.56), we write it in the alternative form

$$e_{(a)}{}^{j} A_{j;k} e_{(b)}{}^{k} = A_{(a),(b)} - \eta^{(n)(m)} \gamma_{(n)(a)(b)} A_{(m)}. \tag{2.61}$$

The quantity on the right-hand side of this equation is called the intrinsic derivative of $A_{(a)}$ in the direction $e_{(b)}$ and written $A_{(a)|(b)}$

$$A_{(a)|(b)} = e_{(a)}{}^{j} A_{j;k} e_{(b)}{}^{k}. \tag{2.62}$$

We thus have the formula,

$$A_{(a)|(b)} = A_{(a),(b)} - \eta^{(n)(m)} \gamma_{(n)(a)(b)} A_{(m)}, \tag{2.63}$$

relating the directional and the intrinsic derivatives.

It is clear from above that we can pass freely from intrinsic derivatives to covariant derivatives and vice versa.

The notion of the intrinsic derivative of vector fields is readily extended to tensor fields in an obvious fashion. Thus, the intrinsic derivative of the Riemann tensor is given by

$$R_{(a)(b)(c)(d)|(f)} = R_{ijkl;m} e_{(a)}{}^{i} e_{(b)}{}^{j} e_{(c)}{}^{k} e_{(d)}{}^{l} e_{(f)}{}^{m}. \tag{2.64}$$

Now expanding

$$R_{(a)(b)(c)(d)|(f)} = [R_{ijkl} e_{(a)}{}^{i} e_{(b)}{}^{j} e_{(c)}{}^{k} e_{(d)}{}^{l}]_{;m} e_{(f)}{}^{m}, \tag{2.65}$$

and replacing the covariant derivatives of the different basis-vectors by the respective rotation-coefficients we find

$$\begin{aligned} R_{(a)(b)(c)(d)|(f)} &= R_{(a)(b)(c)(d),(f)} - \eta^{(n)(m)} [\gamma_{(n)(a)(f)} R_{(m)(b)(c)(d)} + \gamma_{(n)(b)(f)} R_{(a)(m)(c)(d)} \\ &+ \gamma_{(n)(c)(f)} R_{(a)(b)(m)(d)} + \gamma_{(n)(d)(f)} R_{(a)(b)(c)(m)}]. \end{aligned} \tag{2.66}$$

Finally, it is important to observe that the evaluation of the rotation coefficients does not require the evaluation of covariant derivatives. For, defining

$$\lambda_{(a)(b)(c)} = e_{(b)j,k} [e_{(a)}{}^{j} e_{(c)}{}^{k} - e_{(a)}{}^{k} e_{(c)}{}^{j}], \tag{2.67}$$

and rewriting in the form

$$\lambda_{(a)(b)(c)} = [e_{(b)i,j} - e_{(b)j,i}] e_{(a)}{}^{j} e_{(c)}{}^{k}, \tag{2.68}$$

we observe that we can replace the ordinary derivatives of $e_{(b)j}$ and $e_{(b)k}$ by the corresponding covariant derivatives and write

$$\lambda_{(a)(b)(c)} = \gamma_{(a)(b)(c)} - \gamma_{(c)(b)(a)}. \tag{2.69}$$

By virtue of this relation, we have

$$\gamma_{(a)(b)(c)} = \frac{1}{2}[\lambda_{(a)(b)(c)} + \lambda_{(c)(a)(b)} - \lambda_{(b)(c)(a)}], \tag{2.70}$$

and as is manifest from above, the evaluation of $\lambda_{(a)(b)(c)}$ requires only the evaluation of ordinary derivatives.

2.3.2 The Newman - Penrose Formalism

The Newman - Penrose formalism is a tetrad formalism with a special choice of the basis vectors [27]. The choice that is made is a tetrad of null vectors $\mathbf{l}$, $\mathbf{n}$, $\mathbf{m}$ and $\bar{\mathbf{m}}$ of which $\mathbf{l}$ and $\mathbf{n}$ are real and $\mathbf{m}$ and $\bar{\mathbf{m}}$ are complex conjugates of one another. The novelty of the formalism, when it was first proposed by Newman and Penrose in 1962, was precisely in their choice of a null basis: it was a departure from the choice of an orthonormal basis which was customary till then. The underlying motivation for the choice of a null basis was Penrose's strong belief that the essential element of a space-time is its light-cone structure which makes possible the introduction of a spinor basis. And it will appear that the light-cone structure of the space-times of the black hole solutions of general relativity is exactly of the kind that makes the Newman - Penrose formalism most effective for grasping the inherent symmetries of these space-times and revealing their analytical richness.

The Null Basis and the Spin Coefficients

As we have already stated, underlying the Newman - Penrose formalism is the choice of a null basis consisting of a pair of real null-vectors, $\mathbf{l}$ and $\mathbf{n}$, and a pair of complex-conjugate null-vectors $\mathbf{m}$ and $\bar{\mathbf{m}}$. They are required to satisfy the orthogonality conditions,

$$\mathbf{l} \cdot \mathbf{m} = \mathbf{l} \cdot \bar{\mathbf{m}} = \mathbf{n} \cdot \mathbf{m} = \mathbf{n} \cdot \mathbf{m} = 0, \tag{2.71}$$

besides the requirements,

$$\mathbf{l} \cdot \mathbf{l} = \mathbf{n} \cdot \mathbf{n} = \mathbf{m} \cdot \mathbf{m} = \bar{\mathbf{m}} \cdot \bar{\mathbf{m}} = 0, \tag{2.72}$$

that the vectors be null. It is customary to impose on the basis vectors the further normalization conditions,

$$\mathbf{l} \cdot \mathbf{n} = 1 \text{ and } \mathbf{m} \cdot \bar{\mathbf{m}} = -1. \tag{2.73}$$

Then, the fundamental matrix represented by $\eta_{(a)(b)}$ is a constant symmetric matrix of the form

$$[\eta_{(a)(b)}] = [\eta^{(a)(b)}] = \begin{vmatrix} 0 & 1 & 0 & 0 \\ 1 & 0 & 0 & 0 \\ 0 & 0 & 0 & -1 \\ 0 & 0 & -1 & 0 \end{vmatrix}, \tag{2.74}$$

with the correspondence,

$$\mathbf{e}_1 = \mathbf{l}\ ,\ \mathbf{e}_2 = \mathbf{n}\ ,\ \mathbf{e}_3 = \mathbf{m} \text{ and } \mathbf{e}_4 = \bar{\mathbf{m}}. \tag{2.75}$$

The corresponding covariant basis is given by

$$\mathbf{e}^1 = \mathbf{e}_2 = \mathbf{n}\ ,\ \mathbf{e}^2 = \mathbf{e}_1 = \mathbf{l}\ ,\ \mathbf{e}^3 = -\mathbf{e}_4 = -\bar{\mathbf{m}} \text{ and } \mathbf{e}^4 = -\mathbf{e}_3 = -\mathbf{m}. \tag{2.76}$$

The basis vectors, considered as directional derivatives, are designated by special symbols

$$\mathbf{e}_1 = \mathbf{e}^2 = D\ ,\ \mathbf{e}_2 = \mathbf{e}^1 = D^*\ ,\ \mathbf{e}_3 = -\mathbf{e}^4 = \delta \text{ and } \mathbf{e}_4 = -\mathbf{e}^3 = \delta^*. \tag{2.77}$$

The various Ricci rotation-coefficients, now called the spin coefficients, are, similarly, designated by special symbols [24]

$$\begin{aligned}
\kappa = \gamma_{(3)(1)(1)}\ ,\ \rho &= \gamma_{(3)(1)(4)}\ ,\ \varepsilon = \frac{1}{2}(\gamma_{(2)(1)(1)} + \gamma_{(3)(4)(1)}),\\
\sigma = \gamma_{(3)(1)(3)}\ ,\ \mu &= \gamma_{(2)(4)(3)}\ ,\ \gamma = \frac{1}{2}(\gamma_{(2)(1)(2)} + \gamma_{(3)(4)(2)}),\\
\lambda = \gamma_{(2)(4)(4)}\ ,\ \tau &= \gamma_{(3)(1)(2)}\ ,\ \alpha = \frac{1}{2}(\gamma_{(2)(1)(4)} + \gamma_{(3)(4)(4)}),\\
\nu = \gamma_{(2)(4)(2)}\ ,\ \pi &= \gamma_{(2)(4)(1)}\ ,\ \beta = \frac{1}{2}(\gamma_{(2)(1)(3)} + \gamma_{(3)(4)(3)}),
\end{aligned} \tag{2.78}$$

It is clear that the complex conjugate of any quantity can be obtained by replacing the index 3, wherever it occurs, by the index 4, and conversely. This is a general rule.

Since the most simple way of writing Dirac's equation is in the framework of spinor formalism, we shall begin with a review of the spinor analysis and the spinorial basis of the Newman - Penrose formalism to the extent that we shall need them in our present context, based on [24]. Spinors in general were discovered by Cartan in 1913, while their theory was published in 1966 [28].

2.3.3 Spinor Analysis

The idea behind spinors came about from the observation that a four-vector in Minkowski space can be represented equally by a Hermitian matrix and that a unimodular transformation in the complex two-dimensional space induces a Lorentz transformation in the Minkowski space.

Consider a point $x^j (j = 0, 1, 2, 3)$ in Minkowski space [29]; and let

$$(x^0)^2 - (x^1)^2 - (x^2)^2 - (x^3)^2 = 0. \tag{2.79}$$

We now represent the point (x^j) in terms of two complex numbers ξ^0 and ξ^1, and their complex conjugates, $\bar{\xi}^{0'}$ and $\bar{\xi}^{1'}$, in the manner

$$\begin{aligned} x^0 &= +\frac{1}{\sqrt{2}}(\xi^0\bar{\xi}^{0'} + \xi^1\bar{\xi}^{1'}), \\ x^1 &= +\frac{1}{\sqrt{2}}(\xi^0\bar{\xi}^{1'} + \xi^1\bar{\xi}^{0'}), \\ x^2 &= -\frac{i}{\sqrt{2}}(\xi^0\bar{\xi}^{1'} - \xi^1\bar{\xi}^{0'}), \\ x^3 &= +\frac{1}{\sqrt{2}}(\xi^0\bar{\xi}^{0'} - \xi^1\bar{\xi}^{1'}), \end{aligned} \tag{2.80}$$

or, inversely,

$$\begin{aligned} \xi^0\bar{\xi}^{0'} = \frac{1}{\sqrt{2}}(x^0 + x^3) \quad , \quad \xi^0\bar{\xi}^{1'} = \frac{1}{\sqrt{2}}(x^1 + ix^2), \\ \xi^1\bar{\xi}^{0'} = \frac{1}{\sqrt{2}}(x^1 - ix^2) \quad , \quad \xi^1\bar{\xi}^{1'} = \frac{1}{\sqrt{2}}(x^0 - x^3). \end{aligned} \tag{2.81}$$

By these equations,

$$\begin{aligned} (x^0)^2 - (x^1)^2 - (x^2)^2 - (x^3)^2 &= (x^0 + x^3)(x^0 - x^3) - (x^1 + ix^2)(x^1 - ix^2) \\ &= 2(\xi^0\bar{\xi}^{0'}\xi^1\bar{\xi}^{1'} - \xi^0\bar{\xi}^{1'}\xi^1\bar{\xi}^{0'}) \\ &= 0. \end{aligned} \tag{2.82}$$

Therefore, the representation (2.80) guarantees that it is a point on a null ray in Minkowski space, joining the origin with the point (x^j); and it also guarantees that the light ray is future directed since x^0 by this representation, is necessarily positive.

Now let

$$\xi_*{}^A = \alpha^A{}_B\xi^B \text{ and } \bar{\xi}_*{}^{A'} = \bar{\alpha}^{A'}{}_{B'}\xi^{B'} \ (A, B, A', B' = 0, 1), \tag{2.83}$$

represent linear transformations of the complex two-dimensional spaces, (ξ^0, ξ^1) and $(\bar{\xi}^{0'}, \bar{\xi}^{1'})$, where $(\alpha^A{}_B)$ and $(\bar{\alpha}^{A'}{}_{B'})$ are two complex-conjugate matrices. With $x_*{}^j$ defined in terms of $\xi_*{}^A$ and $\bar{\xi}_*{}^{A'}$ in the identical manner (2.80), the linear transformations (2.83) will induce linear transformation,

$$x_*{}^j = \beta^j{}_k x^k, \tag{2.84}$$

in the Minkowskian space with the coefficients $\beta^j{}_k$ given by certain bilinear combinations of the α's and $\bar{\alpha}$'s. We ask for the condition on the transformation (2.83) which will insure that the induced transformation (2.84) in the Minkowskian space is Lorentzian.

By the transformation (2.83), we have in particular

$$\begin{aligned} x_*{}^0 &= \frac{1}{\sqrt{2}}(\alpha^0{}_0\xi^0 + \alpha^0{}_1\xi^1)(\bar{\alpha}^{0'}{}_{0'}\bar{\xi}^{0'} + \bar{\alpha}^{0'}{}_{1'}\xi^{1'}) \\ &+ \frac{1}{\sqrt{2}}(\alpha^1{}_0\xi^0 + \alpha^1{}_1\xi^1)(\bar{\alpha}^{1'}{}_{0'}\bar{\xi}^{0'} + \bar{\alpha}^{1'}{}_{1'}\xi^{1'}) \\ &= \frac{1}{2}(\alpha^0{}_0\bar{\alpha}^{0'}{}_{0'} + \alpha^1{}_0\bar{\alpha}^{1'}{}_{0'})(x^0 + x^3) \\ &+ \frac{1}{2}(\alpha^0{}_1\bar{\alpha}^{0'}{}_{1'} + \alpha^1{}_1\bar{\alpha}^{1'}{}_{1'})(x^0 - x^3) \\ &+ \frac{1}{2}(\alpha^0{}_0\bar{\alpha}^{0'}{}_{1'} + \alpha^1{}_0\bar{\alpha}^{1'}{}_{1'})(x^1 + ix^2) \\ &+ \frac{1}{2}(\alpha^0{}_1\bar{\alpha}^{0'}{}_{0'} + \alpha^1{}_1\bar{\alpha}^{1'}{}_{0'})(x^1 - ix^2). \end{aligned} \tag{2.85}$$

Therefore,

$$\begin{aligned} \beta^0{}_0 + \beta^0{}_3 &= \alpha^0{}_0\bar{\alpha}^{0'}{}_{0'} + \alpha^1{}_0\bar{\alpha}^{1'}{}_{0'}, \\ \beta^0{}_0 - \beta^0{}_3 &= \alpha^0{}_1\bar{\alpha}^{0'}{}_{1'} + \alpha^1{}_1\bar{\alpha}^{1'}{}_{1'}, \\ \beta^0{}_1 - i\beta^0{}_2 &= \alpha^0{}_0\bar{\alpha}^{0'}{}_{1'} + \alpha^1{}_0\bar{\alpha}^{1'}{}_{1'}, \\ \beta^0{}_1 + i\beta^0{}_2 &= \alpha^0{}_1\bar{\alpha}^{0'}{}_{0'} + \alpha^1{}_1\bar{\alpha}^{1'}{}_{0'}. \end{aligned} \tag{2.86}$$

A requirement that the transformation (2.84) is Lorentzian is that

$$(\beta^0{}_0)^2 - (\beta^0{}_1)^2 - (\beta^0{}_2)^2 - (\beta^0{}_3)^2 = 1. \tag{2.87}$$

By equations (2.86), this condition requires

$$\Delta\bar{\Delta} = 1, \tag{2.88}$$

where Δ and $\bar{\Delta}$ denote the determinants of the transformations (2.83). Therefore, a necessary condition that the transformations (2.83) represent a Lorentz transformation is that their determinants be modulus 1, i.e., unimodular; and it is clear that it is also sufficient. In our further considerations, we shall suppose that

$$\Delta = \bar{\Delta} = 1, \tag{2.89}$$

i.e., we shall restrict ourselves to transformations with unit determinants. It is clear that these transformations do not include all Lorentz transformations. But, by including transformations which are the negative of the ones we have considered, e.g., parity transformations ($t \to -t$), etc., we can recover all Lorentz transformations.

We now define spinors ξ^A and $\eta^{A'}$ of rank 1 as complex vectors in a two-dimensional space $(A, A' = 0, 1)$ subject to the transformations

$$\xi_*{}^A = \alpha^A{}_B \xi^B \text{ and } \eta_*{}^{A'} = \bar{\alpha}^{A'}{}_{B'} \eta^{B'} \text{ with } (A, A', B, B' = 0, 1), \tag{2.90}$$

where $\alpha^A{}_B$ and $\bar{\alpha}^{A'}{}_{B'}$ are complex conjugate matrices with unit determinants.

It is important that we distinguish spinors of the two classes: those with the unprimed and those with the primed indices, which are subject to complex-conjugate transformations. Also, we shall restrict capital Latin alphabets for spinor indices.

If ξ^A and η^A are two spinors of the same class, then their determinant

$$\left|\left| \begin{array}{cc} \xi^0 & \xi^1 \\ \eta^0 & \eta^1 \end{array} \right|\right| = \xi^0\eta^1 - \xi^1\eta^0, \tag{2.91}$$

is invariant to unimodular transformations. Therefore, we may define a skew metric, ε_{AB} for the space such that

$$\varepsilon_{AB}\xi^A\eta^B, \tag{2.92}$$

is invariant. By comparison with (2.91) it follows that

$$\varepsilon_{00} = \varepsilon_{11} = 0 \text{ and } \varepsilon_{01} = -\varepsilon_{10} = 1, \tag{2.93}$$

i.e., ε_{AB} is the two-dimensional Levi-Civita symbol. We may, of course, similarly define a metric, $\varepsilon_{A'B'}$ for the primed spinors; it will again be the Levi-Civita symbol.

As in tensor analysis, we may use the metrics ε_{AB} and $\varepsilon_{A'B'}$, to lower the spinor indices; thus

$$\xi_A = \xi^C\varepsilon_{CA}, \tag{2.94}$$

or, explicitly,

$$\xi_0 = -\xi^1 \text{ and } \xi_1 = \xi^0. \tag{2.95}$$

Accordingly, indices can be raised by the Levi-Civita symbol ε^{AB} in the manner

$$\xi^A = \varepsilon^{AC}\xi_C. \tag{2.96}$$

In view of the antisymmetry of ε^{AC} and ε_{AC}, it is important to preserve the order of the indices in equations (2.94) and (2.96) with respect to the index which is contracted. Since

$$\xi_A = \xi^C\varepsilon_{CA} = \varepsilon^{CB}\xi_B\varepsilon_{CA}, \tag{2.97}$$

it follows that

$$\delta^B_A = \varepsilon^{CB}\varepsilon_{CA} = \varepsilon_A{}^B = -\varepsilon^B{}_A. \tag{2.98}$$

It is, of course, clear that by considering spinors with primed indices, we shall obtain the same formulae (2.94) - (2.98) with the indices primed.

As in tensor analysis, we can construct spinors of higher rank,

$$\xi^{AB}\ ,\ \xi_{AB'C}\ ,\ \xi_{ABC'}{}^{D'E}{}_{F'G}\ ,\ \text{etc.}, \tag{2.99}$$

with their appropriate transformation properties. Thus,

$$\xi^{AB'}_{*} = \alpha^{A}{}_{C}\bar{\alpha}^{B'}{}_{D'}\xi^{CD'}. \tag{2.100}$$

It is important to observe that while the order of the indices of each kind is relevant and must be preserved, the relative ordering of the primed and the unprimed indices is of no consequence.

Again, as in tensor analysis, contraction of spinors with respect to a pair of primed, or unprimed, indices can be effected with the metric ε_{AB}, or $\varepsilon_{A'B'}$; but contraction of a primed and unprimed index is, of course, forbidden. Thus, on the other hand,

$$\xi^{A'}{}_{A'} = \varepsilon^{A'B'}\xi_{B'A'}. \tag{2.101}$$

Therefore,

$$\xi_{A'}{}^{A'} = -\xi^{A'}_{A'}. \tag{2.102}$$

In particular,

$$\xi_{A'}\xi^{A'} = 0. \tag{2.103}$$

The Representation of Vectors and Tensors in Terms of Spinors

Equations (2.80) and (2.81) provide a representation of the position vector, x^j, in terms of a pair of complex-conjugate spinors, ξ^A and $\bar{\xi}^{A'}$, which we can express in the manner

$$x^j \leftrightarrow \begin{vmatrix} \xi^0\bar{\xi}^{0'} & \xi^0\bar{\xi}^{1'} \\ \xi^1\bar{\xi}^{0'} & \xi^1\bar{\xi}^{1'} \end{vmatrix} = \frac{1}{\sqrt{2}} \begin{vmatrix} x^0 + x^3 & x^1 + ix^2 \\ x^1 - ix^2 & x^0 - x^3 \end{vmatrix}. \tag{2.104}$$

Quite generally, we associate any four vector X^j with a spinor of the second rank $\xi^{AB'}$ in the manner

$$X^j \leftrightarrow \begin{vmatrix} \xi^{00'} & \xi^{01'} \\ \xi^{10'} & \xi^{11'} \end{vmatrix} = \frac{1}{\sqrt{2}} \begin{vmatrix} X^0 + X^3 & X^1 + iX^2 \\ X^1 - iX^2 & X^0 - X^3 \end{vmatrix}. \tag{2.105}$$

Thus a four vector is associated with a Hermitian matrix.

The invariant associated with the four vector is

$$(X^0)^2 - (X^1)^2 - (X^2)^2 - (X^3)^2 = X_{AB'}X^{AB'} \tag{2.106}$$

or, expressed in terms of the metrics g_{jk}, ε_{AB} and $\varepsilon_{A'B'}$ of the Minkowskian and the spinor spaces,

$$g_{jk}X^jX^k = \varepsilon_{AC}\varepsilon_{B'D'}X^{AB'}X^{CD'}. \tag{2.107}$$

The relationship,

$$X^j \leftrightarrow X^{AB'}, \tag{2.108}$$

is now expressed in the form

$$X^j = \sigma^j{}_{AB'} X^{AB'}, \tag{2.109}$$

or, in its inverse form,

$$X^{AB'} = \sigma^{AB'}{}_j X^j, \tag{2.110}$$

where $\sigma^j{}_{AB'}$ and $\sigma^{AB'}{}_j$, for each j, are constant Hermitian matrices. Relations which are immediate consequence of the foregoing definitions are

$$\sigma^{AB'}{}_j \sigma^j{}_{CD'} = \delta^A_C \delta^{B'}_{D'}, \tag{2.111}$$

and

$$\sigma^j{}_{AB'} \sigma_k{}^{AB'} = \delta^j_k. \tag{2.112}$$

And, finally, we deduce from equations (2.107) and (2.110) that

$$g_{jk} = \varepsilon_{AC} \varepsilon_{B'D'} \sigma^{AB'}{}_j \sigma^{CD'}{}_k, \tag{2.113}$$

and

$$\varepsilon_{AC} \varepsilon_{B'D'} = g_{jk} \sigma^j{}_{AB'} \sigma^k{}_{CD'}. \tag{2.114}$$

It is of interest to note that the matrices $\sigma^j_{AB'}$ and $\sigma_j^{AB'}$, defined by the representation (2.105), are

$$\begin{aligned} \sigma^{AB'}{}_0 &= \frac{1}{\sqrt{2}} \begin{vmatrix} 1 & 0 \\ 0 & 1 \end{vmatrix} \quad , \quad \sigma^{AB'}{}_1 = \frac{1}{\sqrt{2}} \begin{vmatrix} 0 & 1 \\ 1 & 0 \end{vmatrix}, \\ \sigma^{AB'}{}_2 &= \frac{1}{\sqrt{2}} \begin{vmatrix} 0 & i \\ -i & 0 \end{vmatrix} \quad , \quad \sigma^{AB'}{}_3 = \frac{1}{\sqrt{2}} \begin{vmatrix} 1 & 0 \\ 0 & -1 \end{vmatrix}, \end{aligned} \tag{2.115}$$

and

$$\begin{aligned} \sigma^0{}_{AB'} &= \frac{1}{\sqrt{2}} \begin{vmatrix} 1 & 0 \\ 0 & 1 \end{vmatrix} \quad , \quad \sigma^1{}_{AB'} = \frac{1}{\sqrt{2}} \begin{vmatrix} 0 & 1 \\ 1 & 0 \end{vmatrix}, \\ \sigma^2{}_{AB'} &= \frac{1}{\sqrt{2}} \begin{vmatrix} 0 & -i \\ i & 0 \end{vmatrix} \quad , \quad \sigma^3{}_{AB'} = \frac{1}{\sqrt{2}} \begin{vmatrix} 1 & 0 \\ 0 & -1 \end{vmatrix}. \end{aligned} \tag{2.116}$$

It will be observed that, apart from the normalization factor $\frac{1}{\sqrt{2}}$, $\sigma^1{}_{AB'}$, $\sigma^2{}_{AB'}$, and $\sigma^3{}_{AB'}$ are the Pauli spin-matrices.

In terms of the σ-matrices, we can now relate tensors of arbitrary rank with their spinor equivalents. Thus,

$$Y^{jk}{}_p = \sigma^j{}_{AB'} \sigma^k{}_{CD'} \sigma_p{}^{EF'} Y^{AB'CD'}{}_{EF'}, \tag{2.117}$$

and

$$Y^{AB'CD'}{}_{EF'} = \sigma^{AB'}{}_{j}\sigma^{CD'}{}_{k}\sigma^{p}{}_{EF'}Y^{jk}{}_{p}\,. \tag{2.118}$$

By virtue of these relations, we have the correspondence

$$Y^{AB'CD'}{}_{EF'} \leftrightarrow Y^{jk}{}_{p}\,. \tag{2.119}$$

In this sense, equation (2.114) expresses the correspondence

$$\varepsilon_{AC}\varepsilon_{B'D'} \leftrightarrow g_{jk}. \tag{2.120}$$

The Dyad Formalism

Since the space-time of general relativity is locally Minkowskian, we can set up, at each point of the space-time, an orthonormal dyad basis, $\chi_{(F)}{}^{A}$ and $\chi_{(F')}{}^{A'}$ $(F, F', A, A' = 0, 1)$, for spinors even as we set up an orthonormal tetrad basis, $e^{j}_{(a)}(a = 0, 1, 2, 3$ and $j = 0, 1, 2, 3)$ for tensors in a tetrad formalism. And, as in the tetrad formalism, we shall enclose the dyad indices - the lowercase letters of the earlier part of the Latin alphabet - in parentheses. It is, however, convenient to have special symbols for the two basis spinors, $\chi_{(0)}{}^{A}$ and $\chi_{(1)}{}^{A}$. We shall write

$$\chi_{(0)}{}^{A} = o^{A} \text{ and } \chi_{(1)}{}^{A} = l^{A}. \tag{2.121}$$

And the condition of orthonormality is

$$\varepsilon_{AB}o^{A}l^{B} = o^{0}l^{1} - o^{1}l^{0} = o^{B}l^{B} = -o^{A}l^{A} = 1. \tag{2.122}$$

Elementary consequences of these definitions are

$$\varepsilon_{AB}\chi_{(F)}{}^{A}\chi_{(G)}{}^{B} = \chi_{(G)B}\chi^{B}_{(G)} = \varepsilon_{(F)(G)}, \tag{2.123}$$

and

$$\varepsilon^{(F)(G)}\chi_{(F)}{}^{A}\chi_{(G)}{}^{B} = \chi_{(0)}{}^{A}\chi_{(1)}{}^{B} - \chi_{(1)}{}^{A}\chi_{(0)}{}^{B} \tag{2.124}$$

$$= o^{A}l^{B} - l^{A}o^{B} = \varepsilon^{AB}. \tag{2.125}$$

It is also clear that we can raise and lower the dyad indices by $\varepsilon^{(F)(G)}$ and $\varepsilon_{(F)(G)}$. Thus,

$$\chi^{(H)A}\varepsilon_{(H)(F)} = \chi_{F}{}^{A} \text{ and } \varepsilon^{(F)(H)}\chi_{(H)}{}^{A} = \chi^{(F)A}. \tag{2.126}$$

Further consequences are

$$\chi_{(F)A}\chi^{(G)A} = -\chi_{(F)}{}^{A}\chi^{(G)}{}_{A} = \delta^{(G)}_{(F)}, \tag{2.127}$$

and

$$\chi_{(F)A}\chi_{(G)}{}^{A} = -\chi_{(F)}{}^{A}\chi_{(G)A} = \varepsilon_{(F)(G)}. \tag{2.128}$$

As in the tetrad formalism, we can project any spinor ξ_A on to the dyad basis

$$\xi_{(F)} = \xi_A \chi_{(F)}{}^{A}, \tag{2.129}$$

or, explicitly,

$$\xi_{(0)} = \xi_A o^A \text{ and } \xi_{(1)} = \xi_A l^A. \tag{2.130}$$

We also have

$$\xi_A = \xi^{(F)}\chi_{(F)A} = \xi^{(0)}o_A + \xi^{(1)}l_A. \tag{2.131}$$

The spinors o^A and l^A and their complex conjugates determine the null vectors $\mathbf{l}$, $\mathbf{n}$, $\mathbf{m}$ and $\bar{\mathbf{m}}$ by the correspondence

$$\begin{gathered} l^j \leftrightarrow o^A\bar{o}^{B'}\ ,\ m^j \leftrightarrow o^A\bar{l}^{B'}, \\ \bar{m}^j \leftrightarrow l^A\bar{o}^{B'}\ ,\ n^j \leftrightarrow l^A\bar{l}^{B'}. \end{gathered} \tag{2.132}$$

The null vectors satisfy the orthogonality conditions,

$$l^j n_j = o^A\bar{o}^{B'}l_A\bar{l}_{B'} = 1 \text{ and } m^j\bar{m}_j = o^A\bar{l}^{B'}l_A\bar{o}_{B'} = -1, \tag{2.133}$$

while all the remaining scalar products are zero. Thus, the dyad basis determines four null vectors which can be used as a basis for a Newman - Penrose formalism.

The representation (2.132) yields the Hermitian matrices,

$$\sigma^{j}{}_{AB'} \text{ and } \sigma_{AB'}{}^{j}, \tag{2.134}$$

such that

$$\begin{aligned} l^j &= \sigma^{j}{}_{AB'}\chi_{(0)}{}^{A}\bar{\chi}_{(0')}{}^{B'} = \sigma^{j}{}_{AB'}o^A\bar{o}^{B'}, \\ m^j &= \sigma^{j}{}_{AB'}\chi_{(0)}{}^{A}\bar{\chi}_{(1')}{}^{B'} = \sigma^{j}{}_{AB'}o^A\bar{l}^{B'}, \\ \bar{m}^j &= \sigma^{j}{}_{AB'}\chi_{(1)}{}^{A}\bar{\chi}_{(0')}{}^{B'} = \sigma^{j}{}_{AB'}l^A\bar{o}^{B'}, \\ n^j &= \sigma^{j}{}_{AB'}\chi_{(1)}{}^{A}\bar{\chi}_{(1')}{}^{B'} = \sigma^{j}{}_{AB'}l^A\bar{l}^{B'}. \end{aligned} \tag{2.135}$$

Accordingly, we may write

$$\sigma^{j}{}_{AB'} = \frac{1}{\sqrt{2}}\begin{vmatrix} l^j & m^j \\ \bar{m}^j & n^j \end{vmatrix} \text{ and } \sigma_{AB'}{}^{j} = \frac{1}{\sqrt{2}}\begin{vmatrix} n^j & -\bar{m}^j \\ -m^j & l^j \end{vmatrix}. \tag{2.136}$$

Comparison with equations (2.115) and (2.116) shows that the foregoing definitions provide the natural generalizations of the Pauli spin-matrices.

And finally, associated with the directional derivatives,

$$D = l^j\partial_j \ , \ D^* = n^j\partial_j \ , \ \delta = m^j\partial_j \text{ and } \delta^* = \bar{m}^j\partial_j, \tag{2.137}$$

of the Newman - Penrose formalism, we have the spinor equivalents

$$\partial_{00'} = D \ , \ \partial_{11'} = D^* \ , \ \partial_{01'} = \delta \text{ and } \partial_{10'} = \delta^*. \tag{2.138}$$

Covariant Differentiation of Spinor Fields and Spin Coefficients

We now wish to define covariant differentiation of spinor fields. Consistency requires that the definition must be based on the correspondences

$$\nabla_j \leftrightarrow \nabla_{AB'}, \tag{2.139}$$

and

$$\nabla_j X_k = X_{k;j} \leftrightarrow X_{CD';AB'}. \tag{2.140}$$

In accordance with equation (2.117), this last equation requires

$$X_{CD';AB'} = \sigma^k{}_{CD'}\sigma^j{}_{AB'}X_{k;j}. \tag{2.141}$$

Besides, we shall require that the covariant differentiation of spinor fields satisfies the Leibnitz rule, namely,

$$\nabla_{AB'}(S^{\cdots}{}_{\cdots} \times T^{\cdots}{}_{\cdots}) = T^{\cdots}{}_{\cdots}\nabla_{AB'}(S^{\cdots}{}_{\cdots}) + S^{\cdots}{}_{\cdots}\nabla_{AB'}(T^{\cdots}{}_{\cdots}), \tag{2.142}$$

where $S^{\cdots}{}_{\cdots}$ and $T^{\cdots}{}_{\cdots}$ are any two spinor fields. And we shall also require that the operator $\nabla_{AB'}$ is real, i.e.,

$$\nabla_{AB'} = \bar{\nabla}_{A'B}. \tag{2.143}$$

We shall show presently how the foregoing postulates suffice to define uniquely the operation of covariant differentiation. But first, we note that, as in the tetrad formalism, we can define, in analogous fashion, the notion of intrinsic differentiation. Thus, we define the intrinsic derivative of the dyadic component $\xi_{(F)}$, of a spinor along the direction $(F)(G')$ by

$$\xi_{(H)|(F)(G')} = \chi_{(H)}{}^C\xi_{C;AB'}\chi_{(F)}{}^A\xi_{(G)}{}^{B'}, \tag{2.144}$$

or, equivalently,

$$\xi_{(H)|AB'} = \chi_{(H)}{}^C\xi_{C;AB'}. \tag{2.145}$$

The spin coefficients, $\Gamma_{(a)(b)(c)(d')}$, are defined in the dyad formalism by

$$\Gamma_{(A)(B)(G)(H')} = [\chi_{(A)F}]_{;CD'}\chi_{(B)}{}^{F}\chi_{(G)}{}^{C}\chi_{(H')}{}^{D'}. \tag{2.146}$$

It is convenient, for the sake of brevity, to write instead the formula

$$\Gamma_{(A)(B)CD'} = [\chi_{(A)F}]_{;CD'}\chi_{(B)}{}^{F}. \tag{2.147}$$

The spin coefficients, as defined, are symmetric in the first pair of its indices. This symmetry follows from the relation

$$\chi_{(A)F}\chi_{(B)}{}^{F} = \varepsilon_{(A)(B)}. \tag{2.148}$$

For, by this relation, we have

$$\begin{aligned}\Gamma_{(A)(B)CD'} &= -[\chi_{(B)}{}^{F}]_{;CD'}\chi_{(A)F} \\ &= +[\chi_{(B)F}]_{;CD'}\chi_{(A)}{}^{F} = \Gamma_{(B)(A)CD'}.\end{aligned} \tag{2.149}$$

An alternative form of equation (2.147) follows by contraction with $\chi^{(B)}{}_{E}$ and making use of the relations included in equations (2.127). Thus,

$$[\chi_{(A)E}]_{;CD'} = -\chi^{(B)}{}_{E}\Gamma_{(B)(A)CD'} = \chi_{(B)E}\Gamma^{(B)}{}_{(A)CD'}. \tag{2.150}$$

We shall now show how, with the spin coefficients as defined, the intrinsic derivatives of the dyadic components of the spinors of the first rank, $\xi_{(F)}$ and $\xi^{(F)}$, can be expressed; and this, by the Leibnitz rule, will clearly suffice to obtain the covariant derivatives of spinors of arbitrary rank. Thus,

$$\begin{aligned}\xi_{(F)|BC'} &= \chi_{(F)}{}^{A}\xi_{A;BC'} \\ &= [\xi_{A}\chi_{(F)}{}^{A}]_{;BC'} - \xi_{A}[\chi_{(F)}{}^{A}]_{;BC'}.\end{aligned} \tag{2.151}$$

The quantity in the first square brackets on the right-hand side is a scalar, namely, $\xi_{(F)}$. Therefore, by equation (2.150),

$$\xi_{(F)|BC'} = \xi_{(F),BC'} - \xi_{A}\Gamma^{(D)}{}_{(F)BC'}\chi_{(D)}{}^{A}, \tag{2.152}$$

or, equivalently,

$$\xi_{(F)|BC'} = \xi_{(F),BC'} + \Gamma_{(D)(F)BC'}\chi^{(D)}. \tag{2.153}$$

Similarly, we find

$$\xi^{(F)}{}_{|BC'} = \xi^{(F)}{}_{,BC'} + \Gamma^{(F)}{}_{(D)BC'}\chi^{(D)}, \tag{2.154}$$

and

$$\xi^{A}{}_{;BC'} = \chi^{A}{}_{(F)}(\xi^{(F)}{}_{,BC'} + \Gamma_{(D)}{}^{(F)}{}_{BC'}\xi^{(D)}). \tag{2.155}$$

In view of the symmetry of the spin coefficients in the first pair of the dyadic indices, it is clear that twelve coefficients will have to be specified. In the Newman - Penrose formalism, these coefficients are assigned special symbols which are listed below.

$$\begin{aligned}
\Gamma_{(0)(0)00'} = \kappa \ , \ \Gamma_{(0)(0)10'} = \rho \quad &, \quad \Gamma_{(0)(0)01'} = \sigma \ , \ \Gamma_{(0)(0)11'} = \tau, \\
\Gamma_{(0)(1)00'} = \Gamma_{(1)(0)00'} = \varepsilon \quad &, \quad \Gamma_{(0)(1)10'} = \Gamma_{(1)(0)10'} = \alpha, \\
\Gamma_{(0)(1)01'} = \Gamma_{(1)(0)01'} = \beta \quad &, \quad \Gamma_{(0)(1)11'} = \Gamma_{(1)(0)11'} = \gamma, \\
\Gamma_{(1)(1)00'} = \pi \ , \ \Gamma_{(1)(1)10'} = \lambda \quad &, \quad \Gamma_{(1)(1)01'} = \mu \ , \ \Gamma_{(1)(1)11'} = \nu.
\end{aligned} \tag{2.156}$$

This completes our account of spinor analysis and the spinorial basis of the Newman - Penrose formalism.

2.3.4 Dirac's Equation

As is well known, in the relativistic theory of spin half particles, the wave function is represented by a pair of spinors, P^A and $\bar{Q}^{A'}$; and in Minkowski space, Dirac's equations governing them are [30]

$$\sigma^j{}_{AB'}\partial_j P^A + i\mu_* \bar{Q}_{B'} = 0, \tag{2.157}$$

and

$$\sigma^j{}_{AB'}\partial_j Q^A + i\mu_* \bar{P}_{B'} = 0, \tag{2.158}$$

where $\sigma^j{}_{AB'}$ are the Pauli matrices and $\frac{1}{\sqrt{2}}\mu_*$ is the mass of the particle. The factor $\sqrt{2}$ in the definition of the mass arises from the fact that the Pauli matrices as defined in equation (2.116) differ from their customary definitions by the factor $\frac{1}{\sqrt{2}}$.

In the Newman - Penrose formalism in a curved space-time, we take over equations (2.157) and (2.158) with the covariant derivatives replacing the ordinary derivatives and the σ-matrices, defined in equations (2.137), replacing the Pauli matrices. The required equations are, therefore,

$$\sigma^j{}_{AB'} P^A{}_{;j} + i\mu_* \bar{Q}^{C'} \varepsilon_{C'B'} = 0, \tag{2.159}$$

and

$$\sigma^j{}_{AB'} Q^A{}_{;j} + i\mu_* \bar{P}^{C'} \varepsilon_{C'B'} = 0, \tag{2.160}$$

where

$$\sigma^j{}_{AB'} = \frac{1}{\sqrt{2}} \begin{vmatrix} l^j & m^j \\ \bar{m}^j & n^j \end{vmatrix}. \tag{2.161}$$

We show now write out the explicit forms of these equations in terms of the spin coefficients we have defined.

Consider equation (2.159) for $B' = 0$. We have

$$\sigma^{j}{}_{00'} P^{0}{}_{;j} + \sigma^{j}{}_{10'} P^{1}{}_{;j} - i\mu_* \bar{Q}^{1'} = 0, \tag{2.162}$$

or, by virtue of equations (2.137), (2.138), (2.154), and (2.161),

$$(\partial_{00'} P^0 + \Gamma^{0}{}_{b00'} P^b) + (\partial_{10'} P^1 + \Gamma^{1}{}_{b10'} P^b) - i\mu_* \bar{Q}^{1'} = 0, \tag{2.163}$$

or, more explicitly,

$$(D + \Gamma_{1000'} - \Gamma_{0010'}) P^0 + (\delta^* + \Gamma_{1100'} - \Gamma_{0110'}) P^1 - i\mu_* \bar{Q}^{1'} = 0. \tag{2.164}$$

Now replacing the various spin coefficients in equation (2.164) by their named symbols listed in (2.156), we obtain

$$(D + \varepsilon - \rho) P^0 + (\delta^* + \pi - \alpha) P^1 - i\mu_* \bar{Q}^{1'} = 0. \tag{2.165}$$

Similarly, equation (2.159) for $B' = 1$, yields

$$(D^* + \mu - \gamma) P^1 + (\delta + \beta - \tau) P^0 + i\mu_* \bar{Q}^{0'} = 0. \tag{2.166}$$

Equation (2.160) provides the same equations (2.165) and (2.166) with P and Q interchanged. It is, however, convenient to consider the complex conjugate of equation (2.160) and further write

$$F_1 = P^0 \ , \ F_2 = P^1 \ , \ G_1 = \bar{Q}^{1'} \text{ and } G_2 = -\bar{Q}^{0'}. \tag{2.167}$$

The resulting equations are

$$\begin{aligned}
(D + \epsilon - \rho) F_1 + (\delta^* + \pi - \alpha) F_2 &= i\mu_* G_1, \\
(D^* + \mu - \gamma) F_2 + (\delta + \beta - \tau) F_1 &= i\mu_* G_2, \\
(D + \epsilon^* - \rho^8) G_2 - (\delta + \pi^* - \alpha^\alpha) G_1 &= i\mu_* F_2, \\
(D^* + \mu^* - \gamma^*) G_1 - (\delta^* + \beta^* - \tau^*) G_2 &= i\mu_* F_1.
\end{aligned} \tag{2.168}$$

These are the Dirac equations in the Newman - Penrose formalism.

2.3.5 In the Kerr Space-time

For the Kerr space-time, the tetrad basis in the Newman - Penrose formalism is given by

$$\begin{aligned}
l^j &= \frac{1}{\Delta} \left(r^2 + a^2, \Delta, 0, a \right), \\
n^j &= \frac{1}{2\rho^2} \left(r^2 + a^2, -\Delta, 0, a \right), \\
m^j &= \frac{1}{\sqrt{2}\bar{\rho}} \left(ia \sin\theta, 0, 1, i \csc\theta \right),
\end{aligned} \tag{2.169}$$

where

$$\rho^2 = \bar{\rho}\bar{\rho}^* = r^2 + a^2\cos^2\theta, \tag{2.170}$$

while the spin-coefficients are

$$\kappa = \sigma = \lambda = \nu = \varepsilon = 0,$$

$$\tilde{\rho} = -\frac{1}{\bar{\rho}^*}\ ,\ \beta = \frac{\cot\theta}{2\sqrt{2}\bar{\rho}}\ ,\ \pi = \frac{ia\sin\theta}{\sqrt{2}(\bar{\rho}^*)^2}\ ,\ \tau = -\frac{ia\sin\theta}{\sqrt{2}\rho^2}, \tag{2.171}$$

$$\mu = -\frac{\Delta}{2\bar{\rho}^*\rho^2}\ ,\ \gamma = \mu + \frac{r-M}{2\rho^2}\ ,\ \alpha = \pi - \beta^*. \tag{2.172}$$

So in the Kerr space-time and with massless particles ($\mu_* = 0$), equations (2.168) reduce to

$$\begin{aligned}
\left(\mathcal{D}_0 + \frac{1}{\bar{\rho}^*}\right)F_1 + \frac{1}{\sqrt{2}\bar{\rho}^*}\mathcal{L}_{\frac{1}{2}}F_2 = 0,\\
\frac{\Delta}{2\rho^2}\mathcal{D}^\dagger_{\frac{1}{2}}F_2 - \frac{1}{\sqrt{2}\bar{\rho}}\left(\mathcal{L}^\dagger_{\frac{1}{2}} + \frac{ia\sin\theta}{\bar{\rho}^*}\right)F_1 = 0,\\
\left(\mathcal{D}_0 + \frac{1}{\bar{\rho}}\right)G_2 - \frac{1}{\sqrt{2}\bar{\rho}}\mathcal{L}^\dagger_{\frac{1}{2}}G_1 = 0,\\
\frac{\Delta}{2\rho^2}\mathcal{D}^\dagger_{\frac{1}{2}}G_1 + \frac{1}{\sqrt{2}\bar{\rho}^*}\left(\mathcal{L}_{\frac{1}{2}} - \frac{ia\sin\theta}{\bar{\rho}}\right)G_1 = 0,
\end{aligned} \tag{2.173}$$

where

$$\begin{aligned}
\mathcal{D}_n = \partial_r + i\frac{K}{\Delta} + 2n\frac{r-M}{\Delta} \quad ,\quad \mathcal{D}^\dagger_n = \partial_r - i\frac{K}{\Delta} + 2n\frac{r-M}{\Delta},\\
\mathcal{L}_n = \partial_\theta + Q + n\cot\theta \quad ,\quad \mathcal{L}^\dagger_n = \partial_\theta - Q + n\cot\theta,
\end{aligned} \tag{2.174}$$

and

$$K = (r^2+a^2)\omega + am\ ,\ Q = a\omega\sin\theta + m\csc\theta. \tag{2.175}$$

The forms of equations (2.173) suggest that in place of F_1 and G_2 we define

$$f_1 = \bar{\rho}^* F_1\ ,\ g_2 = \bar{\rho}G_2. \tag{2.176}$$

Also writing f_2 and g_1 in place of F_2 and G_1 we find that equations (2.173) become

$$\mathcal{D}_0 f_1 + \frac{1}{\sqrt{2}}\mathcal{L}_{\frac{1}{2}} f_2 = 0 \ , \ \Delta\mathcal{D}^\dagger_{\frac{1}{2}} f_2 - \sqrt{2}\mathcal{L}^\dagger_{\frac{1}{2}} f_1 = 0,$$
$$\mathcal{D}_0 g_2 - \frac{1}{\sqrt{2}}\mathcal{L}^\dagger_{\frac{1}{2}} g_1 = 0 \ , \ \Delta\mathcal{D}^\dagger_{\frac{1}{2}} g_1 + \sqrt{2}\mathcal{L}_{\frac{1}{2}} g_2 = 0. \tag{2.177}$$

It is now apparent that the variables can be separated by the substitutions

$$f_1(r,\theta) = R_{-\frac{1}{2}}(r)S_{-\frac{1}{2}}(\theta) \ , \ f_2(r,\theta) = R_{\frac{1}{2}}(r)S_{\frac{1}{2}}(\theta),$$
$$g_1(r,\theta) = R_{\frac{1}{2}}(r)S_{-\frac{1}{2}}(\theta) \ , \ g_2(r,\theta) = R_{-\frac{1}{2}}(r)S_{\frac{1}{2}}(\theta), \tag{2.178}$$

where $R_{\pm\frac{1}{2}}(r)$ and $S_{\pm\frac{1}{2}}(\theta)$ are functions, respectively, of r and θ only. With these substitutions, equations (2.177) yield

$$\mathcal{D}_0 R_{-\frac{1}{2}} = \lambda_1 R_{\frac{1}{2}} \ , \ \frac{1}{\sqrt{2}}\mathcal{L}_{\frac{1}{2}} S_{\frac{1}{2}} = -\lambda_1 S_{-\frac{1}{2}},$$
$$\Delta\mathcal{D}^\dagger_{\frac{1}{2}} R_{\frac{1}{2}} = \lambda_2 R_{-\frac{1}{2}} \ , \ \sqrt{2}\mathcal{L}^\dagger_{\frac{1}{2}} S_{-\frac{1}{2}} = \lambda_2 S_{\frac{1}{2}},$$
$$\mathcal{D}_0 R_{-\frac{1}{2}} = \lambda_3 R_{\frac{1}{2}} \ , \ \frac{1}{\sqrt{2}}\mathcal{L}^\dagger_{\frac{1}{2}} S_{-\frac{1}{2}} = \lambda_3 S_{\frac{1}{2}}, \tag{2.179}$$
$$\Delta\mathcal{D}^\dagger_{\frac{1}{2}} R_{\frac{1}{2}} = \lambda_4 R_{-\frac{1}{2}} \ , \ \sqrt{2}\mathcal{L}_{\frac{1}{2}} S_{\frac{1}{2}} = -\lambda_4 S_{-\frac{1}{2}},$$

where $\lambda_1, ..., \lambda_4$ are four constants of separation. However, it is manifest that the consistency of the foregoing equations requires that

$$\lambda_1 = \lambda_3 = \frac{1}{2}\lambda_2 = \frac{1}{2}\lambda_4 = \lambda. \tag{2.180}$$

We are thus left with two pairs of equations,

$$\mathcal{D}_0 R_{-\frac{1}{2}} = \lambda R_{\frac{1}{2}} \ , \ \Delta\mathcal{D}^\dagger_{\frac{1}{2}} R_{\frac{1}{2}} = 2\lambda R_{-\frac{1}{2}}, \tag{2.181}$$

and

$$\mathcal{L}_{\frac{1}{2}} S_{\frac{1}{2}} = -\sqrt{2}\lambda S_{-\frac{1}{2}} \ , \ \mathcal{L}^\dagger_{\frac{1}{2}} S_{-\frac{1}{2}} = \sqrt{2}\lambda S_{\frac{1}{2}}. \tag{2.182}$$

It is convenient at this stage to replace $\sqrt{2}\lambda$ by λ and $\sqrt{2}R_{-\frac{1}{2}}$ by $R_{-\frac{1}{2}}$. With these replacements, equations (2.181) and (2.182) become

$$\Delta^{\frac{1}{2}}\mathcal{D}_0 R_{-\frac{1}{2}} = \lambda\Delta^{\frac{1}{2}} R_{\frac{1}{2}} \ , \ \Delta^{\frac{1}{2}}\mathcal{D}^\dagger_{\frac{1}{2}}\Delta^{\frac{1}{2}} R_{\frac{1}{2}} = \lambda R_{-\frac{1}{2}}, \tag{2.183}$$

and

$$\mathcal{L}_{\frac{1}{2}} S_{\frac{1}{2}} = -\lambda S_{-\frac{1}{2}} \ , \ \mathcal{L}^{\dagger}_{\frac{1}{2}} S_{-\frac{1}{2}} = \lambda S_{\frac{1}{2}}. \tag{2.184}$$

We can eliminate $\Delta^{\frac{1}{2}} R_{\frac{1}{2}}$ from equations (2.183) to obtain an equation for $R_{-\frac{1}{2}}$. Thus,

$$\left[\Delta \mathcal{D}^{\dagger}_{\frac{1}{2}} \mathcal{D}_0 - \lambda^2\right] R_{-\frac{1}{2}} = 0, \tag{2.185}$$

and $\Delta^{\frac{1}{2}} R_{\frac{1}{2}}$ satisfies the complex-conjugate equation.

Similarly, we can eliminate $S_{\frac{1}{2}}$ from equations (2.184) to obtain an equation for $S_{-\frac{1}{2}}$, thus,

$$\left[\mathcal{L}_{\frac{1}{2}} \mathcal{L}^{\dagger}_{\frac{1}{2}} + \lambda^2\right] S_{-\frac{1}{2}} = 0, \tag{2.186}$$

and $S_{\frac{1}{2}}$ satisfies the adjoint equation.

Now that the radial and angular equations have been derived for both the scalar and the spin half particles in the Kerr space-time; they can be used to study the conformal nature of the near region of a Kerr black hole in chapter 3 and for the calculation of the QNM frequencies of a Kerr black hole in chapter 5.

Chapter 3

Hidden Conformal Symmetry

It has been stated that an extreme Kerr black hole could be holographically described by an two-dimensional chiral conformal field theory with non-vanishing temperature $T_L = \frac{1}{2\pi}$ and the central charge $c_L = 12J$, where J is the angular momentum of the Kerr black hole. In this chiral representation, it was then possible to reproduce the Bekenstein-Hawking entropy by using the Cardy formula. Such a correspondence was soon generalized to various extreme black holes [31].

In particular, the extreme black holes with multiple $U(1)$ symmetries are especially interesting. For such cases, it turns out that for each $U(1)$ there is a dual holographic conformal field theory description correspondingly [32].

Every novel conformal field theory is defined with respect to a Killing symmetry of translation along an angular variable, which could be the linear combination of original two Killing symmetries.

The conformal field theory dual to an extreme black hole is actually not chiral. It was pointed out that there is actually a right-moving sector with the same central charge [33]. But the excitations are suppressed in the extreme limit. When one considers the scattering off of the extreme black hole, the black hole becomes near-extremal, the right-moving sector is excited. In the near-horizon limit, the modes of interest are the ones near the super-radiant boundary.

The symmetry of interest for this dissertation forms the basis of two-dimensional conformal field theory, so it would be of use to first review this theory, before applying it to the Kerr black hole, and this done in the following section.

This chapter seeks to study the conformal nature of the four dimensional Kerr black hole in the near region, in terms of both the scalar solution space and the spin-half solution space. But first it is necessary to briefly describe conformal field theory and then define what the Kerr black hole near region is.

3.1 Conformal Field Theory

Conformal field theories have been at the centre of much attention during the last fifteen

years since they are relevant for at least three different areas of modern theoretical physics, including a central role in string theory. (At present the most promising candidate for a unifying theory of all forces.) Conformal field theories have also had a major impact on various aspects of modern mathematics.

From an abstract point of view, conformal field theories are Euclidean quantum field theories that are characterized by the property that their symmetry group contains, in addition to the Euclidean symmetries, local conformal transformations, i.e., transformations that preserve angles but not lengths. The local conformal symmetry is of special importance in two dimensions since the corresponding symmetry algebra is infinite-dimensional in this case. As a consequence, two-dimensional conformal field theories have an infinite number of conserved quantities, and are completely solvable by symmetry considerations alone [34].

3.1.1 Conformal Transformations

Consider flat space-time in d dimensions, that is, $\mathbb{R}^d$ endowed with a flat metric $g_{\mu\nu}$ (which can be taken as either euclidean or lorentzian) and coordinates x^μ, $\mu = 0, ..., d-1$. First recall that Poincaré transformations are the set of transformations

$$x^\mu \to x^{'\mu}(x), \tag{3.1}$$

leaving the components of the flat metric (with a lorentzian signature) unchanged

$$g_{\mu\nu} \to g^{'}_{\mu\nu}(x^{'}(x)) = g_{\mu\nu}(x).$$

This statement can also be expressed from the "active" point of view by demanding that the squared "Minkowskian norm" $\mathrm{d}s^2$ of a vector with components $\mathrm{d}x^\mu$ be preserved under (3.1):

$$\mathrm{d}s^2 = g_{\mu\nu}\mathrm{d}x^\mu \mathrm{d}x^\nu \to \mathrm{d}s^{'2} = g_{\mu\nu}\mathrm{d}x^{'\mu}\mathrm{d}x^{'\nu} = \mathrm{d}s^2,$$

that is

$$g_{\mu\nu}\frac{\partial x^{'\mu}}{\partial x^\alpha}\frac{\partial x^{'\nu}}{\partial x^\beta} = \Lambda(x) g_{\alpha\beta}. \tag{3.2}$$

For flat space the scale factor $\Lambda(x) = 1$ corresponds to the Poincaré group consisting of translations and rotations, respectively Lorentz transformations.

Conformal transformations are defined as the set of transformations (3.1) leaving the components of the metric tensor invariant up to a scale

$$g_{\mu\nu} \to g^{'}_{\mu\nu}(x^{'}(x)).$$

Condition (3.2) expresses that the scalar product of basis vectors of the tangent space is conserved only up to a local scale factor (possibly depending on the (point). In particular, angles are preserved by conformal transformations. Equivalently, conformal transformations are such that

$$\mathrm{d}s^2 \to ds^{'2} = \Lambda^{-1}(x) ds^2. \tag{3.3}$$

3.1.2 Two Dimensional Conformal Symmetry

We will be working with an Euclidean metric, such that the line element is $(\mathrm{d}x^1)^2 + (\mathrm{d}x^2)^2$. We introduce complex coordinates

$$z = x^1 + ix^2 \text{ and } \bar{z} = x^1 - ix^2,$$

in which the metric reads $\mathrm{d}s^2 = \mathrm{d}z\mathrm{d}\bar{z}$. Notice it is only in two dimensions that the metric in complex coordinates factorizes into $\mathrm{d}z$ and $\mathrm{d}\bar{z}$. Consequently, any change of coordinates

$$z \to f(z) = z + \alpha(z) \ , \ \bar{z} \to \bar{f}(\bar{z}) = \bar{z} + \bar{\alpha}(\bar{z}),$$

with f and $\bar{f}$ depending only upon z and $\bar{z}$ respectively, will satisfy (3.3), because

$$\mathrm{d}s^2 \to \mathrm{d}s'^2 = \left(\frac{\mathrm{d}f}{\mathrm{d}z}\right)\left(\frac{\mathrm{d}\bar{f}}{\mathrm{d}\bar{z}}\right)\mathrm{d}s^2.$$

Actually, these are the only conformal transformations in two dimensions.

The solutions of the four dimensional Laplace equation

$$\left(\frac{\partial^2}{\partial x^2} + \frac{\partial^2}{\partial y^2} + \frac{\partial^2}{\partial z^2} + \frac{\partial^2}{\partial \omega^2}\right) U = 0,$$

are related to the ordinary hypergeometric function ${}_2F_1(a, b, c; z)$.

The hypergeometric function is intimately associated with the Laplace and wave equations in four dimensional space (along with their extensions into the complex). They arise from the variable separation of these equations and the conformal symmetry groups lead to many of the properties of these functions. In fact, hypergeometric functions can be used to form representations of the two-dimensional conformal group.

The hypergeometric differential equation is given by

$$x(1-x)y'' + [c - (a+b+1)x]y' - aby = 0,$$

where $|x| < 1$, y is a function of x and $c > 0$. This differential equation is solved by functions of the following form

$$y = \frac{\Gamma(c)}{\Gamma(a)\Gamma(b)} \sum_{n=0}^{\infty} \frac{\Gamma(a+n)\Gamma(b+n)}{\Gamma(c+n)} \frac{x^n}{n!}.$$

3.2 The Near Region of the Kerr Black Hole

The full solution spaces of both the scalar and spin-half particles in the Kerr space-time do not have any apparent symmetries, so the first step is to limit the solution space by placing a condition on either the particles or the source of the space-time curvature, which is done when considering the near region.

The near region is defined by the following condition [35]

$$\omega M \ll 1, \tag{3.4}$$

i.e., that the wavelength of the particle excitation is large compared to the radius of curvature. In this case the geometry can be divided into two regions

$$\begin{aligned} r &\ll \frac{1}{\omega}, \implies \text{“NEAR”} , \\ r &\gg M, \implies \text{“FAR”} , \end{aligned} \tag{3.5}$$

which have significant overlap in the matching region

$$M \ll r \ll \frac{1}{\omega}, \implies \text{“MATCHING”} .$$

The wave equations in the near and far regions can be solved in terms of familiar special functions, and a full solution is obtained by matching near and far solutions together along a surface in the matching region.

We note that the region, defined by condition (3.4), is not the same as the often discussed “near-horizon” region of the geometry defined by $r - r_+ \ll M$. Indeed, for sufficiently small ω, the value of r in the near region defined by (3.5) can be arbitrarily large. For a generic non-extreme Kerr black hole, the near-horizon geometry is just Rindler space, while the structure of the near region is more complicated.

We view the far region as an asymptotic region where the scattering experiments are set up. The black hole is thought of as encompassing the whole “near” region. Waves are sent from the far region into the matching region, which is the interface for interactions with the black hole.

The next two sections first reduce the radial (and angular) equations of both the scalar and spin-half particles using the near region condition, then they try to manipulate the reduced equations to see if either of them fit the necessary form for a two-dimensional conformal symmetry.

3.3 Scalar Solution Space

The full solution space of the scalar particle, which is governed by equations (2.37) and (2.38), does not have an apparent two dimensional conformal symmetry. But once the solution space is reduced using the near region condition, i.e., (3.4), the governing equations reduce to forms that have an easily identifiable two dimensional conformal symmetry. This section, which closely follows [35], is broken up into the reduction of the governing equations, the re-expression of these reduced equations in conformal coordinates and then the interpretation of the conformal nature of the reduced scalar solution space.

3.3.1 The Near Region Equations

For the purpose of this section, it would be better to re-express equation (2.38) in the following form

$$\begin{aligned} A_{l,m}R &= \frac{\mathrm{d}}{\mathrm{d}r}\left(\Delta\frac{\mathrm{d}}{\mathrm{d}r}R\right) \\ &+ \left[\frac{(2Mr_+\omega - am)^2}{(r-r_+)(r_+-r_-)} - \frac{(2Mr_-\omega - am)^2}{(r-r_-)(r_+-r_-)} + (r^2+2M(r+2M))\omega^2\right]R, \end{aligned} \tag{3.6}$$

which becomes

$$\frac{\mathrm{d}}{\mathrm{d}r}\left(\Delta\frac{\mathrm{d}}{\mathrm{d}r}R\right) + \left[\frac{(2Mr_+\omega - am)^2}{(r-r_+)(r_+-r_-)} - \frac{(2Mr_-\omega - am)^2}{(r-r_-)(r_+-r_-)}\right]R = A_{l,m}R, \tag{3.7}$$

in the near region limit and equation (2.37) simplifies to

$$\frac{\mathrm{d}}{\mathrm{d}\theta}\left(\sin\theta\frac{\mathrm{d}}{\mathrm{d}\theta}S\right) - \frac{m^2}{\sin^2\theta}S = -A_l S,$$

which is the standard Laplacian for the 2-sphere. The solutions $e^{im\phi}S(\theta)$ are the spherical harmonics, and the separation constants are

$$A_l = l(l+1).$$

Equation (3.7) is solved by hypergeometric functions. As hypergeometric functions transform in representations of $SL(2,R)$, this suggests the existence of a hidden conformal symmetry.

3.3.2 The Conformal Representation

In order to describe the $SL(2,R)_L \times SL(2,R)_R$ symmetry of the near region scalar field equation, it is convenient for to us adapt conformal coordinates $(\omega^{\pm}, y)$, which are defined in terms of (t, r, ϕ) by

$$\begin{aligned} \omega^+ &= \sqrt{\frac{r-r_+}{r-r_-}}e^{2\pi T_R\phi}, \\ \omega^- &= \sqrt{\frac{r-r_+}{r-r_-}}e^{2\pi T_L\phi - \frac{t}{2M}}, \\ y &= \sqrt{\frac{r_+-r_-}{r-r_-}}e^{\pi(T_L\phi+T_R) - \frac{t}{4M}}, \end{aligned}$$

where

$$T_R = \frac{r_+-r_-}{4\pi a} \text{ and } T_R = \frac{r_++r_-}{4\pi a}.$$

Next we define locally the vector fields

$$\begin{aligned} H_1 &= i\partial_+, \\ H_0 &= i(\omega^+\partial_+ + \frac{1}{2}y\partial_y), \\ H_{-1} &= i((\omega^+)^2\partial_+ + \omega^+ y\partial_y - y^2\partial_-), \end{aligned}$$

and

$$\begin{aligned} \bar{H}_1 &= i\partial_-, \\ \bar{H}_0 &= i(\omega^-\partial_- + \frac{1}{2}y\partial_y), \\ \bar{H}_{-1} &= i((\omega^-)^2\partial_- + \omega^- y\partial_y - y^2\partial_+). \end{aligned}$$

These obey the $SL_2(\mathbb{R})$ Lie bracket algebra,

$$[H_0, H_\pm] = \mp iH_\pm \ , \ [H_{-1}, H_1] = -2iH_0,$$

and similarly for $(\bar{H}_0, \bar{H}_{\pm 1})$. The $SL_2(\mathbb{R})$ quadratic Casimir is

$$\begin{aligned} \mathcal{H}^2 = \bar{\mathcal{H}} = &= -H_0^2 + \frac{1}{2}(H_1H_{-1} + H_{-1}H_1). \\ &= \frac{1}{4}(y^2\partial_y^2 - y\partial_y) + y^2\partial_+\partial_-. \end{aligned}$$

In terms of the (t, r, ϕ) coordinates, the vector fields are

$$\begin{aligned} H_1 &= ie^{-2\pi T_R\phi}\left(\Delta^{\frac{1}{2}}\partial_r + \frac{1}{2\pi T_R}\frac{r-M}{\Delta^{\frac{1}{2}}}\partial_\phi + \frac{2T_L}{T_R}\frac{Mr-a^2}{\Delta^{\frac{1}{2}}}\partial_t\right), \\ H_0 &= \frac{i}{2\pi T_R}\partial_\phi + 2iM\frac{T_L}{T_R}\partial_t, \\ H_{-1} &= ie^{2\pi T_R\phi}\left(-\Delta^{\frac{1}{2}}\partial_r + \frac{1}{2\pi T_R}\frac{r-M}{\Delta^{\frac{1}{2}}}\partial_\phi + \frac{2T_L}{T_R}\frac{Mr-a^2}{\Delta^{\frac{1}{2}}}\partial_t\right), \end{aligned} \tag{3.8}$$

and

$$\begin{aligned} \bar{H}_1 &= ie^{-2\pi T_L\phi + \frac{t}{2M}}\left(\Delta^{\frac{1}{2}}\partial_r - \frac{a}{\Delta^{\frac{1}{2}}}\partial_\phi - 2M\frac{r}{\Delta^{\frac{1}{2}}}\partial_t\right), \\ \bar{H}_0 &= -2iM\partial_t, \\ \bar{H}_{-1} &= ie^{2\pi T_L\phi - \frac{t}{2M}}\left(-\Delta^{\frac{1}{2}}\partial_r - \frac{a}{\Delta^{\frac{1}{2}}}\partial_\phi - 2M\frac{r}{\Delta^{\frac{1}{2}}}\partial_t\right), \end{aligned} \tag{3.9}$$

and the Casimir becomes

$$\mathcal{H}^2 = \bar{\mathcal{H}}^2 = \frac{\mathrm{d}}{\mathrm{d}r}\Delta\frac{\mathrm{d}}{\mathrm{d}r} + \frac{(2Mr_+\omega - am)^2}{(r-r_+)(r_+-r_-)} - \frac{(2Mr_-\omega - am)^2}{(r-r_-)(r_+-r_-)}.$$

The near region wave equation (3.7) can be written as

$$\mathcal{H}^2 = \bar{\mathcal{H}}^2 = l(l+1).$$

We see that the scalar Laplacian has reduced to the $SL_2(\mathbb{R})$ Casimir. The $SL_2(\mathbb{R})_L \times SL_2(\mathbb{R})_R$ weights of the field Ψ are

$$(h_L, h_R) = (l, l).$$

3.3.3 The Interpretation

From this result one might think that the solutions of the Kerr scalar wave equation in the near region form $SL_2(\mathbb{R})$ representations. In fact this is not the case, because the vector fields (3.7) and (3.9), which generate the $SL_2(\mathbb{R})$ symmetries are not globally defined. They are not periodic under the angular identification

$$\phi \sim \phi + 2\pi. \tag{3.10}$$

Thus these symmetries can not be used to generate new global solutions from old ones. This can be interpreted as the statement that the $SL_2(\mathbb{R})_L \times SL_2(\mathbb{R})_R$ symmetry is spontaneously broken by the periodic identification of the angular coordinate ϕ. Indeed, under the identification (3.10) the conformal coordinates are identified as

$$\omega^+ \sim e^{4\pi^2 T_R}\omega^+ \ , \ \omega^- \sim e^{4\pi^2 T_L}\omega^- \ , \ y \sim e^{2\pi^2(T_L+T_R)}y.$$

The identification is generated by the $SL_2(\mathbb{R})_L \times SL_2(\mathbb{R})_R$ group element

$$e^{-4i\pi^2 T_R H_0 - 4i\pi^2 T_L \bar{H}_0}.$$

Hence the $SL_2(\mathbb{R})_L \times SL_2(\mathbb{R})_R$ symmetry is broken down to the $U(1)_L \times U(1)_R$ subgroup generated by $(H_0, \bar{H}_0)$.

The relation between conformal and Boyer-Lindquist coordinates is reminiscent of the relation between Minkowski and Rindler coordinates in flat space-time. The periodic identification suggest that the Kerr black hole should be dual to a finite temperature (T_L, T_R) mixed state in dual CFT. This provides an effective way to determine the temperatures in the dual CFT.

3.4 Spin-Half Solution Space

With the governing equations of the spin-half solution space, equations (2.185) and (2.186), derived in chapter 2, it was attempted for this dissertation to follow a similar procedure as that of the scalar solution space in order to see if the spin-half solution space also has a two dimensional conformal symmetry in the near region. The first part of this section shows how the spin-half equations reduce in the near region.

3.4.1 The Near Region Equations

When the differential operators are expanded and $S_{-\frac{1}{2}}$ is relabeled as S, equation (2.186) becomes

$$\frac{1}{\sin\theta}\frac{\mathrm{d}}{\mathrm{d}\theta}\left(\sin\theta\frac{\mathrm{d}}{\mathrm{d}\theta}S\right)+\left[\left(\frac{1}{2}-a\omega\cos\theta\right)^2-\left(\frac{m-\frac{1}{2}\cos\theta}{\sin\theta}\right)^2-\frac{3}{4}-2a\omega m-a^2\omega^2\right]S=-\lambda^2 S,$$

which simplifies to

$$\frac{1}{\sin\theta}\frac{\mathrm{d}}{\mathrm{d}\theta}\left(\sin\theta\frac{\mathrm{d}}{\mathrm{d}\theta}S\right)+\left[-a\omega\cos\theta-\left(\frac{m-\frac{1}{2}\cos\theta}{\sin\theta}\right)^2-\frac{1}{2}-2a\omega m\right]S=-\lambda^2 S, \quad (3.11)$$

in the near region.

When the differential operators are expanded and $R_{-\frac{1}{2}}$ is relabeled as R, equation (2.185) becomes

$$\Delta\frac{\mathrm{d}^2}{\mathrm{d}r^2}R+(-iK+(r-M))\frac{\mathrm{d}}{\mathrm{d}r}R+\frac{1}{\Delta}(K^2+i(K'\Delta-K\Delta')+i(r-M)K)R=\lambda^2 R. \quad (3.12)$$

In order to determine if the spin-half field equation has a two-dimensional conformal symmetry, it would be useful to re-express equation (3.12) in a similar form to the scalar field equation. This can be done by changing the dependence of R on r, i.e.,

$$R\to pR,$$

where

$$\ln p=\frac{1}{2}\ln\Delta-\frac{1}{2}\int\frac{-iK+(r-M)}{\Delta}\mathrm{d}r,$$

which yields a new spin-half radial equation given by

$$\frac{\mathrm{d}}{\mathrm{d}r}\left(\Delta\frac{\mathrm{d}}{\mathrm{d}r}R\right)+\frac{1}{4}\frac{1}{\Delta}((5K-i(r-M))(K-i(r-M))+2\Delta(1+6i\omega r))R=\lambda^2 R. \quad (3.13)$$

Rewriting equation (3.13) in two parts, one of which has a hypergeometric form

$$\frac{\mathrm{d}}{\mathrm{d}r}\left(\Delta\frac{\mathrm{d}}{\mathrm{d}r}R\right)+(\frac{1}{\Delta}4M\omega(2M^2\omega-am)r-\frac{1}{\Delta}a^2(4M^2\omega^2-m^2))R,$$

and the other part comprises of the "additional" terms:

$$\frac{1}{4}\frac{1}{\Delta}((5\omega^2)r^4+(6i\omega)r^3+(1+10am\omega-18iM\omega+10a^2\omega^2)r^2$$

$$+(-6iam-2M+6ia^2\omega+16amM\omega-32M^3\omega^2)r$$

$$+(2a^2+a^2m^2+6iamM-M^2+10a^3m\omega+6ia^2M\omega+5a^4\omega^2+16a^2M^2\omega^2))R,$$

which simplifies to

$$\frac{1}{4}\frac{1}{\Delta}(r^2 + (-6iam - 2M)r + (2a^2 + a^2m^2 + 6iamM - M^2))R, \tag{3.14}$$

in the near region.

3.4.2 Discussion

Since the terms in (3.14) are not negligible in the near region, the radial equation of the spin-half solution space does not have the necessary hypergeometric form, which is the condition for two dimensional conformal symmetry, at least as presented by [35]. This does not necessarily mean that the near region spin-half solution space has no (hidden) two dimensional conformal symmetry, just that it cannot be identified in the same way as it was in the near region scalar solution space.

Chapter 4

Quasinormal Mode Theory

We are familiar with the fact that the ringing of a bell or the strum of a guitar invariably produces a "characteristic sound". Such systems respond to any excitation by selecting a set of natural real frequencies, the normal frequencies, and their response is given as a superposition of stationary modes, the normal modes. Black holes have a characteristic sound as well. As a simple demonstration we may let a Gaussian gravitational wave-packet evolve on the Schwarzschild geometry. The results, at the linearized level, are shown in figures 4.1 [19].

A striking feature, first uncovered by Vishveshwara [36] and clearly apparent in figures 4.1, is that the signal is dominated, during a certain time, by damped single frequency oscillations. The frequency and damping of these oscillations depend only on the parameters characterizing the black hole, which in the Schwarzschild case is its mass. They are completely independent of the particular initial configuration that cause the excitation of such vibrations. That such characteristic oscillations always appear and dominate the signal at intermediate times, in any event involving black holes, has been tested time and time again. It has been verified at the linearized level [36], in which the fields are treated as a perturbation in the single black hole space-time, but also for example, on fully numerical simulations of black hole-black hole collision processes [37], or stellar collapse [38]. They are therefore characteristic of black holes. These characteristic oscillations have been termed "quasinormal modes" and the associated frequencies "quasinormal frequencies" [39]. The "normal" part derives from the obvious similarity between these and normal mode systems. There are, however, important differences between these two systems, which justifies the "quasi": first, QNMs are not stationary modes, since they are exponentially damped. This is merely reflecting the fact that the black hole space-time is radiating energy away to infinity, through the form of gravitational waves (or any massless field). When describing a resonant system, such as a bell, a guitar or a star, one often makes the convenient and sometimes accurate assumption that there is no damping. This then leads to a complete normal mode expansion of the field. The stationary mode expansion is just reflecting the no energy loss assumption. As soon as one turns to the more realistic situation, by allowing a dissipation mechanism, one expects no such naive stationary normal mode expansion to exist. Black hole oscillations occupy a very special place here. It is impossible, even in principle, even in

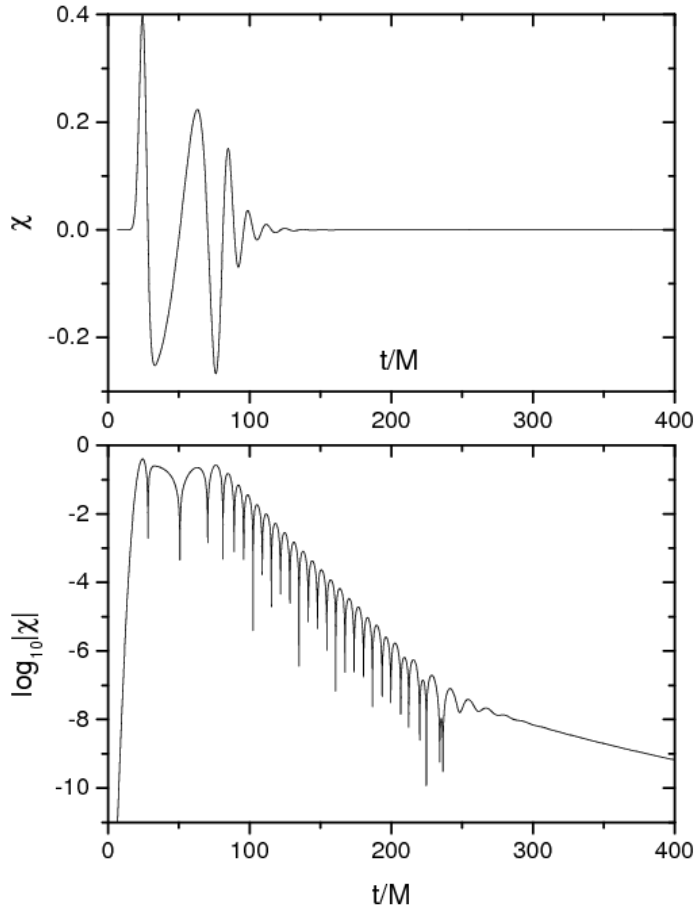

Figure 4.1: *The top figure shows the evolution of a gravitational Gaussian wave-packet in the neighbourhood of a Schwarzschild black hole and the bottom figure shows a log plot of the same wave-packet.*

the most idealized scenario, to turn off the dissipation mechanism. In fact, black holes are made from the fabric of space-time, and any space-time oscillation implies the generation of gravitational waves, carrying energy away to infinity. Indeed the very equations describing black hole oscillations are nothing more than a description of gravitational waves. QNMs were first discussed in the black hole context, but from the above discussion one anticipates they will also appear in other dissipative physical systems, such as a vibrating string coupled to a surrounding medium (and therefore transmitting energy to infinity through it), laser cavities or a star when one does not neglect gravitational radiation. Another important difference between normal and QNMs is the completeness issue, which is a rather subtle one, mathematically. The response of a normal mode system can be given for all times as a superposition of normal modes.However, QNMs seem to appear only over a limited time interval; this is also shown in figures 4.1, where it is seen that at very late times quasinormal ringing gives way to a power-law fall-off. A thorough account of QNMs in asymptotically flat space-times, their properties, a thorough comparison between normal and QNM systems, and a discussion about the incompleteness of QNMs can be found in the classical reviews by Kokkotas and Schmidt [19] and Nollert [40], and references therein.

4.1 Definition

Most of the problems concerning wave propagation in black hole space-times can be reduced to a second order partial differential equation of the form

$$\frac{\partial^2}{\partial x^2}\Psi - \frac{\partial^2}{\partial t^2}\Psi - V\Psi = 0. \tag{4.1}$$

Here x is a spatial variable, usually but not always ranging (in special coordinate system) from $-\infty$ to $+\infty$. When dealing with black hole space-times the horizon is usually at $-\infty$, and for the rest of this discussion we shall assume so. Also, V is an x-dependent potential. To define in a phenomenological way what a QNM is, we shall proceed in the usual way by assuming a time dependence

$$\Psi(t, x) = e^{-i\omega t}\phi(x). \tag{4.2}$$

Inserting this into (4.1) we get an ordinary differential equation in the spatial variable x,

$$\frac{\mathrm{d}^2}{\mathrm{d}x^2}\phi + (\omega^2 - V)\phi = 0. \tag{4.3}$$

The form (4.2) is not restrictive, because equation (4.1) is linear, so once we have a solution for (4.3), a general time dependent solution can be given as a continuous Fourier transform of such solutions. The form (4.3) is ideal to study QNMs in a way that parallels a normal mode analysis. We shall now restrict ourselves to asymptotically flat space-times so that the potential V is positive and satisfies

$$\begin{gathered} V \to 0, x \to -\infty, \\ V \to 0, x \to +\infty. \end{gathered} \tag{4.4}$$

Therefore, such potentials do not allow bound states, and this makes it impossible to do a normal mode expansion. The idea that the evolution of Ψ will generally involve a superposition of these QNMs can be shown to be correct by use of Laplace transforms. We refer the reader to [19]. Nevertheless, we saw that the signal is somehow dominated by characteristic oscillations (Figures 4.1), so we shall blindly continue with our analysis. Having in mind the form (4.4) of the potential, we have that near the boundaries $-\infty$ and $+\infty$ the solution behaves as plane waves,

$$\phi \sim e^{\pm i\omega x}, x \to \pm\infty.$$

The boundary conditions defining QNMs are that toward the boundaries the solutions should be purely outgoing at infinity and ingoing at the horizon ($x = -\infty$),

$$\begin{aligned} \phi &\sim e^{-i\omega x}, x \to -\infty, \\ \phi &\sim e^{+i\omega x}, x \to +\infty. \end{aligned} \tag{4.5}$$

Here ingoing at the horizon means entering into the black hole, therefore leaving the domain we are studying. These are physically motivated boundary conditions. Only a discrete set of complex frequencies satisfy these boundary conditions, i.e., the QNM frequencies and the associated wave-functions ϕ, which are the solutions of (4.3) are the QNMs. It has been proved by Vishveshwara [8] that for the Schwarzschild geometry the QNM frequencies must have a negative imaginary part; this has also been found true for other geometries like the Kerr space-time. This means on the one hand that QNMs decay exponentially in time, and the physical significance of this is that the black hole space-time is loosing energy in the form of gravitational waves. On the other hand, this also means that the space-time is stable. In addition, the imaginary part being negative makes the numerical calculation of the QNM frequencies a non-trivial task: according to the boundary conditions (4.5), and to the fact that the QNM frequencies have a negative imaginary part, one has that QNMs grow exponentially at the boundaries. Now, in order to tell if a certain frequency is or not a QNM frequency one must check that, for example, there is only an outgoing $e^{i\omega x}$ piece at infinity, or in other words, one must check that near infinity the $e^{-i\omega x}$ piece is absent. However, this last term is exponentially suppressed in relation to the other, so one must be able to distinguish numerically an exponentially small term from an exponentially large one. This has always been, and still is, a major obstacle when it comes down to an actual computation of QNM frequencies. Still brute numerical force sometimes works. Chandrasekhar and Detweiler [9] have succeeded in finding some of the Schwarzschild QNM frequencies this way, in 1975. Since then, numerous techniques have been developed. Some of them are analytical tools like the WKB(J) technique of Schultz and Will [41], later refined to third order [42], and recently extended to sixth order [14], or the "potential fit" [10] one, in which one tries to fit the Schwarzschild potential to one which enables us to find an exact result. However, the most successful attempt has been developed by Leaver [12], using a continued fraction form of the equations, which is rather easily implemented numerically. With the exception of the WKB method, which will be discussed in greater detail in a later section of this dissertation, a complete account of all these techniques, and many others are given

in [19, 40]. While there are a few exceptions, there are no analytical solutions that exactly satisfy the boundary conditions (4.5), so one has to resort to any numerical or approximate method to find them.

4.2 Semi-analytic Techniques

In this dissertation we shall make use of two semi-analytical techniques to calculate QNM frequencies, specifically:

4.2.1 WKB(J) Method

This method is named after physicists Wentzel, Kramers and Brillouin, who developed it in 1926 [43]. In 1923, mathematician Harold Jeffreys had developed a general method of approximating solutions to linear, second-order differential equations, which includes the Schrödinger equation. But even though the Schrödinger equation was developed two years later, Wentzel, Kramers and Brillouin were apparently unaware of this earlier work, so Jeffreys is often not given credit.

Before we describe the exact situations where we can use the WKB(J) method, let's first consider the example

$$\epsilon^2 \frac{\mathrm{d}^2 y}{\mathrm{d}x^2} + y = 0,$$

with the condition that

$$0 < \epsilon \ll 1. \tag{4.6}$$

Note that there are two solutions to this differential equation

$$y(x, \epsilon) \sim e^{\pm \frac{ix}{\epsilon}},$$

since

$$\frac{\mathrm{d}y}{\mathrm{d}x} \sim \pm \frac{i}{\epsilon} e^{\pm \frac{ix}{\epsilon}},$$

and

$$\frac{\mathrm{d}^2 y}{\mathrm{d}x^2} \sim -\frac{1}{\epsilon^2} e^{\pm \frac{ix}{\epsilon}}.$$

It is important to notice that this solution oscillates rapidly on a scale of $O(\epsilon^1)$. These are the types of problems that are ideal for the WKB(J) method because we want to be able to assume that the solution is in a specific form. We will discuss this idea further when the ansatz is discussed later on. In general, we can use the WKB method to solve problems of the following form

$$\epsilon^2 \frac{\mathrm{d}^2 y}{\mathrm{d}x^2} + Q(x) y = 0, \tag{4.7}$$

with the condition (4.6) being true, and where $Q(x)$ is a smooth and positive on the $O(\epsilon^0)$ scale.

Again, we can use the WKB method here because the solution(s) will have rapid oscillations on a scale $O(\epsilon^1)$ with an amplitude and phase, which both vary on a scale $O(\epsilon^0)$, i.e., they both vary slowly. We can only use the WKB method in these situations because it requires an ansatz, in which we assume that solutions have this specific form.

We will now solve the general differential equation (4.7) with condition (4.6) using the WKB(J) method. As discussed previously, we will assume that the solution to this differential equation is in the following form (our ansatz)

$$y(x,\epsilon) = A(x,\epsilon)e^{\frac{iu(x)}{\epsilon}},$$

then

$$\frac{\mathrm{d}y}{\mathrm{d}x} = \left(A' + A\frac{iu'}{\epsilon}\right)e^{\frac{iu(x)}{\epsilon}},$$

and

$$\frac{\mathrm{d}^2y}{\mathrm{d}x^2} = \left(-\frac{(u')^2}{\epsilon^2} + \frac{i}{\epsilon}(Au'' + 2A'u') + A''\right)e^{\frac{iu(x)}{\epsilon}}.$$

So our differential equation becomes

$$(-(u')^2A + i\epsilon(Au'' + 2A'u') + \epsilon^2A'')e^{\frac{iu}{\epsilon}} + Q(x)e^{\frac{iu(x)}{\epsilon}} = 0.$$

Now we let

$$\begin{aligned} A(x,\epsilon) &= A_0(x) + \epsilon A_1(x) + ..., \\ A'(x,\epsilon) &= A_0'(x) + \epsilon A_1'(x) + ..., \\ A''(x,\epsilon) &= A_0''(x) + \epsilon A_1''(x) + ... \end{aligned}$$

Then we collect like terms in order to find $A(x,\epsilon)$ and $u(x)$. First we find the terms of order $O(\epsilon^0)$

$$\begin{aligned} -(u')^2e^{\frac{iu}{\epsilon}} + Q(x)e^{\frac{iu}{\epsilon}} &= 0, \\ \implies Q(x) &= (u')^2, \\ \implies u(x) &= \pm\int_{x_0}^{x}\sqrt{Q(s)}ds. \end{aligned}$$

Then we find the terms of order $O(\epsilon)$

$$\begin{aligned} (i\epsilon A_0u'' + 2i\epsilon A_0')e^{\frac{iu}{\epsilon}} &= 0, \\ \implies A_0u'' + 2A_0'u' &= 0, \\ \implies \frac{A_0}{2\sqrt{Q(x)}} + 2A_0'\sqrt{Q(x)} &= 0. \end{aligned}$$

If we solve this, we find that

$$A_0 = C(Q(x))^{-\frac{1}{4}}.$$

Thus we have a one-term (first order) approximation to the solution of (4.7)

$$y(x,\epsilon) \sim (Q(x))^{-\frac{1}{4}} e^{\pm\frac{i}{\epsilon}\int_{x_0}^{x}\sqrt{Q(s)}ds}.$$

It is known that the black hole perturbations can be reduced to a second-order ordinary differential equation of the form [24]

$$\frac{\mathrm{d}^2}{\mathrm{d}x^2}\psi(x) + Q(x,\omega)\psi(x) = 0, \tag{4.8}$$

which is valid for the three types of black holes: Schwarzschild, Reissner-Nordström and Kerr. The function $Q(x,\omega)$, for the first two types of black hole, has the form $\omega^2 - V(x)$ where ω is the complex frequency of the oscillation and $V(x)$ is the real potential. The potential $V(x)$ is a positive function of x, the spin weight of the the field s and the angular harmonic index l, but it is independent of ω. For the Kerr black hole, the function $Q(x,\omega)$ is more complicated and there is no clear separation between ω and $V(x)$ for electromagnetic ($s = \pm 1$) and gravitational ($s = \pm 2$) perturbations. For this reason Seidel and Iyer [13] have transformed the standard equation and expanded $Q(x,\omega)$ in powers of $a\omega$ to avoid working, in principle, on the complex plane. What follows avoids using the transformation or expansion and deals with the standard equation. Similar results are achieved with a simpler method.

The boundary condition for the QNMs of a perturbed black hole is that the waves are ingoing at the horizon and outgoing at infinity. With this condition it is possible to solve the eigenvalue problem (4.8) either numerically or semi-analytically and to determine the complex QNM frequencies. From the known methods like [12], only the one introduced by Leaver can determine the frequencies of both the weakly and the strongly damped modes of a black hole, the semi-analytical method like [42], proved to give very good results for the QNM frequencies, though only for small damping. The attempt [44] to improve this method for normal modes with larger imaginary parts was not that successful, since it determines only the imaginary parts of the frequencies with a satisfactory accuracy, but it does not show the same success for the determination of the real part of the frequency.

Equation (4.8), which describes the perturbations of a black hole, is a second-order ordinary differential equation, which is equivalent to the one-dimensional Schrödinger equation for a particle encountering a potential barrier. Thus techniques used extensively in quantum mechanics can be used for studying equation (4.8). The Bohr-Sommerfield (BS) rule (or connection formulae) seems to be especially useful. Using this rule, it is possible to reproduce not only the Schutz-Will formula, but also to give a way to extend the accuracy of that formula, by taking higher order terms [14]. The BS formula has already been proven to give in quantum mechanics, not only accurate but in some cases exact results. The method improves the accuracy as the eigenvalue of the problem, i.e., the energy, increases [45]. The corresponding eigenvalue for the black hole case is the frequency of the oscillation.

The classical form of the BS rule for equations of the type (4.8) is

$$\int_{x_A}^{x_B} (Q(x))^{\frac{1}{2}} dx = \left(n + \frac{1}{2}\right)\pi, \tag{4.9}$$

where x_A, x_B are the two roots of $Q(x) = 0$ or else the two turning points. A more general form can be found in [45], which is valid for complex potentials and in this form it is possible to extend it to the complex z-plane

$$\oint_C \sum_{k=0}^{\infty} S'_{2k}(z)dz \approx 2i\left(n+\frac{1}{2}\right)\pi, \tag{4.10}$$

where the contour C encircles the two turning points, which are connected by a branch cut on the the real z-axis. The even order terms of the WKB(J) expansion have the following form [45]

$$\begin{aligned} S_0(x) &= \pm\int^x (Q(t))^{\frac{1}{2}}\mathrm{d}t, \\ S_2(x) &= \pm\int^x \left[\frac{Q''(t)}{8(Q(t))^{\frac{3}{2}}(t)} - \frac{5(Q'(t))^2}{8(Q(t))^{\frac{3}{2}}(t)}\right]dt.... \end{aligned}$$

Although all the terms for $k > 0$ are infinite at the two turning points, the integral (4.10) is finite because the contour encircles the turning points without passing through them. The advantage of relation (4.10) is its generalization of relation (4.9) on the complex plane and its ability to handle the Bardeen-Press [46] potential for the Schwarzschild black hole perturbation as well as the complex Teukolsky [24] potential for the Kerr black hole.

Next the BS rule will be used in the case where the complex frequency has a small imaginary part. In this case the two turning points are close to the peak of the potential and not very far apart. Thus it is possible to take a Taylor expansion of the potential close to its peaks x_0 (i.e., $Q(x)$ approximated by a parabola)

$$Q(x) = Q_0 + \frac{1}{2}Q''_0(x-x_0)^2 + O((x-x_0))^3, \tag{4.11}$$

where $Q_0 = Q(x_0) < 0$ and $Q''_0 = \frac{\mathrm{d}^2Q}{\mathrm{d}x^2}|_{x=x_0} > 0$. Then by substituting (4.11) into (4.10), the problem is reduced in the solution of the integral equation

$$\int_{x_A}^{x_B}\left[Q_0 + \frac{1}{2}Q''_0(x-x_0)^2\right]^{\frac{1}{2}}\mathrm{d}x = \left(n+\frac{1}{2}\right)\pi, \tag{4.12}$$

where $x_{A,B} = x_0 \mp \left[-2\frac{Q_0}{Q''_0}\right]^{\frac{1}{2}}$. A straight integration of (4.12) gives

$$Q_0 = \pm i[2Q''_0]^{\frac{1}{2}}\left(n+\frac{1}{2}\right),$$

which is exactly the Schutz-Will formula [41].

Once the black hole radial perturbation equation is written in the following form

$$\frac{\mathrm{d}^2}{\mathrm{d}x^2}\psi + Q\psi = 0, \tag{4.13}$$

where $Q = \omega^2 - V$, with x being the tortoise coordinate and V being the black hole potential; the WKB(J) formula for calculating the QNM frequencies can be used. The WKB(J) formula, up to sixth order, is

$$i \times \frac{Q_0}{(-2Q_0'')^{\frac{1}{2}}} - \sum_{j=2}^{6} \Lambda_j = \alpha,$$

where the Λ_j ' s are the second through sixth order corrections to the WKB(J) approximation, with the second and third corrections are given by

$$\Lambda_2 = \frac{i}{(-2Q_0'')^{\frac{1}{2}}} \left[\frac{1}{8} \left(\frac{Q_0^{(4)}}{Q_0''} \right) \left(\frac{1}{4} + \alpha^2 \right) - \frac{1}{288} \left(\frac{Q_0'''}{Q_0''} \right) \left(7 + 60\alpha^2 \right) \right],$$

$$\begin{aligned} \frac{-2Q_0''}{\alpha} \times \Lambda_3 &= \frac{5}{6912} \left(\frac{Q_0'''}{Q_0''} \right)^4 \left(77 + 188\alpha^2 \right) - \frac{1}{384} \left(\frac{(Q_0'')^2 Q_0^4}{Q_0''} \right) \left(51 + 100\alpha^2 \right) \\ &\quad + \frac{1}{2304} \left(\frac{Q_0^4}{Q_0''} \right)^2 \left(67 + 68\alpha^2 \right) + \frac{1}{288} \left(\frac{(Q_0''')(Q_0)^5}{Q_0''} \right) \left(19 + 28\alpha^2 \right) \\ &\quad - \frac{1}{288} \left(\frac{Q_0^6}{Q_0''} \right)^2 \left(5 + 4\alpha^2 \right). \end{aligned}$$

Here

$$\alpha = n + \frac{1}{2},$$

where $n = 0, 1, 2, ...$ is the mode number of the QNM frequency and

$$Q_0^{(n)} = \frac{\mathrm{d}^{(n)}}{dx^{(n)}} Q|_{x=x_{max}},$$

with x_{max} being the point were the black hole potential is at its maximum.

The fourth through sixth order corrections to the WKB(J) method are given in appendix B.

4.2.2 Asymptotic Iteration Method

The second semi-analytical technique approach we shall use is the AIM. This technique for solving differential equations numerically was presented by Cifti *et al.* in 2003 [15] and it is described below.

Consider the homogeneous linear, second-order differential equation for the function $y(x)$,

$$y'' = \lambda_0(x) y' + s_0(x) y, \tag{4.14}$$

where $\lambda_0(x)$ and $s_0(x)$ are functions in $C_\infty(a, b)$. In order to find a general solution to this equation, we rely on the symmetric structure of the right-hand of (4.14) [15]. Indeed, if we differentiate (4.14) with respect to x, we find that

$$y''' = \lambda_1(x) y' + s_1(x) y,$$

where

$$\lambda_1 = \lambda_0' + s_0 + (\lambda_0)^2 \text{ and } s_1 = s_0' + s_0\lambda_0.$$

If we write the second derivative of equation (4.14), we get

$$y'''' = \lambda_2(x)y' + s_2(x)y,$$

where

$$\lambda_2 = \lambda_1' + s_1 + \lambda_0\lambda_1 \text{ and } s_1 = s_0' + s_0\lambda_0.$$

Thus, for the $(n+1)^{th}$ and the $(n+2)^{th}$ derivatives, $n = 1, 2, ...$, we have

$$y^{(n+1)} = \lambda_{n-1}(x)y' + s_{n-1}(x)y, \tag{4.15}$$

and

$$y^{(n+2)} = \lambda_n(x)y' + s_n(x)y,$$

respectively, where

$$\lambda_n = \lambda_{n-1}' + s_{n-1} + \lambda_0\lambda_{n-1} \text{ and } s_{n-1} = s_0' + s_0\lambda_{n-1}. \tag{4.16}$$

From the ratio of the $(n+1)^{th}$ and the $(n+2)^{th}$ derivatives, we have

$$\frac{\mathrm{d}}{\mathrm{d}x}\ln\left(y^{(n+1)}\right) = \frac{y^{(n+2)}}{y^{(n+1)}} = \frac{\lambda_n(y' + \frac{s_n}{\lambda_n})}{\lambda_{n-1}(y' + \frac{s_{n-1}}{\lambda_{n-1}})}. \tag{4.17}$$

We now introduce the 'asymptotic' aspect of the method. If we have, for sufficiently large n,

$$\frac{s_n}{\lambda_n} = \frac{s_{n-1}}{\lambda_{n-1}} = \alpha,$$

then (4.17) reduces to

$$\frac{\mathrm{d}}{\mathrm{d}x}\ln\left(y^{(n+1)}\right) = \frac{\lambda_n}{\lambda_{n-1}},$$

which yields

$$y^{(n+1)}(x) = C_1 e^{\left(\int^x \frac{\lambda_n(t)}{\lambda_{n-1}(t)}dt\right)} = C_1\lambda_{n-1}e^{\left(\int^x \alpha + \lambda_0 dt\right)}, \tag{4.18}$$

where C_1 is the integration constant and the right-hand side equation from (4.16) and the definition of α. Substituting (4.18) into (4.15), we obtain the first-order differential equation

$$y' + \alpha = C_1\lambda_{n-1}e^{\left(\int^x \alpha + \lambda_0 \mathrm{d}t\right)},$$

which, in turn, yields the general solution to (4.14) as

$$y(x) = e^{\left(-\int^x \alpha \mathrm{d}t\right)}\left[C_2 + C_1\int^x e^{\left(\int^t (\lambda_0(\tau) + 2\alpha(\tau))\mathrm{d}\tau\right)}\mathrm{d}t\right].$$

The QNM frequencies are obtained from the quantization condition [16], by setting $\delta_n = 0$, where δ_n is given by

$$\delta_n = s_n\lambda_{n-1} - s_{n-1}\lambda_n, \tag{4.19}$$

which is equivalent to imposing a termination to the number of iterations.

Improved Asymptotic Iteration Method

Cho *et al.* [16] have presented an improved version of the AIM which circumvents the unpleasant feature of the recursion relations in equations (4.16), that at each iteration one must take the derivatives of λ_n and s_n. This is where we will slow down the numerical operation and produce problems with regards to precision. Thus, we shall use their method, that is we expand λ_n and s_n as Taylor series around the point y_0, where the AIM is implemented

$$\lambda_k(y) = \sum_{j=0}^{\infty} c_k^j (y - y_0)^j,$$

and

$$s_k(y) = \sum_{j=0}^{\infty} d_k^j (y - y_0)^j,$$

where c_k^j and d_k^j are the jth Taylor coefficients of $\lambda_k(y)$ and $s_k(y)$ respectively. Substituting these expressions into equations (4.16) leads to

$$c_k^j = (j+1)c_{k-1}^{j+1} + d_{k-1}^j + \sum_{p=0}^{j} c_0^j c_{k-1}^{j-p},$$

and

$$d_k^j = (j+1)d_{k-1}^{j+1} + \sum_{p=0}^{j} d_0^j c_{k-1}^{j-p}.$$

In terms of these coefficients, the termination condition (4.19) can be written as

$$d_k^0 c_{k-1}^0 - d_{k-1}^0 c_k^0 = 0,$$

and thus we have reduced the AIM into a set of recursion relations which no longer require derivative operations.

The Boundary Conditions in the Asymptotic Iteration Method

Note that while the form of the equation used for the WKB(J) method to calculate QNM frequencies, already incorporates the boundary conditions necessary for QNMs, it is required to directly include them when using the AIM.

According to Leaver [12] and Jing *et al.* [47], the Kerr boundary conditions for QNMs can be incorporated into the radial equation, by re-expressing the radial function in the following form

$$\psi(r) = \left(1 - \frac{r_-}{r}\right)^{-s-i\sigma_-} \left(1 - \frac{r_+}{r}\right)^{s-i\sigma_+} \left(\frac{r_+}{r}\right)^{-ir_+\omega} e^{i\omega r}\chi(r), \tag{4.20}$$

where

$$\sigma_\pm = \frac{1}{r_+ - r_-}[(r_\pm^2 + a^2)\omega + am],$$

and s is either 0 or $\frac{1}{2}$ for scalar or spin-half perturbations, respectively.

Armed with this information, we can now proceed to calculate the QNM frequencies for the AIM, and the WKB method presented earlier, in the next chapter.

Chapter 5

Quasinormal Mode Frequencies

Chapter 4, which discussed the theory of QNMs, showed that the radial (perturbation) equation of the particle of interest was what was necessary for QNM frequency calculations. The radial (perturbation) equations for both the scalar and spin-half particles were derived in chapter 2, however, they were not in the correct form, so first they needed to be manipulated accordingly.

Once the radial equation was manipulated into the correct QNM forms, Mathematica 8 was used to determine the QNM frequencies. In the case of the black hole with no angular momentum ($a = 0.00$), i.e., the Schwarzschild limit, the NSolve function was used to calculate the QNM frequencies in both the WKB(J) method and the AIM. For the cases with angular momentum ($0.00 < a < 1.00$), the FindRoot function was used, with the Schwarzschild limit value used as the initial "guess". Fifteen iterations were used for the AIM.

5.1 Scalar Perturbations

5.1.1 Equation Manipulation

The WKB(J) Method

Th scalar radial equation (2.38), is slightly altered to give

$$\frac{\mathrm{d}}{\mathrm{d}r}\left(\Delta\frac{\mathrm{d}}{\mathrm{d}r}R\right) - V\cdot R = 0, \tag{5.1}$$

where

$$V = -\frac{1}{\Delta}((K - 2(r^2 + a^2))^2 - \Delta\lambda),$$

with $\lambda = A_{l,m} + a^2\omega^2 - 2am\omega$.

Before the QNM frequencies can be calculated, equation (5.1) needs to be changed into the standard form. One of the ways this is accomplished is by first choosing the radial field, R to have the following form

$$R(r) = (r^2 + a^2)^{-\frac{1}{2}}\psi(r),$$

and then changing to the Tortoise coordinate x, which is related to the original coordinate r by

$$\frac{\mathrm{d}r}{\mathrm{d}x} = \frac{\Delta}{r^2 + a^2}, \tag{5.2}$$

which changes equation (5.1) to

$$\frac{\mathrm{d}^2}{\mathrm{d}x^2}\psi + (\omega^2 - V)\psi = 0. \tag{5.3}$$

The 'new' potential is

$$V = \frac{2am(r^2 + a^2)\omega - a^2m^2 + \Delta\lambda}{(r^2 + a^2)^2} + G^2 + \frac{\mathrm{d}}{\mathrm{d}x}G,$$

with

$$G = \frac{r\Delta}{(r^2 + a^2)^2}.$$

Equation (5.3) is in the standard form for QNM frequency determination, which is also the correct form for using the WKB(J) method to calculate them.

The Asymptotic Iteration Method

Because the AIM works better on a compact domain, we define a new variable $y = 1 - \frac{r_+}{r}$, which ranges from 0 at the event horizon ($r = r_+$) to 1 at spatial infinity. Then it is necessary to incorporate the boundary conditions, which expressed in the new compact domain is

$$\psi(y) = \left(1 - \frac{r_-}{r_+}(1 - y)\right)^{-i\sigma_-} y^{-\sigma_+}(1 - y)^{-r_+\omega} e^{i\omega\frac{r_+}{1-y}}\chi(y).$$

By making the change of coordinate and the change of function, equation (5.3) takes the form

$$\chi(y) = \lambda_0(y) + s_0(y), \tag{5.4}$$

where

$$\lambda_0 = -2\frac{1}{g}\frac{\mathrm{d}g}{\mathrm{d}y} - \frac{1}{f}\frac{\mathrm{d}f}{\mathrm{d}y},$$

and

$$s_0 = -\frac{1}{g}\frac{\mathrm{d}^2g}{\mathrm{d}y^2} - \frac{1}{f}\frac{\mathrm{d}f}{\mathrm{d}y} \times \frac{1}{g}\frac{\mathrm{d}g}{\mathrm{d}y} - \frac{1}{f^2}\left(\omega^2 - V|_{r=r_+(1-y)^{-1}}\right),$$

with

$$f = \left(\frac{\Delta}{r^2 + a^2}\frac{\mathrm{d}y}{\mathrm{d}r}\right)|_{r=r_+(1-y)^{-1}},$$

and

$$g = (1 - y)^{-2i\omega}\left(1 - \frac{r_-}{r_+}(1 - y)\right)^{i\sigma_-} y^{-i\sigma_+} e^{i\omega r_+(1-y)^{-1}}.$$

Equation (5.4) is now in the correct form to use the AIM for QNM frequency calculations.

5.1.2 Results and Discussion

As presented in tables 5.1 and 5.2 are the QNM frequencies for the scalar perturbations of the Kerr black hole with the two "extreme" (minimum and maximum for this dissertation) values of the angular momentum per unit mass, i.e., $a = 0.00$ and $a = 0.80$. m was set to 0, while the angular number l was given values of 0, 1, 2 and 3 and the mode number n was varied from 0 to $l - 1$.

Table 5.1: *The Quasinormal Mode Frequencies for the Scalar Perturbations of the Kerr Black Hole, when* $a = 0.00$.

l	n	Numerical	Third Order WKB(J)	Sixth Order WKB(J)	AIM
0	0	0.1105 - 0.1049i	0.1046 - 0.1152i	0.1105 - 0.1008i	0.1103 - 0.1046i
			(5.34% , 9.82%)	(<0.01% , 3.91%)	(0.18% , 0.29%)
1	0	0.2929 - 0.0977i	0.2911 - 0.0989i	0.2929 - 0.0978i	0.2929 - 0.0977i
			(0.61% , 1.23%)	(<0.01% , 0.10%)	(<0.01% , <0.01%)
	1	0.2645 - 0.3063i	0.2622 - 0.3074i	0.2645 - 0.3065i	0.2645 - 0.3063i
			(0.87% , 0.36%)	(<0.01% , 0.07%)	(<0.01% , <0.01%)
2	0	0.4836 - 0.0968i	0.4832 - 0.0968i	0.4836 - 0.0968i	0.4836 - 0.0968i
			(0.08% , <0.01%)	(<0.01% , <0.01%)	(<0.01% , <0.01%)
	1	0.4639 - 0.2956i	0.4632 - 0.2958i	0.4638 - 0.2956i	0.4639 - 0.2956i
			(0.15% , 0.07%)	(0.02% , <0.01%)	(<0.01% , <0.01%)
	2	0.4305 - 0.5086i	0.4317 - 0.5034i	0.4304 - 0.5087i	0.4306 - 0.5086i
			(0.28% , 1.02%)	(0.02% , 0.02%)	(0.02% , <0.01%)
3	0		0.6752 - 0.0965i	0.6754 - 0.0965i	0.6754 - 0.0965i
					(<0.01% , <0.01%)
	1		0.6604 - 0.2923i	0.6607 - 0.2923i	0.6607 - 0.2923i
					(<0.01% , <0.01%)
	2		0.6348 - 0.4941i	0.6336 - 0.4960i	0.6336 - 0.4960i
					(<0.01% , <0.01%)
	3		0.6022 - 0.7011i	0.5984 - 0.7114i	0.5989 - 0.7113i
					(0.08% , 0.01%)

Included in table 5.1 are the numerically determined QNM frequencies for $l = 0$ to $l = 2$ published by Leaver [12]. Even though the WKB(J) method has been used to calculate the Schwarzschild limit QNM frequencies before, up to sixth order, and the values published by Seidel *et al.* [13] and by Konoplya [14], the calculations were redone for this work. The percentages bracketed under each QNM frequency for $l = 0$ to $l = 2$, are the percentage differences between the calculated value and the numerical value published by Leaver, while for $l = 3$ the percentages compare the AIM to sixth order WKB(J) values.

In table 5.2, all three values were calculated for this work, even though published values are available for the third order WKB(J), at least graphically. Since the WKB(J) is a generally accepted semi-analytical technique for QNM frequency calculations, the percentages

Table 5.2: *The Quasinormal Mode Frequencies for the Scalar Perturbations of the Kerr Black Hole, when* $a = 0.80$.

l	n	Third Order WKB(J)	Sixth Order WKB(J)	AIM
0	0	0.1005 - 0.1007i	0.1211 - 0.0897i	0.1141 - 0.0939i
				(5,78% , 4.68%)
1	0	0.3029 - 0.0891i	0.3053 - 0.0893i	0.3052 - 0.0892i
				(0.03% , 0.11%)
	1	0.2758 - 0.2779i	0.2821 - 0.2755i	0.2817 - 0.2756i
				(0.14% , 0.04%)
2	0	0.5035 - 0.0885i	0.5041 - 0.0886i	0.5041 - 0.0886i
				(<0.01% , <0.01%)
	1	0.4866 - 0.2693i	0.4885 - 0.2690i	0.4885 - 0.2689i
				(<0.01% , 0.04%)
	2	0.4585 - 0.4570i	0.4607 - 0.4581i	
3	0	0.7037 - 0.0884i	0.7040 - 0.0884i	0.7040 - 0.0884i
				(<0.01% , <0.01%)
	1	0.6917 - 0.2670i	0.6925 - 0.2669i	0.6925 - 0.2669i
				(<0.01% , <0.01%)
	2	0.6701 - 0.4498i	0.6708 - 0.4503i	
	3	0.6416 - 0.6369i	0.6414 - 0.6407i	

below the AIM values are the differences to the sixth order WKB(J) values.

Based off tables 5.1 and 5.2, as a increases, the real part of the QNM frequency increases, while the imaginary part of the QNM frequency decreases.

Included in appendix C are the tables, C.1 - C.3, which give the scalar perturbation Kerr black hole QNM frequencies calculated for values of $a = 0.20$, $a = 0.40$ and $a = 0.60$, with the same variations of l and n.

Figures 5.1 - 5.3 show the dependence of the QNM frequencies on n (with constant l), i.e., that as n increases the real part of the QNM frequency decreases, while the imaginary part of the QNM frequency increases.

Figures 5.4 - 5.6 show the dependence of the QNM frequencies on l (with constant n), i.e., that as l increases the real part of the frequency increases, while the imaginary part of the frequency decreases.

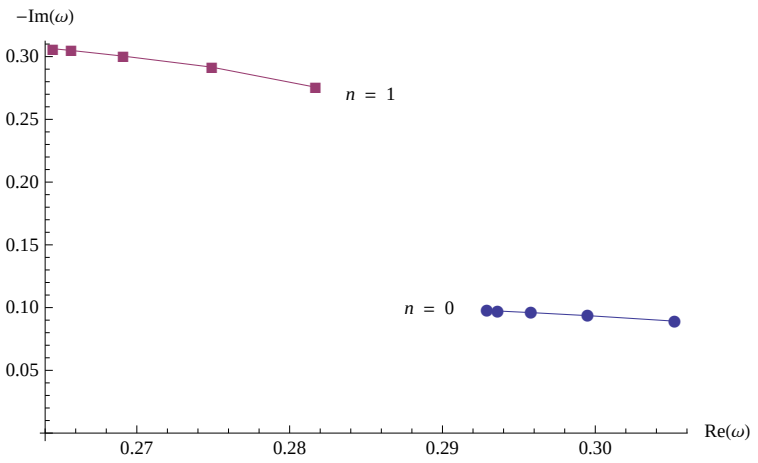

Figure 5.1: *The Quasinormal Mode Frequencies for the Scalar Perturbations of the Kerr Black Hole, when* $l = 1$.

5.2 Spin-Half Perturbations

5.2.1 Equation Manipulation

The WKB(J) Method

With a choice of x, which is an independent variable, defined by

$$\frac{\mathrm{d}r}{\mathrm{d}x} = \frac{\Delta}{\bar{K}},$$

where $\bar{K} = \frac{K}{\omega}$, then the operators $\mathcal{D}_0$ and $\mathcal{D}_0^\dagger$ take the simple forms

$$\mathcal{D}_0 = \frac{\bar{K}}{\Delta}\left(\frac{\mathrm{d}}{\mathrm{d}x} + i\omega\right) \text{ and } \mathcal{D}_0^\dagger = \frac{\bar{K}}{\Delta}\left(\frac{\mathrm{d}}{\mathrm{d}x} - i\omega\right).$$

The radial equations then become

$$\left(\frac{\mathrm{d}}{\mathrm{d}x} - i\omega\right) P_{\frac{1}{2}} = \lambda \frac{\Delta^{\frac{1}{2}}}{\bar{K}} P_{-\frac{1}{2}} \tag{5.5}$$

and

$$\left(\frac{\mathrm{d}}{\mathrm{d}x} + i\omega\right) P_{-\frac{1}{2}} = \lambda \frac{\Delta^{\frac{1}{2}}}{\bar{K}} P_{\frac{1}{2}} \tag{5.6}$$

with $\Delta^{\frac{1}{2}} R_{\frac{1}{2}} = P_{\frac{1}{2}}$ and $R_{-\frac{1}{2}} = P_{-\frac{1}{2}}$.

Letting

$$Z_\pm = P_{\frac{1}{2}} \pm P_{-\frac{1}{2}},$$

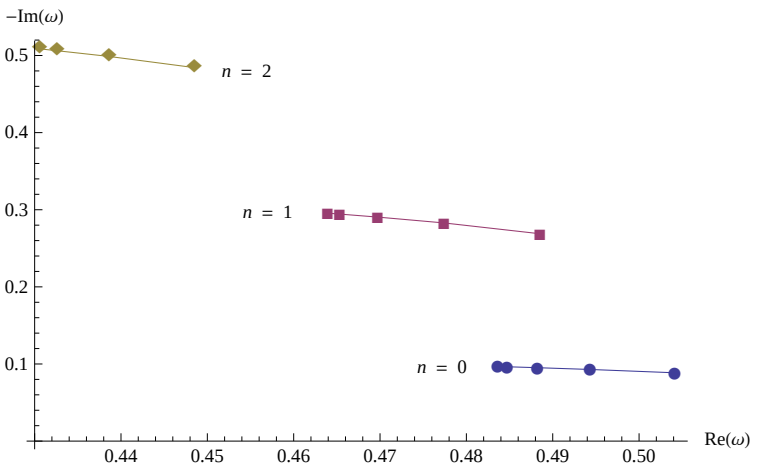

Figure 5.2: *The Quasinormal Mode Frequencies for the Scalar Perturbations of the Kerr Black Hole, when* $l = 2$.

we can combine equations (5.5) and (5.6) to give

$$\left(\frac{\mathrm{d}}{\mathrm{d}x} - \lambda\frac{\Delta^{\frac{1}{2}}}{\bar{K}}\right) Z_+ = i\omega Z_-,$$

and

$$\left(\frac{\mathrm{d}}{\mathrm{d}x} + \lambda\frac{\Delta^{\frac{1}{2}}}{\bar{K}}\right) Z_- = i\omega Z_+.$$

From these equations, we readily obtain the pair of one-dimensional wave-equations,

$$\left(\frac{\mathrm{d}^2}{\mathrm{d}x^2} + \omega^2\right) = V_\pm Z_\pm, \tag{5.7}$$

where

$$V_\pm = \lambda^2\frac{\Delta}{\bar{K}^2} \pm \lambda\frac{\mathrm{d}}{\mathrm{d}x}\left(\frac{\Delta^{\frac{1}{2}}}{\bar{K}}\right).$$

Selecting the positive part of equation (5.7) and rewriting it, with $Z_+ = \psi$ and $V = V_+$, yields

$$\frac{\mathrm{d}^2}{\mathrm{d}x^2}\psi + (\omega^2 - V)\psi = 0, \tag{5.8}$$

which is now in the standard QNMs form and the WKB(J) method can be used to calculate the QNM frequencies.

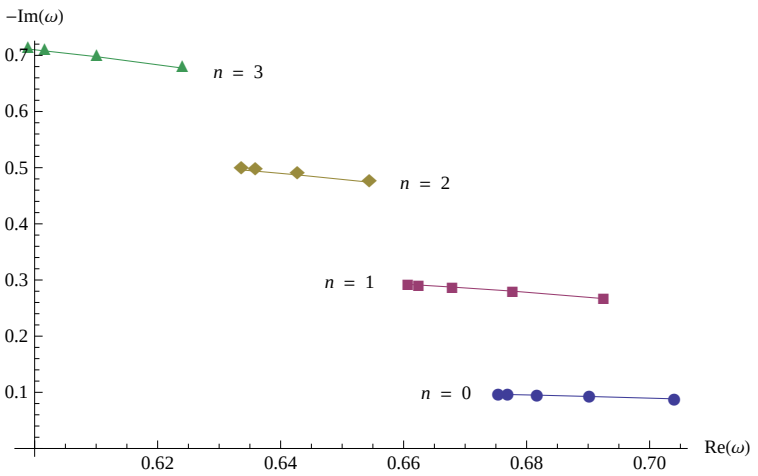

Figure 5.3: *The Quasinormal Mode Frequencies for the Scalar Perturbations of the Kerr Black Hole, when* $l = 3$.

The Asymptotic Iteration Method

Because the AIM works better on a compact domain, we define a new variable $y^2 = 1 - \frac{r_+}{r}$, which ranges from 0 at the event horizon ($r = r_+$) to 1 at spatial infinity. Then it is necessary to incorporate the boundary conditions, which expressed in the new compact domain is

$$\psi(y) = \left(1 - \frac{r_-}{r_+}(1-y^2)\right)^{-\frac{1}{2}-i\sigma_-} (y^2)^{\frac{1}{2}-\sigma_+}(1-y^2)^{-r_+\omega} e^{i\omega\frac{r_+}{1-y^2}}\chi(y).$$

By making the change of coordinate and the change of function, equation (5.8) takes the form

$$\chi(y) = \lambda_0(y) + s_0(y), \tag{5.9}$$
$$\lambda_0 = -2\frac{1}{g}\frac{\mathrm{d}g}{\mathrm{d}y} - \frac{1}{f}\frac{\mathrm{d}f}{\mathrm{d}y},$$

and

$$s_0 = -\frac{1}{g}\frac{\mathrm{d}^2 g}{\mathrm{d}y^2} - \frac{1}{f}\frac{\mathrm{d}f}{\mathrm{d}y} \times \frac{1}{g}\frac{\mathrm{d}g}{\mathrm{d}y} - \frac{1}{f^2}\left(\omega^2 - V|_{r=r_+(1-y^2)^{-1}}\right),$$

with

$$f = \left(\frac{\Delta}{K}\frac{\mathrm{d}y^{\frac{1}{2}}}{\mathrm{d}r}\right)|_{r=r_+(1-y^2)^{-1}},$$

and

$$g = (1-y^2)^{-2i\omega}\left(1 - \frac{r_-}{r_+}(1-y^2)\right)^{-\frac{1}{2}-i\sigma_-} (y^2)^{\frac{1}{2}-i\sigma_+} e^{i\omega r_+(1-y^2)^{-1}}.$$

Equation (5.9) is now in the correct form to use the AIM for QNM frequency calculations.

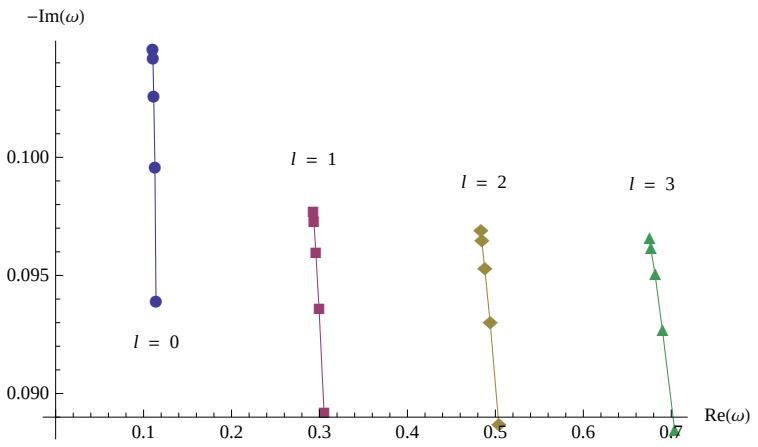

Figure 5.4: *The Quasinormal Mode Frequencies for the Scalar Perturbations of the Kerr Black Hole, when* $n = 0$.

5.2.2 Results and Discussion

As presented in tables 5.3 and 5.4 are the QNM frequencies for the spin-half perturbations of the Kerr black hole with the two "extreme" (minimum and maximum for this dissertation) values of the angular momentum per unit mass, i.e., $a = 0.00$ and $a = 0.80$. m was set to 0, while the angular number l was given values of 0, 1, 2 and 3 and the mode number n was varied from 0 to $l - 1$.

Included in table 5.3 are the numerically determined QNM frequencies published by Jing [48]. Even though the WKB(J) method has been used to calculate the Schwarzschild limit QNM frequencies before, up to sixth order, and the values published by Cho [49] and by Konoplya [14], the calculations were redone for this work. The AIM values are novel to this work. The percentages bracketed under each QNM frequency for $l = 0$ to $l = 2$, is the percentage difference between the calculated value and the numerical value published by Jing. While for $l = 3$, the AIM values are compared to the sixth order WKB(J) values.

Included in table 5.4 are the numerically determined QNM frequencies published by Jing *et al.* [47]. Both the third and sixth order WKB(J) values along with the AIM values are novel to this work. The percentages bracketed under each QNM frequency, are the percentage difference between the calculated value and the numerical value published by Jing, at least for $l = 0$ and $l = 1$. For $l = 2$ and $l = 3$, the AIM values are compared to the sixth order WKB(J) values.

Based off tables 5.3 and 5.4, as a increases, the real part of the QNM frequency increases, while the imaginary part of the QNM frequency decreases.

Included in appendix C are the tables, C.4 - C.6, which give the spin-half perturbation Kerr black hole QNM frequencies calculated for values of $a = 0.20$, $a = 0.40$ and $a = 0.60$, with the same variations of l and n.

Figures 5.7 - 5.9 show the dependence of the QNM frequencies on n (with constant l),

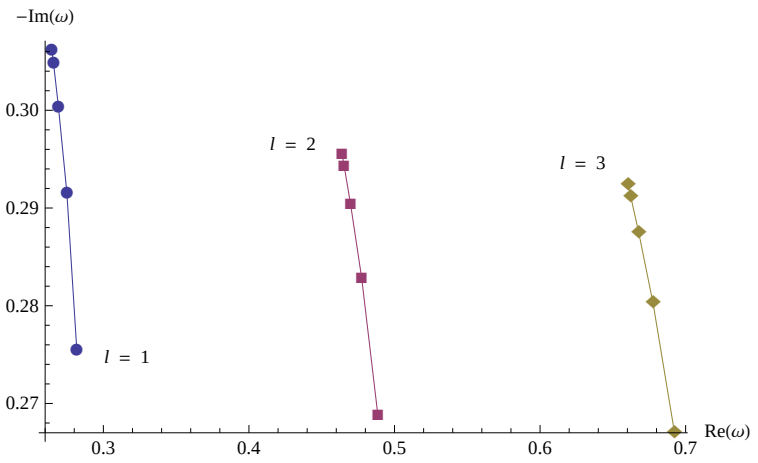

Figure 5.5: *The Quasinormal Mode Frequencies for the Scalar Perturbations of the Kerr Black Hole, when* $n = 1$.

i.e., that as n increases the real part of the QNM frequency decreases, while the imaginary part of the QNM frequency increases.

Figures 5.10 and 5.12 show the dependence of the QNM frequencies on l (with constant n), i.e., that as l increases the real part of the frequency increases, while the imaginary part of the frequency decreases.

The missing values, for the QNM frequencies calculated using the AIM, in some of the tables are because the values returned by Mathematica 8 on the computer used, were so far off the numerical / sixth order WKB(J) values, it was a clear indication of computation error and were therefore left out.

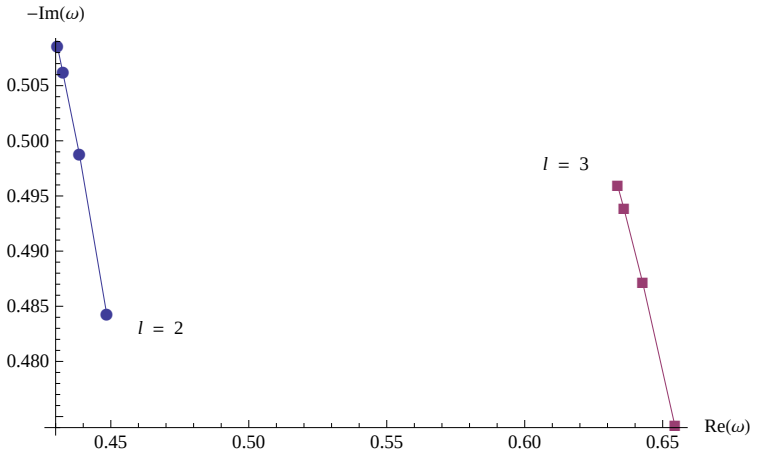

Figure 5.6: *The Quasinormal Mode Frequencies for the Scalar Perturbations of the Kerr Black Hole, when* $n = 2$.

Table 5.3: *The Quasinormal Mode Frequencies for the Spin-Half Perturbations of the Kerr Black Hole, when* $a = 0.00$.

l	n	Numerical	Third Order WKB(J)	Sixth Order WKB(J)	AIM
0	0	0.1830 - 0.0970i	0.1765 - 0.1001i	0.1827 - 0.0949i	0.1830 - 0.0969i
			(3.55% , 3.20%)	(0.16% , 2.16%)	(<0.01% , 0.10%)
1	0	0.3800 - 0.0964i	0.3786 - 0.0965i	0.3801 - 0.0964i	0.3800 - 0.0964i
			(0.37% , 0.10%)	(0.03% , <0.01%)	(<0.01% , <0.01%)
	1	0.3558 - 0.2975i	0.3536 - 0.2987i	0.3559 - 0.2973i	0.3568 - 0.2976i
			(0.62% , 0.40%)	(0.03% , 0.07%)	(0.28% , 0.03%)
2	0	0.5741 - 0.0963i	0.5737 - 0.0963i	0.5741 - 0.0963i	0.5741 - 0.0963i
			(0.07% , <0.01%)	(<0.01% , <0.01%)	(<0.01% , <0.01%)
	1	0.5570 - 0.2927i	0.5562 - 0.2930i	0.5570 - 0.2927i	0.5573 - 0.2928i
			(0.14% , 0.10%)	(<0.01% , <0.01%)	(0.05% , 0.03%)
	2	0.5266 - 0.4997i	0.5273 - 0.4972i	0.5265 - 0.4997i	0.5189 - 0.5213i
			(0.13% , 0.50%)	(0.02% , <0.01%)	(1.46% , 4.32%)
3	0		0.7672 - 0.0963i	0.7674 - 0.0963i	0.7674 - 0.0963i
					(<0.01% , <0.01%)
	1		0.7540 - 0.2910i	0.7543 - 0.2910i	0.7544 - 0.2910i
					(0.01% , <0.01%)
	2		0.7305 - 0.4909i	0.7298 - 0.4919i	0.7267 - 0.4928i
					(0.42% , 0.18%)
	3		0.6999 - 0.6957i	0.6967 - 0.7023i	

Table 5.4: *The Quasinormal Mode Frequencies for the Spin-Half Perturbations of the Kerr Black Hole, when* $a = 0.80$.

l	n	Numerical	Third Order WKB(J)	Sixth Order WKB(J)	AIM
0	0	0.1932 - 0.0891i	0.1883 - 0.0896i	0.1914 - 0.0865i	0.1920 - 0.0872i
			(2.54% , 0.56%)	(0.93% , 2.92%)	(0.62% , 2.13%)
1	0	0.3993 - 0.0893i	0.3956 - 0.0881i	0.3967 - 0.0880i	0.3965 - 0.0880i
			(0.93% , 1.34%)	(0.65% , 1.46%)	(0.70% , 1.46%)
	1	0.3789 - 0.2728i	0.3751 - 0.2701i	0.3777 - 0.2687i	
			(1.00% , 0.99%)	(0.32% , 1.50%)	
2	0		0.5984 - 0.0881i	0.5987 - 0.0881i	0.5987 - 0.0882i
					(<0.01% , 0.11%)
	1		0.5844 - 0.2669i	0.5855 -0.2667i	0.5847 - 0.2644i
					(0.14% , 0.86%)
	2		0.5600 - 0.4512i	0.5609 - 0.4517i	
3	0		0.8000 - 0.0882i	0.8001 - 0.0882i	0.8001 - 0.0882i
					(<0.01% , <0.01%)
	1		0.7895 - 0.2659i	0.7900 - 0.2658i	0.7900 - 0.2655i
					(<0.01% , 0.11%)
	2		0.7702 - 0.4471i	0.7706 - 0.4473i	
	3		0.7443 - 0.6320i	0.7436 - 0.6345i	

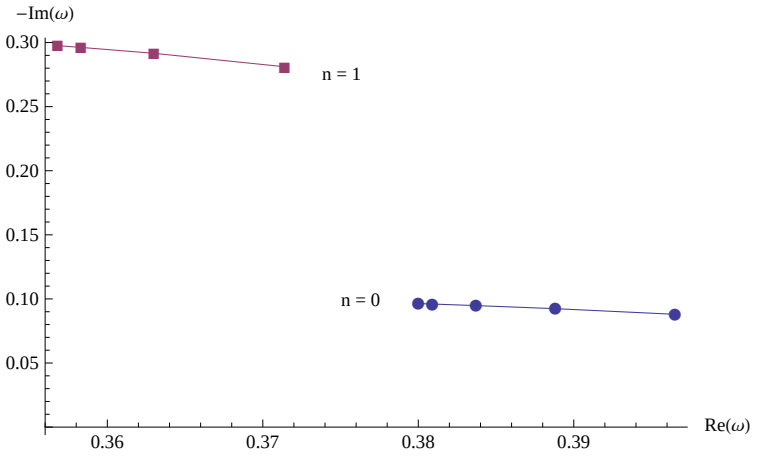

Figure 5.7: *The Quasinormal Mode Frequencies for the Spin-Half Perturbations of the Kerr Black Hole, when* $l = 1$.

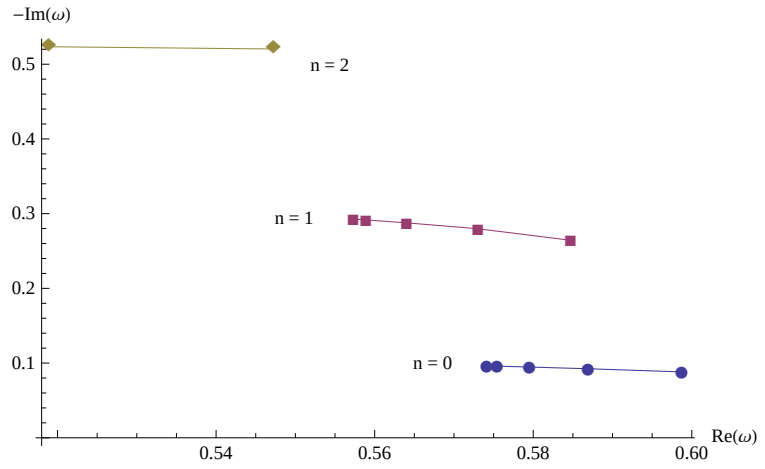

Figure 5.8: *The Quasinormal Mode Frequencies for the Spin-Half Perturbations of the Kerr Black Hole, when* $l = 2$.

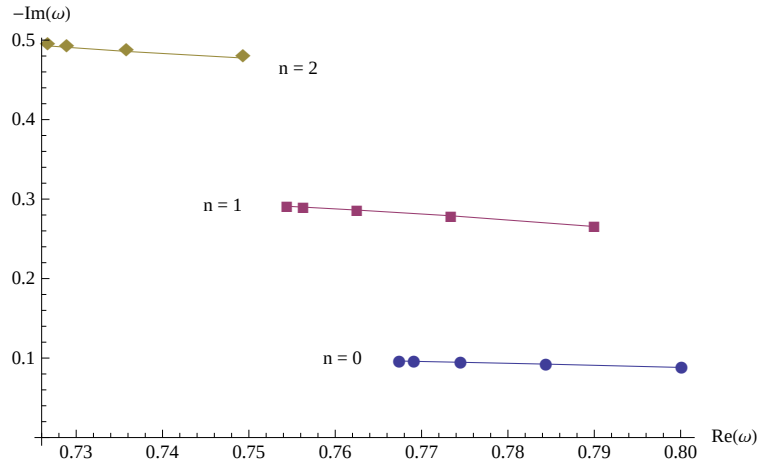

Figure 5.9: *The Quasinormal Mode Frequencies for the Spin-Half Perturbations of the Kerr Black Hole, when* $l = 3$.

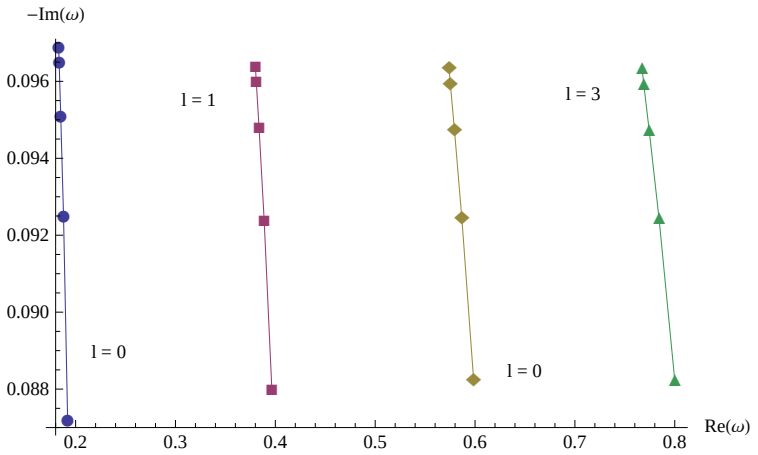

Figure 5.10: *The Quasinormal Mode Frequencies for the Spin-Half Perturbations of the Kerr Black Hole, when* $n = 0$.

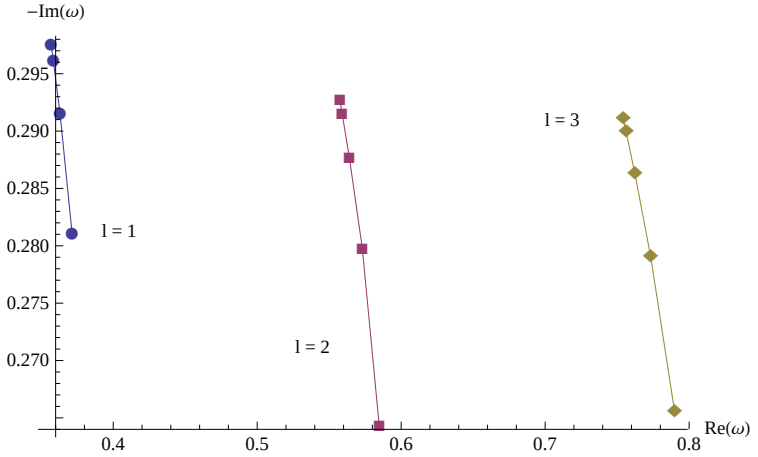

Figure 5.11: *The Quasinormal Mode Frequencies for the Spin-Half Perturbations of the Kerr Black Hole, when* $n = 1$.

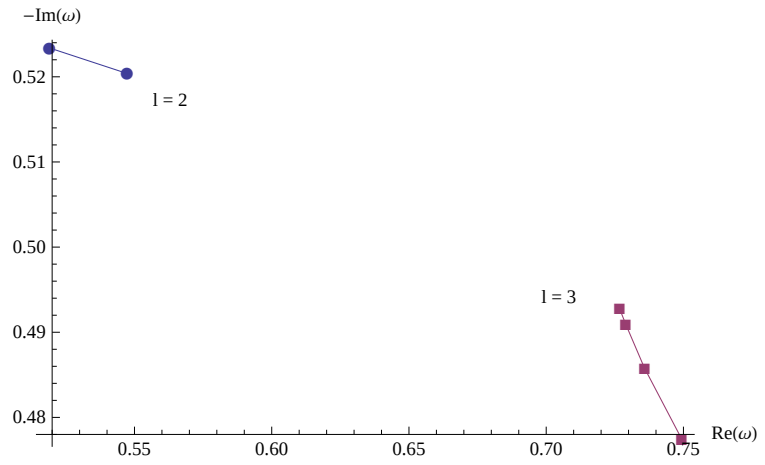

Figure 5.12: *The Quasinormal Mode Frequencies for the Spin-Half Perturbations of the Kerr Black Hole, when* $n = 2$.

Chapter 6

Conclusion

6.1 Hidden Conformal Symmetry

The near region condition that lead to the discovery of a two dimensional conformal symmetry "hidden" in the Kerr scalar solution space, was not enough to reveal a similar symmetry in the Kerr spin-half solution space. Or to be more specific, the non-hypergeometric terms in the spin-half radial equation were not negligible in the near region limit, so it was not apparent that the solution space had a two dimensional conformal symmetry.

6.2 Quasinormal Modes

6.2.1 Scalar Perturbations

In the case of the scalar perturbations of a Kerr black hole, there appears to be no published numerical values for the QNM frequencies. All past tabulated calculations seem to focus on gravitational perturbations. There are, however, diagrams of the scalar perturbations for QNM frequencies of a Kerr black hole calculated using the third order WKB(J) method [13] and they compare favourably, at least visually, with the third order WKB(J) method values recalculated in this dissertation.

When Konoplya first derived the fourth through sixth order corrections to the the WKB(J) method and published the expressions, he included a demonstration of their improved accuracy over the third order WKB(J) method when compared to numerically calculated values [14]. So for the purpose of this dissertation, the QNM frequencies calculated using the sixth order WKB(J) method are what the AIM values are compared to, in order to have an idea how accurate the AIM is. As such the accuracy of the AIM, as compared to the numerical method or the sixth order WKB(J) method, was at its highest when a was at its lowest, i.e., 0, n was at its lowest, i.e., 0, and l was at its highest, i.e., 3. However Mathematica 8 did evaluate the necessary expressions, etcetera, significantly faster for the sixth order WKB(J) method than for the AIM.

6.2.2 Spin-Half Perturbations

Unlike the case of the scalar perturbations, there are previously published numerical values for the QNM frequencies that result from the spin-half perturbations of a Kerr black hole [47], at least for the angular numbers of $l = 0$ and $l = 1$. For the QNM frequencies when $l = 2$ and $l = 3$, the AIM values were then compared to the sixth order WKB(J) method values.

The accuracy of the AIM, as compared to the numerical method or the sixth order WKB(J) method, was at its highest when a was at its lowest, i.e., 0, n was at its lowest, i.e., 0, and l was at its highest, i.e., 3. Once again, Mathematica 8 did evaluate the necessary expressions, etcetera significantly faster for the sixth order WKB(J) method than for the AIM.

6.3 Possible Future Directions

6.3.1 Hidden Conformal Symmetry

Since the start of this dissertation in 2010, there have been many articles published about the hidden conformal symmetry of a variety of black holes, ranging from the simple extension of the Kerr to the Kerr - Newman black hole by adding an electric charge, which was done by Wang *et al.* [50], to the extremal Kaluza-Klein black hole by Huang [51]. Just like the original work by Strominger *et al.* [35], these hidden conformal symmetries were found for the scalar particle solution space in the near region of the black hole. As of the end of this dissertation, no one has published an article about the presence / absence of a similar hidden conformal symmetry for the spin-half particle solution space in the near region of the Kerr or any other black holes.

It may be that the spin-half solution space in the near region has a different conformal symmetry to the scalar solution space in the near region, so any further study would warrant comparisons to the functions that transform under other representations.

It may be possible to follow similar procedures as in this dissertation to derive the Hawking radiation of fermions, depending on the form of the near horizon solutions [52].

6.3.2 Quasinormal Modes

As of the end of this dissertation, no one has published an article that uses either the sixth order WKB(J) method or the AIM to calculate the QNM frequencies of anything but the non - spin-half perturbations of a variety of Schwarzschild black holes [14, 16].

This dissertation only used the sixth order WKB(J) method and AIM to calculate the QNM frequencies for the scalar and spin-half perturbations of a four dimensional Kerr black hole.

The possible extensions for the Kerr black hole are different types of perturbations of the Kerr black hole, working in a space-time that is not asymptotically flat or working in higher dimensions. The importance of these extensions are described below.

In the context of the Einstein - Maxwell equations, the most general solution describing stationary axisymmetric black holes is the Kerr - Newman metric (with electric charge Q) [53], but for astrophysical black holes the electric charge is likely to be negligible. So it would be instructive to study different kinds of perturbations for Kerr black holes such as electromagnetic and gravitational perturbations.

The study of black hole QNMs has a long history, where most of the studies are for asymptotically flat space-times. The discovery of the AdS / CFT correspondence [21] and the expanding universe motivated the investigation of QNMs in de Sitter [54] and anti - de Sitter [20] space-times in the past several years.

Electromagnetic perturbations are of interest due to the AdS / CFT conjecture since they can be seen as perturbations for some generic supergravity gauge field. In addition, the Maxwell field is an important field with different features from scalar or gravitational fields, which makes it worth studying. On the other hand, gravitational perturbations have the additional interest of arising from any other type of perturbation, be it scalar, electromagnetic, Weyl, etc., which in turn disturb the background geometry. Therefore, questions like the stability of space-time for scalar or other perturbations, have a direct dependence on the stability to gravitational perturbations.

Classical general relativity in more than four space-time dimensions has been the subject of increasing attention in recent years. Among the reasons why it should be interesting to study this extension of Einstein's theory, and particular its black hole solutions, we may mention that

- String theory contains gravity and requires more than four dimensions [4].
- The AdS / CFT correspondence relates the properties of a d - dimensional black hole with those of a quantum field theory in $d-1$ dimensions [18].
- The production of higher dimensional black holes in future colliders becomes a conceivable possibility in scenarios involving large extra dimensions and TeV scale gravity [55].

Just as the study of quantum field theories with a field content very different than any conceivable extension of the Standard Model has been a very useful endeavor throwing light on general features of quantum fields, we believe that endowing General Relativity with a tunable parameter, namely the space-time dimensionality d, should also lead to valuable insights into the nature of the theory, in particular of its most basic objects: the black holes. For instance, four dimensional black holes are known to possess a number of remarkable features, such as uniqueness, spherical topology, dynamical stability, and the laws of black hole mechanics. One would like to know which of these are peculiar to four dimensions, and which hold more generally. At the very least, this study will lead to a deeper understanding of classical black holes and of what space-time can do at its most extreme.

Bibliography

[1] R. Kerr. Gravitational field of a spinning mass as an example of algebraically special metrics. *Phys. Rev. Lett.*, 11, 1963.

[2] K. Schwarzschild. Central mass black hole. *Phys. Math. Klasse*, 1916.

[3] J. Maldacena. The large n limit of superconformal field theories and supergravity. *Adv. Theor. Math. Phys.*, 2, 1998.

[4] A. Strominger and C. Vafa. Microscopic origin of the berkenstein-hawking entropy. *Phys. Rev. Lett.*, B, 1996.

[5] A. Strominger. Black hole entropy from near-horizon microstates. *JHEP*, 1998.

[6] R. F. Stark and T. Piran. Gravitational-wave emission from rotating gravitational collapse. *Phys. Rev. Lett.*, 44, 1980.

[7] S. Detweiler and R. Ove. Instability of some black holes. *Phys. Rev. Lett.*, 51, 1983.

[8] C. V. Vishveshwara. Stability of the schwarzschild metric. *Phys. Rev. D*, 1, 1970.

[9] S. Chandrasekhar and S. Detweiler. The quasi-normal modes of the schwarzschild black hole. *Proc. Roy. Soc. Lond.*, A, 1975.

[10] V. Ferrari and B. Mashhoon. New approach to the quasinormal modes of a black hole. *Phys. Rev. D*, 30, 1084.

[11] D. Gunter. A study of the coupled gravitational and electromagnetic perturbations to the reissner–nordstrom black hole: The scattering matrix, energy conversion, and quasi-normal modes. *Phil. Trans. R. Soc. London*, 296, 1980.

[12] E. W. Leaver. An analytic representation for the quasi-normal modes of kerr black holes. *Proc. Roy. Soc. Lond.*, A, 1985.

[13] E. Seidel and S. Iyer. Black-hole normal modes: A wkb approach. iv. kerr black holes. *Phys. Rev. D*, 41, 1990.

[14] R. A. Konoplya. Quasinormal behavior of the d-dimensional schwarzschild black hole and the higher order wkb approach. *Phys. Rev. D*, 68, 2003.

[15] H. Cifti, R. Hall, and N. Saad. Asymptotic iteration method for eigenvalue problems. *J. Phys. A : Math. Gen.*, 36, 2003.

[16] H. T. Cho, A. S. Cornell, J. Doukas, and W. Naylor. Black hole quasinormal modes using the asymptotic iteration method. *Classical and Quantum Gravity*, 27, 2010.

[17] J. D. Bekenstein. Black holes and entropy. *Phys. Rev. D*, 7, 1973.

[18] O. Aharony, S. S. Gubser, J. M. Maldacena, H. Ooguri, and Y. Oz. Large n field theories, string theory and gravity. *Phys. Rept.*, 323, 2000.

[19] K. D. Kokkotas and Schmidt B. G. Quasi-normal modes of stars and black holes. *Living Rev. Relativ.*, 2, 1999.

[20] G. T. Horowitz and V. E. Hubeny. Quasinormal modes of ads black holes and the approach to thermal equilibrium. *Phys. Rev. D*, 62, 2000.

[21] D. Birmingham, I. Sachs, and S. N. Solodukhin. Conformal field theory interpretation of black hole quasinormal modes. *Phys. Rev. Lett.*, 2002.

[22] J. B. Hartle. *Gravity - An Introduction to Einstein's Relativity.* Addison Wesley, California, USA, 2003.

[23] S. R. Dolan. Black holes and wave mechanics. *arXiv:1007.5097*, 2008.

[24] S. Chandrasekhar. *The Mathematical Theory of Black Holes.* Oxford University Press, New York, USA, 1983.

[25] M. Visser. The kerr spacetime: A brief introduction. *arXiv:0706.0622 [gr-qc]*, 2008.

[26] L. Ryder. *Introduction to General Relativity.* Cambridge University Press, 2009.

[27] E. T. Newman and R. Penrose. The newman-penrose formalism. *J. Math. Phys.*, 3, 1962.

[28] E. Cartan. *The Theory of Spinors.* The M.I.T. Press, 1966.

[29] B. Mukhopadhyay. Dirac equation in kerr geometry. *Indian J. Phys*, B, 1991.

[30] V. B. Berestetskii, E. M. Lifshitz, L. P. Pitaevskii, L. D. Landau, and E. M. Lifshitz. *Courses in Theoretical Physics*, volume 4. Pergamon Press, 1971.

[31] M. Guica, T. Hartman, W. Song, and A. Strominger. The kerr / cft correspondence. *Phys. Rev. D*, 80, 2009.

[32] T. Hartman, K. Murata, T. Nishioka, and A. Strominger. Cft duals for extreme black holes. *JHEP*, 2009.

[33] Y. Matsuo, T. Tsukioka, and C. M. Yoo. Another realization of kerr / cft correspondence. *Nuclear Physics B*, 825, 2010.

[34] M. R. Gaberdiel. An introduction to conformal field theory. *Reports on Progress in Physics*, 1999.

[35] A. Castro, A. Maloney, and A. Strominger. Hidden conformal symmetry of the kerr black hole. *Phys. Rev. D*, 82, 2010.

[36] C. V. Vishveshwara. Scattering of gravitational radiation by a schwarzschild black-hole. *Nature*, 227, 1970.

[37] L. L. Smarr. *Sources of Gravitational Radiation: Proceedings of the Battelle Seattle Workshop*. Cambridge University Press, 1979.

[38] R. Gleiser, C. O. Nicasio, H. Price, and J. Pullin. Colliding black holes: How far can the close approximation go? *Phys. Rev. Lett.*, 77, 1996.

[39] W. H. Press. Long wave trains of gravitational waves from a vibrating black hole. *Astrophys.*, 170, 1971.

[40] H. P. Nollert. Quasinormal modes: the characteristic 'sound' of black holes and neutron stars. *Classical and Quantum Gravity*, 16, 1999.

[41] B. F. Schutz and C. M. Will. Black hole normal modes - a semianalytic approach. *Astrophys.*, 291, 1985.

[42] S. Iyer and C. M. Will. Black-hole normal modes: A wkb approach. i. foundations and application of a higher-order wkb analysis of potential-barrier scattering. *Phys. Rev. D*, 35, 1987.

[43] T. Kawai and Y. Takei. *Algebraic Analysis of Singular Perturbation Theory*. American Mathematical Society, 2005.

[44] J. W. Guinn, C. M. Will, Y Kojima, and B. F. Schutz. High-overtone normal modes of schwarzschild black holes. *Classical and Quantum Gravity*, 7, 1990.

[45] C. M. Bender and S. A. Orszag. *Advanced Mathematical Methods for Scientists and Engineers*. McGraw Hill, 1978.

[46] J. M. Bardeen and W. H. Press. Radiation fields in the schwarzschild background. *J. Math. Phys.*, 14, 1973.

[47] J. Jing and Q. Pan. Dirac quasinormal frequencies of the kerr-newman black hole. *Nuclear Physics B*, 728, 2005.

[48] J. Jing. Dirac quasinormal modes of schwarzschild black hole. *Phys. Rev. D*, 71, 2005.

[49] H. T. Cho. Dirac quasinormal modes in schwarzschild black hole spacetimes. *Phys. Rev. D*, 68, 2003.

[50] Y.-Q. Wang and Y.-X. Liu. Hidden conformal symmetry of the kerr-newman black hole. *Journal of High Energy Physics*, 2010.

[51] Y.-C. Huang and F.-F. Yuan. Hidden conformal symmetry of extremal kaluza-klein black hole in four dimensions. *Journal of High Energy Physics*, 2011.

[52] I. Agullo, J. Navarro-Salas, G. J. Olmo, and L. Parker. Hawking radiation by kerr black holes and conformal symmetry. *arxXiv:1006.4404 [hep-th]*, 2010.

[53] M. Heusler. Stationary black holes: Uniqeness and beyond. *Living Rev. Relativ.*, 1998.

[54] P. R. Brady, C. M. Chambers, W. Krivan, and P. Laguna. Telling tails in the presence of a cosmological constant. *Phys. Rev. D*, 1997.

[55] M. Cavaglia. Black hole and brane production in tev gravity: A review. *Int. J. Mod. Phys.*, A, 2003.

[56] R. M. Wald. Energy limits of the penrose process. *Astrophys.*, 191, 1974.

[57] W. Unruth. Separability of the neutrino equations in a kerr background. *Phys. Rev. Lett.*, 1973.

Appendix A

The Penrose Process

The Penrose mechanism is a process theorized by Roger Penrose [56] wherein energy can be extracted from a rotating black hole. That extraction is made possible because the rotational energy of the black hole is located, not inside the event horizon of the the black hole, but on the outside of it in a region of the the Kerr space-time called the ergosphere, a region in which a particle moves concurrently with the rotating space-time. In the process, an object enters into the ergosphere of the black hole, and once it enters the ergosphere, it is split into two. The momentum of the two pieces can be arranged so that one piece escapes to infinity, whilst the other falls past the outer event horizon into the hole. The escaping piece can possibly have greater mass-energy than the original in-falling piece of matter, whereas the in-falling piece has negative mass-energy. In summary, the process results in a decrease in the angular momentum of the black hole, and that reduction corresponds to a transference of energy whereby the momentum lost is converted to energy extracted.

A mathematical description on how this mechanism is possible for a scalar particle is given below.

In the interest of determining the overall effect a Kerr black hole has on a scalar particle, it is convenient to change equation (2.38) to Tortoise coordinates using relationship (5.2). The result of which is

$$\left[\frac{\mathrm{d}^2}{\mathrm{d}x^2}+\frac{2r\Delta}{(r^2+a^2)^2}\frac{\mathrm{d}}{\mathrm{d}x}+\left(\omega^2-\frac{4Mam\omega r-m^2a^2+\Delta A}{(r^2+a^2)^2}\right)\right]R(x)=0. \tag{A.1}$$

The overall effect can be understood by looking at the two limits of the scalar particle's position from the black hole:

1. Equation (A.1) can be re-written as

$$\left[\frac{\mathrm{d}^2}{\mathrm{d}x^2}+\frac{2}{r}\cdot\frac{1+\frac{a^2}{r^2}-\frac{2M}{r}}{(1+\frac{a^2}{r^2})^2}\frac{\mathrm{d}}{\mathrm{d}x}+\left(\omega^2-\frac{1}{r^2}\cdot\frac{\frac{4Mam\omega}{r}-\frac{m^2a^2}{r^2}+(1+\frac{a^2}{r^2}-\frac{2M}{r})A}{(1+\frac{a^2}{r^2})^2}\right)\right]R(x)=0.$$

When the particle is very far away from the black hole, i.e, $r\to\infty$, $\mathrm{d}x$ can be exchanged

with dr and all the terms that are greater than $O(\frac{1}{r})$ can be eliminated, leaving

$$\left[\frac{\mathrm{d}^2}{\mathrm{d}r^2} + \frac{2}{r}\frac{\mathrm{d}}{\mathrm{d}x} + \omega^2\right] R(r) = 0.$$

This is the differential equation for a spherical wave and has the solution

$$R(r) = \frac{1}{r}(Ae^{i\omega r} + Be^{-i\omega r}),$$

where A and B are the coefficients of the outgoing and incoming waves, respectively.

2. Using the definition (2.9), equation (A.1) can be re-written as

$$\left[\frac{\mathrm{d}^2}{\mathrm{d}x^2} + \frac{2r\Delta}{(\Delta + 2Mr)^2}\frac{\mathrm{d}}{\mathrm{d}x} + \left(\omega^2 - \frac{4Mam\omega r - m^2a^2 + \Delta A}{(\Delta + 2Mr)^2}\right)\right] R(x) = 0.$$

When the particle is close to the outer horizon of the black hole, i.e., $r \to r_+$ or $\Delta \to 0$, the above equation simplifies to

$$\left[\frac{\mathrm{d}^2}{\mathrm{d}x^2} + (\omega')^2\right] R(x) = 0,$$

where

$$\frac{\omega'}{m} = \frac{\omega}{m} - \frac{a}{2Mr_+}.$$

This is the differential equation of a simple wave and has the solution

$$R(x) = Fe^{i\omega' x} + Ge^{-i\omega' x}, \tag{A.2}$$

where F and G are the coefficients of the outgoing and incoming waves, respectively.

The wave equivalent of the Penrose Process is known as superradiance. The super radiant modes are given by ω'.

The Stress-Energy tensor is just a convenient physical quantity that describes the density flux of energy and momentum in space-time, for a particular set of equations. In the case of a scalar field, the components of the tensor are given by

$$T_{\mu\nu} = \frac{1}{2}\Psi *_{(,\mu}\ \Psi_{,\nu)} + g_{\mu\nu}|\Psi *_{,\sigma}\ \Psi^{,\sigma}|.$$

The radial power increase of the rotating black hole is given by

$$\frac{\mathrm{d}E^r}{\mathrm{d}t} = \int_A T_{tr}g^{rr}\sqrt{-\mathbf{g}}\mathrm{d}\theta\mathrm{d}\phi,$$

where T_{tr} is the component of the Stress-Energy tensor that has to do with the power flux in the radial direction and in this case is given by

$$T_{tr} = \frac{1}{2}\Psi *_{(,t}\ \Psi_{,r)}. \tag{A.3}$$

Using equation (2.34), with equation (A.2), in equation (A.3) yields

$$T_{tr} = -\frac{1}{4\pi}\omega\omega'\left(\frac{r^2+a^2}{\Delta}\right)(|F|^2 - |G|^2)|S|^2,$$

where $|F|^2$, $|G|^2$ and $|S|^2$ are all positive definite constants. The final expression for the radial increase of the rotating black hole is given by

$$\frac{\mathrm{d}E^r}{\mathrm{d}t} = -\frac{1}{4\pi}\omega\omega'(r^2+a^2)(|F|^2 - |G|^2)\int_A |S|^2 d\Omega, \tag{A.4}$$

where $d\Omega = \sin\theta \mathrm{d}\theta\mathrm{d}\phi$. Since the initial parameters of the rotating black are not set by the observer, it is only possible to obtain a spectrum of results by changing the parameters of the initial scalar particle. So by limiting equation (A.4) to only the incoming wave, i.e., setting $F = 0$, and evaluating at the outer horizon, it simplifies to

$$\frac{\mathrm{d}E^r}{\mathrm{d}t} = \frac{1}{4\pi}\omega\omega'(2Mr_+)|G|^2\int_A |S|^2 d\Omega. \tag{A.5}$$

For power to flow out of the black hole, it is necessary to have

$$\frac{\mathrm{d}E^r}{\mathrm{d}t} < 0,$$

and since all the constants in (A.5) are positive (definite), including the area integral of $|S|^2$, it is required that

$$\omega\omega' < 0.$$

Since $\omega > 0$, we must have $\omega' < 0$ or

$$0 < \frac{\omega}{m} < \frac{a}{2Mr_+}.$$

Therefore, in order for a scalar particle to extract energy from a a rotating black hole, it is necessary for its ratio of the angular frequency to it's angular number of the scalar particle is less than the angular frequency of the rotating black hole's outer horizon.

According to Unruth [57], while superradiance is possible for scalar, electromagnetic and gravitational fields, it is not possible for sermonic fields.

Appendix B

Sixth Order WKB(J) Corrections

Here we shall follow the designations: Q_0 means the value of the "potential" at its peak, i.e., when x, the tortoise coordinate is equal to x_0. So Q_j^k is the kth power of the jth derivate with respect to x of Q.

The fourth through sixth corrections to the WKB(J) approximation are given below.

$$\begin{aligned}
\Lambda_4 &= \frac{1}{597196800\sqrt{2}Q_2^7\sqrt{Q_2}}(2536975Q_3^6 - 9886275Q_2Q_3^4Q_4 + 5319720Q_2^2Q_3^3Q_5 \\
&- 225Q_2^2Q_3^2(-40261Q_4^2 + 9688Q_2Q_6) + 3240Q_2^3Q_3(-1889Q_4Q_5 + 220Q_2Q_7) \\
&- 729Q_2^3(1425Q_4^3 - 1400Q_2Q_4Q_6 + 8Q_2(-123Q_5^2 + 25Q_2Q_8)))
\end{aligned}$$

$$\begin{aligned}
&+ \frac{(n+\frac{1}{2})^2}{4976640\sqrt{2}Q_2^7\sqrt{Q_2}}(348425Q_3^6 - 1199925Q_2Q_3^4Q_4 + 57276Q_2^2Q_3^3Q_5 \\
&- 45Q_2^2Q_3^2(-20671Q_4^2 + 4552Q_2Q_6) + 1980Q_2^3Q_3(-489Q_4Q_5 + 52Q_2Q_7) \\
&- 27Q_2^3(2845Q_4^3 - 2360Q_2Q_4Q_6 + 56Q_2(-31Q_5^2 + 5Q_2Q_8)))
\end{aligned}$$

$$\begin{aligned}
&+ \frac{(n+\frac{1}{2})^4}{2488320\sqrt{2}Q_2^7\sqrt{Q_2}}(192925Q_3^6 - 581625Q_2Q_3^4Q_4 + 234360Q_2^2Q_3^3Q_5 \\
&- 45Q_2^2Q_3^2(-8315Q_4^2 + 1448Q_2Q_6) + 1080Q_2^3Q_3(-161Q_4Q_5 + 12Q_2Q_7) \\
&- 27Q_2^3(625Q_4^3 - 440Q_2Q_4Q_6 + 8Q_2(-63Q_5^2 + 5Q_2Q_8))).
\end{aligned}$$

$$
\begin{aligned}
\Lambda_5 &= \frac{(n+\frac{1}{2})}{57330892800Q_2^{10}}(2768256Q_{10}Q_2^7 - 1078694575Q_3^8 + 5357454900Q_2Q_3^6Q_4 \\
&- 2768587920Q_2^2Q_3^5Q_5 + 90Q_2^2Q_3^4(-88333625Q_4^2 + 12760664Q_2Q_6) \\
&- 4320Q_2^3Q_3^3(-1451425Q_4Q_5 + 91928Q_2Q_7) - 27Q_2^4(7628525Q_4^4 - 9382480Q_2Q_4^2Q_6) \\
&+ 64Q_2^2(19277Q_6^2 + 37764Q_5Q_7) + 576Q_2Q_4(-21577Q_5^2 + 2505Q_2Q_8) \\
&+ 540Q_2^3Q_3^2(6515475Q_4^3 - 3324792Q_2Q_4Q_6 + 16Q_2(-126468Q_5^2 + 12679Q_2Q_8)) \\
&- 432Q_2^4Q_3(5597075Q_4^2Q_5 - 854160Q_2Q_4Q_7 + 8Q_2(-145417Q_5Q_6 + 6685Q_2Q_9)))
\end{aligned}
$$

$$
\begin{aligned}
&+ \frac{(n+\frac{1}{2})^3}{477757440Q_2^{10}}(31104Q_{10}Q_2^7 - 42944825Q_3^8 + 193106700Q_2Q_3^6Q_4 \\
&- 90039120Q_2^2Q_3^5Q_5 + 30Q_2^2Q_3^4(-8476205Q_4^2 + 1102568Q_2Q_6) \\
&- 4320Q_2^3Q_3^3(-41165Q_4Q_5 + 2312Q_2Q_7) - 9Q_2^4(445825Q_4^4 - 472880Q_2Q_4^2Q_6) \\
&+ 64Q_2^2(829Q_6^2 + 1836Q_5Q_7) + 4032Q_2Q_4(-179Q_5^2 + 15Q_2Q_8) \\
&+ 180Q_2^3Q_3^2(532615Q_4^3 - 241224Q_2Q_4Q_6 + 16Q_2(-9352Q_5^2 + 799Q_2Q_8)) \\
&- 144Q_2^4Q_3(392325Q_4^2Q_5 - 51600Q_2Q_4Q_7 + 8Q_2(-8853Q_5Q_6 + 335Q_2Q_9)))
\end{aligned}
$$

$$
\begin{aligned}
&+ \frac{(n+\frac{1}{2})^5}{1194393600Q_2^{10}}(10368Q_{10}Q_2^7 - 66578225Q_3^8 + 272124300Q_2Q_3^6Q_4 \\
&- 112336560Q_2^2Q_3^5Q_5 + 9450Q_2^2Q_3^4(-33775Q_4^2 + 3656Q_2Q_6) \\
&- 151200Q_2^3Q_3^3(-1297Q_4Q_5 + 56Q_2Q_7) - 27Q_2^4(89075Q_4^4 - 83440Q_2Q_4^2Q_6) \\
&+ 64Q_2^2(131Q_6^2 + 396Q_5Q_7) + 576Q_2Q_4(-343Q_5^2 + 15Q_2Q_8) \\
&+ 540Q_2^3Q_3^2(188125Q_4^3 - 71400Q_2Q_4Q_6 + 16Q_2(-3052Q_5^2 + 177Q_2Q_8)) \\
&- 432Q_2^4Q_3(118825Q_4^2Q_5 - 11760Q_2Q_4Q_7 + 8Q_2(-2303Q_5Q_6 + 55Q_2Q_9))).
\end{aligned}
$$

$$
\begin{aligned}
\Lambda_6 &= \frac{-i}{202263389798400Q_2^{12}\sqrt{2Q_2}}(-171460800Q_{12}Q_2^9 + 1714608000Q_{11}Q_2^8Q_3 \\
&- 10268596800Q_{10}Q_2^7Q_3^2 + 970010662775Q_3^{10} + 3772137600Q_{10}Q_2^8Q_4 \\
&- 6262634175525Q_2Q_3^8Q_4 + 137829831961500Q_2^2Q_3^6Q_4^2 - 11954148125850Q_2^3Q_3^4Q_4^3 \\
&+ 3449170577475Q_2^4Q_3^2Q_4^4 - 144528059025Q_2^5Q_4^5 + 3352602187200Q_2^2Q_3^7Q_5 \\
&- 12300730092000Q_2^3Q_3^5Q_4Q_5 + 11994129604800Q_2^4Q_3^3Q_4^2Q_5 - 2624788605600Q_2^5Q_3Q_4^3Q_5 \\
&+ 2580769643760Q_2^4Q_3^4Q_5^2 - 3453909784416Q_2^5Q_3^2Q_4Q_5^2 + 438440697072Q_2^6Q_4^2Q_5^2 \\
&+ 260524397952Q_2^6Q_3Q_5^3 - 1475306441280Q_2^3Q_3^6Q_6 + 4329682610400Q_2^4Q_3^4Q_4Q_6 \\
&- 2865128172480Q_2^5Q_3^2Q_4^2Q_6 + 233443879200Q_2^6Q_4^3Q_6 - 1660199804928Q_2^5Q_3^3Q_5Q_6 \\
&+ 1281705296256Q_2^6Q_3Q_4Q_5Q_6 - 87403857408Q_2^7Q_5^2Q_6 + 231105873600Q_2^6Q_3^2Q_6^2 \\
&- 68412859200Q_2^7Q_4Q_6^2 + 552968700480Q_2^4Q_3^5Q_7 - 1231789749120Q_2^5Q_3^3Q_4Q_7 \\
&+ 470726303040Q_2^6Q_3Q_4^2Q_7 + 413953400448Q_2^6Q_3^2Q_5Q_7 - 126242178048Q_2^7Q_4Q_5Q_7 \\
&- 91489305600Q_2^7Q_3Q_6Q_7 + 5619715200Q_2^8Q_7^2 - 175752294480Q_2^5Q_3^4Q_8 \\
&+ 271759652640Q_2^6Q_3^2Q_4Q_8 - 39736040400Q_2^7Q_4^2Q_8 - 73378363968Q_2^7Q_3Q_5Q_8 \\
&+ 9773265600Q_2^8Q_6Q_8 + 47107126080Q_2^6Q_3^3Q_9 - 43345290240Q_2^7Q_3Q_4Q_9 \\
&+ 7400248128Q_2^8Q_5Q_9)
\end{aligned}
$$

$$
\begin{aligned}
&- \frac{(n+\frac{1}{2})^2 i}{687970713600Q_2^{12}\sqrt{2Q_2}}(-4551552Q_{12}Q_2^9 + 60279552Q_{11}Q_2^8Q_3 \\
&- 425036160Q_{10}Q_2^7Q_3^2 + 73727194625Q_3^{10} + 116743680Q_{10}Q_2^8Q_4 \\
&- 443649208275Q_2Q_3^8Q_4 + 901144103850Q_2^2Q_3^6Q_4^2 - 711096726150Q_2^3Q_3^4Q_4^3 \\
&+ 182164306725Q_2^4Q_3^2Q_4^4 - 6289615575Q_2^5Q_4^5 + 222467624400Q_2^2Q_3^7Q_5 \\
&- 746418445200Q_2^3Q_3^5Q_4Q_5 + 653423900400Q_2^4Q_3^3Q_4^2Q_5 - 124319674800Q_2^5Q_3Q_4^3Q_5 \\
&+ 143980943040Q_2^4Q_3^4Q_5^2 - 169712521920Q_2^5Q_3^2Q_4Q_5^2 + 18188188416Q_2^6Q_4^2Q_5^2 \\
&+ 11240861184Q_2^6Q_3Q_5^3 - 91198200240Q_2^3Q_3^6Q_6 + 241513732080Q_2^4Q_3^4Q_4Q_6 \\
&- 140030897040Q_2^5Q_3^2Q_4^2Q_6 + 9200103120Q_2^6Q_4^3Q_6 - 84218693760Q_2^5Q_3^3Q_5Q_6 \\
&+ 55248386688Q_2^6Q_3Q_4Q_5Q_6 - 3173043456Q_2^7Q_5^2Q_6 + 10464952896Q_2^6Q_3^2Q_6^2 \\
&- 2403421632Q_2^7Q_4Q_6^2 + 31637744640Q_2^4Q_3^5Q_7 - 62649953280Q_2^5Q_3^3Q_4Q_7 \\
&+ 20409822720Q_2^6Q_3Q_4^2Q_7 + 18860532480Q_2^6Q_3^2Q_5Q_7 - 4693344768Q_2^7Q_4Q_5Q_7 \\
&- 3625731072Q_2^7Q_3Q_6Q_7 + 188054784Q_2^8Q_7^2 - 9155635200Q_2^5Q_3^4Q_8 \\
&+ 12238024320Q_2^6Q_3^2Q_4Q_8 - 1405278720Q_2^7Q_4^2Q_8 - 2866700160Q_2^7Q_3Q_5Q_8 \\
&+ 303295104Q_2^8Q_6Q_8 + 2210705280Q_2^6Q_3^3Q_9 - 1685525760Q_2^7Q_3Q_4Q_9 + 235488384Q_2^8Q_5Q_9)
\end{aligned}
$$

$$
\begin{aligned}
- & \frac{(n+\frac{1}{2})^4 i}{20065812480 Q_2^{12}\sqrt{2Q_2}}(-66528 Q_{12}Q_2^9 + 1245888 Q_{11}Q_2^8 Q_3 \\
- & 11158560 Q_{10}Q_2^7 Q_3^2 + 4668804525 Q_3^{10} + 2116800 Q_{10}Q_2^8 Q_4 \\
- & 25898331375 Q_2 Q_3^8 Q_4 + 47959232650 Q_2^2 Q_3^6 Q_4^2 - 33861927750 Q_2^3 Q_3^4 Q_4^3 \\
+ & 7454763225 Q_2^4 Q_3^2 Q_4^4 - 184988475 Q_2^5 Q_4^5 + 11891917800 Q_2^2 Q_3^7 Q_5 \\
- & 36105463800 Q_2^3 Q_3^5 Q_4 Q_5 + 27953667000 Q_2^4 Q_3^3 Q_4^2 Q_5 - 4457716200 Q_2^5 Q_3 Q_4^3 Q_5 \\
+ & 6285855240 Q_2^4 Q_3^4 Q_5^2 - 6471756144 Q_2^5 Q_3^2 Q_4 Q_5^2 + 565259688 Q_2^6 Q_4^2 Q_5^2 \\
+ & 380939328 Q_2^6 Q_3 Q_5^3 - 4375251160 Q_2^3 Q_3^6 Q_6 + 10317018600 Q_2^4 Q_3^4 Q_4 Q_6 \\
- & 5113813320 Q_2^5 Q_3^2 Q_4^2 Q_6 + 238888440 Q_2^6 Q_4^3 Q_6 - 3203871552 Q_2^5 Q_3^3 Q_5 Q_6 \\
+ & 1758685824 Q_2^6 Q_3 Q_4 Q_5 Q_6 - 88566912 Q_2^7 Q_5^2 Q_6 + 335466432 Q_2^6 Q_3^2 Q_6^2 \\
- & 55073088 Q_2^7 Q_4 Q_6^2 + 1351294560 Q_2^4 Q_3^5 Q_7 - 2341442880 Q_2^5 Q_3^3 Q_4 Q_7 \\
+ & 626542560 Q_2^6 Q_3 Q_4^2 Q_7 + 619520832 Q_2^6 Q_3^2 Q_5 Q_7 - 123524352 Q_2^7 Q_4 Q_5 Q_7 \\
- & 96574464 Q_2^7 Q_3 Q_6 Q_7 + 4048704 Q_2^8 Q_7^2 - 341160120 Q_2^5 Q_3^4 Q_8 \\
+ & 386210160 Q_2^6 Q_3^2 Q_4 Q_8 - 30837240 Q_2^7 Q_4^2 Q_8 - 78073632 Q_2^7 Q_3 Q_5 Q_8 \\
+ & 5848416 Q_2^8 Q_6 Q_8 + 70415520 Q_2^6 Q_3^3 Q_9 - 43424640 Q_2^7 Q_3 Q_4 Q_9 + 5255712 Q_2^8 Q_5 Q_9)
\end{aligned}
$$

$$
\begin{aligned}
- & \frac{(n+\frac{1}{2})^6 i}{300987187200 Q_2^{12}\sqrt{2Q_2}}(-72576 Q_{12}Q_2^9 + 1886976 Q_{11}Q_2^8 Q_3 \\
- & 22135680 Q_{10}Q_2^7 Q_3^2 + 27463538375 Q_3^{10} + 2903040 Q_{10}Q_2^8 Q_4 \\
- & 141448688325 Q_2 Q_3^8 Q_4 + 240655765350 Q_2^2 Q_3^6 Q_4^2 - 152907158250 Q_2^3 Q_3^4 Q_4^3 \\
+ & 28724479875 Q_2^4 Q_3^2 Q_4^4 - 413669025 Q_2^5 Q_4^5 + 59058073200 Q_2^2 Q_3^7 Q_5 \\
- & 164264209200 Q_2^3 Q_3^5 Q_4 Q_5 + 113654696400 Q_2^4 Q_3^3 Q_4^2 Q_5 - 15166342800 Q_2^5 Q_3 Q_4^3 Q_5 \\
+ & 26061194880 Q_2^4 Q_3^4 Q_5^2 - 23876233920 Q_2^5 Q_3^2 Q_4 Q_5^2 + 1767189312 Q_2^6 Q_4^2 Q_5^2 \\
+ & 1292433408 Q_2^6 Q_3 Q_5^3 - 18902165520 Q_2^3 Q_3^6 Q_6 + 40256773200 Q_2^4 Q_3^4 Q_4 Q_6 \\
- & 17116974000 Q_2^5 Q_3^2 Q_4^2 Q_6 + 483582960 Q_2^6 Q_4^3 Q_6 - 11384150400 Q_2^5 Q_3^3 Q_5 Q_6 \\
+ & 5285056896 Q_2^6 Q_3 Q_4 Q_5 Q_6 - 246903552 Q_2^7 Q_5^2 Q_6 + 992779200 Q_2^6 Q_3^2 Q_6^2 \\
- & 101860416 Q_2^7 Q_4 Q_6^2 + 4966859520 Q_2^4 Q_3^5 Q_7 - 7661606400 Q_2^5 Q_3^3 Q_4 Q_7 \\
+ & 1683037440 Q_2^6 Q_3 Q_4^2 Q_7 + 1861574400 Q_2^6 Q_3^2 Q_5 Q_7 - 316141056 Q_2^7 Q_4 Q_5 Q_7 \\
- & 235146240 Q_2^7 Q_3 Q_6 Q_7 + 8895744 Q_2^8 Q_7^2 - 1042372800 Q_2^5 Q_3^4 Q_8 \\
+ & 1016789760 Q_2^6 Q_3^2 Q_4 Q_8 - 52436160 Q_2^7 Q_4^2 Q_8 - 189060480 Q_2^7 Q_3 Q_5 Q_8 \\
+ & 9217152 Q_2^8 Q_6 Q_8 + 175190400 Q_2^6 Q_3^3 Q_9 - 87816960 Q_2^7 Q_3 Q_4 Q_9 + 10378368 Q_2^8 Q_5 Q_9)
\end{aligned}
$$

Appendix C

Additional Results

Included in this appendix are the tabulated QNM frequencies for both the scalar and spin-half perturbations of the four dimensional Kerr black hole, when the angular momentum per unit mass has values of $a = 0.20$, $a = 0.40$ and $a = 0.60$.

Table C.1: *The Quasinormal Mode Frequencies for the Scalar Perturbations of the Kerr Black Hole, when* $a = 0.20$.

l	n	Third Order WKB(J)	Sixth Order WKB(J)	AIM
0	0	0.1050 - 0.1144i	0.1108 - 0.1004i	0.1106 - 0.1042i
				(0.18% , 3.78%)
1	0	0.2918 - 0.0976i	0.2936 - 0.0974i	0.2936 - 0.0973i
				(<0.01% , 0.10%)
	1	0.2633 - 0.3060i	0.2657 - 0.3052i	0.2657 - 0.3049i
				(<0.01% , 0.10%)
2	0	0.4843 - 0.0964i	0.4847 - 0.0964i	0.4847 - 0.0964i
				(<0.01% , <0.01%)
	1	0.4646 - 0.2946i	0.4653 - 0.2944i	0.4653 - 0.2944i
				(<0.01% , <0.01%)
	2	0.4335 - 0.5013i	0.4324 - 0.5064i	0.4326 - 0.5062i
				(0.05% , 0.04%)
3	0	0.6767 - 0.0961i	0.6769 - 0.0961i	0.6769 - 0.0961i
				(<0.01% , <0.01%)
	1	0.6622 - 0.2912i	0.6624 - 0.2911i	0.6624 - 0.2911i
				(<0.01% , <0.01%)
	2	0.6370 - 0.4921i	0.6359 - 0.4939i	0.6359 - 0.4939i
				(<0.01% , <0.01%)
	3	0.6048 - 0.6981i	0.6013 - 0.7082i	0.6016 - 0.7080i
				(0.05% , 0.03%)

Table C.2: *The Quasinormal Mode Frequencies for the Scalar Perturbations of the Kerr Black Hole, when* $a = 0.40$.

l	n	Third Order WKB(J)	Sixth Order WKB(J)	AIM
0	0	0.1055 - 0.1120i	0.1118 - 0.0994i	0.1115 - 0.1026i
				(0.27% , 0.21%)
1	0	0.2939 - 0.0962i	0.2957 - 0.0962i	0.2958 - 0.0960i
				(0.03% , 0.21%)
	1	0.2664 - 0.3015i	0.2692 - 0.3008i	0.2691 - 0.3004i
				(0.04% , 0.13%)
2	0	0.4877 - 0.0952i	0.4882 - 0.0952i	0.4882 - 0.0952i
				(<0.01% , <0.01%)
	1	0.4689 - 0.2907i	0.4697 - 0.2905i	0.4697 - 0.2905i
				(<0.01% , <0.01%)
	2	0.4391 - 0.4944i	0.4384 - 0.4990i	0.4386 - 0.4988i
				(0.05% , 0.04%)
3	0	0.6815 - 0.0950i	0.6817 - 0.0950i	0.6817 - 0.0950i
				(<0.01% , <0.01%)
	1	0.6676 - 0.2875i	0.6679 - 0.2874i	0.6679 - 0.2874i
				(<0.01% , <0.01%)
	2	0.6435 - 0.4856i	0.6427 - 0.4872i	0.6427 - 0.4872i
				(<0.01% , <0.01%)
	3	0.6128 - 0.6887i	0.6098 - 0.6978i	0.6101 - 0.6976i
				(0.05% , 0.03%)

Table C.3: *The Quasinormal Mode Frequencies for the Scalar Perturbations of the Kerr Black Hole, when* $a = 0.60$.

l	n	Third Order WKB(J)	Sixth Order WKB(J)	AIM
0	0	0.1049 - 0.1074i	0.1149 - 0.0960i	0.1129 - 0.0996i
				(1.74% , 0.63%)
1	0	0.2975 - 0.0937i	0.2995 - 0.0938i	0.2995 - 0.0936i
				(<0.01% , 0.21%)
	1	0.2711 - 0.2929i	0.2751 - 0.2920i	0.2749 - 0.2916i
				(0.07% , 0.14%)
2	0	0.4938 - 0.0929i	0.4943 - 0.0929i	0.4943 - 0.0929i
				(<0.01% , <0.01%)
	1	0.4762 - 0.2831i	0.4774 - 0.2830i	0.4774 - 0.2829i
				(<0.01% , 0.04%)
	2	0.4480 - 0.4811i	0.4485 - 0.4845i	0.4485 - 0.4843i
				(0.05% , 0.04%)
3	0	0.6900 - 0.0926i	0.6902 - 0.0926i	0.6902 - 0.0926i
				(<0.01% , <0.01%)
	1	0.6772 - 0.2803i	0.6777 - 0.2802i	0.6777 - 0.2802i
				(<0.01% , <0.01%)
	2	0.6547 - 0.4730i	0.6544 - 0.4742i	0.6544 - 0.4742i
				(<0.01% , <0.01%)
	3	0.6258 - 0.6704i	0.6239 - 0.6776i	0.6240 - 0.6774i
				(0.02% , 0.03%)

Table C.4: *The Quasinormal Mode Frequencies for the Spin-Half Perturbations of the Kerr Black Hole, when* $a = 0.20$.

l	n	Numerical	Third Order WKB(J)	Sixth Order WKB(J)	AIM
0	0	0.1836 - 0.0967i	0.1773 - 0.0997i	0.1837 - 0.0942i	0.1835 - 0.0965i
			(3.43% , 3.10%)	(0.05% , 2.59%)	(0.05% , 0.21%)
1	0	0.3811 - 0.0961i	0.3796 - 0.0962i	0.3810 - 0.0960i	0.3809 - 0.0960i
			(0.39% , 0.10%)	(0.03% , 0.10%)	(0.05% , 0.10%)
	1	0.3572 - 0.2964i	0.3550 - 0.2974i	0.3572 - 0.2969i	0.3583 - 0.2962i
			(0.62% , 0.34%)	(<0.01% , 0.17%)	(0.31% , 0.07%)
2	0		0.5750 - 0.0960i	0.5754 - 0.0959i	0.5754 - 0.0959i
					(<0.01% , <0.01%)
	1		0.5578 - 0.2918i	0.5586 - 0.2915i	0.5589 - 0.2916i
					(0.05% , 0.03%)
	2		0.5294 - 0.4951i	0.5287 - 0.4975i	
3	0		0.7689 - 0.0959i	0.7691 - 0.0950i	0.7691 - 0.0959i
					(<0.01% , 0.95%)
	1		0.7559 - 0.2899i	0.7563 - 0.2898i	0.7563 - 0.2899i
					(<0.01% , 0.03%)
	2		0.7328 - 0.4889i	0.7321 - 0.4899i	0.7289 - 0.4910i
					(0.44% , 0.22%)
	3		0.7028 - 0.6928i	0.6997 - 0.6993i	

Table C.5: *The Quasinormal Mode Frequencies for the Spin-Half Perturbations of the Kerr Black Hole, when* $a = 0.40$.

l	n	Numerical	Third Order WKB(J)	Sixth Order WKB(J)	AIM
0	0	0.1854 - 0.0956i	0.1798 - 0.0982i	0.1844 - 0.0932i	0.1851 - 0.0951i
			(3.02% , 2.72%)	(0.54% , 2.51%)	(0.16% , 0.52%)
1	0	0.3843 - 0.0951i	0.3825 - 0.0949i	0.3838 - 0.0948i	0.3837 - 0.0948i
			(0.47% , 0.21%)	(0.13% , 0.32%)	(0.16% , 0.32%)
	1	0.3614 - 0.2930i	0.3592 - 0.2931i	0.3612 - 0.2918i	0.3630 - 0.2916i
			(0.61% , 0.03%)	(0.06% , 0.41%)	(0.44% , 0.48%)
2	0		0.5791 - 0.0948i	0.5795 - 0.0947i	0.5795 - 0.0947i
					(<0.01% , <0.01%)
	1		0.5628 - 0.2880i	0.5636 - 0.2878i	0.5640 - 0.2877i
					(0.07% , 0.03%)
	2		0.5357 - 0.4883i	0.5352 - 0.4905i	0.5472 - 0.5204i
					(2.24% , 6.10%)
3	0		0.7744 - 0.0947i	0.7745 - 0.0947i	0.7745 - 0.0947i
					(<0.01% , <0.01%)
	1		0.7620 - 0.2862i	0.7624 - 0.2862i	0.7625 - 0.2862i
					(0.01% , <0.01%)
	2		0.7400 - 0.4825i	0.7395 - 0.4834i	0.7358 - 0.4858i
					(0.50% , 0.50%)
	3		0.7114 - 0.6835i	0.7086 - 0.6893i	

Table C.6: *The Quasinormal Mode Frequencies for the Spin-Half Perturbations of the Kerr Black Hole, when* $a = 0.60$.

l	n	Numerical	Third Order WKB(J)	Sixth Order WKB(J)	AIM
0	0	0.1885 - 0.0934i	0.1838 - 0.0953i	0.1870 - 0.0909i	0.1879 - 0.0925i
			(2.49% , 2.03%)	(0.80% , 2.68%)	(0.32% , 0.96%)
1	0	0.3901 - 0.0931i	0.3877 - 0.0925i	0.3888 - 0.0924i	0.3888 - 0.0924i
			(0.62% , 0.64%)	(0.33% , 0.75%)	(0.33% , 0.75%)
	1	0.3687 - 0.2861i	0.3662 - 0.2849i	0.3682 - 0.2837i	0.3714 - 0.2811i
			(0.68% , 0.42%)	(0.13% , 0.84%)	(0.73% , 1.75%)
2	0		0.5866 - 0.0924i	0.5869 - 0.0924i	0.5869 - 0.0924i
					(<0.01% , <0.01%)
	1		0.5715 - 0.2806i	0.5724 - 0.2804i	0.5730 - 0.2798i
					(0.10% , 0.21%)
	2		0.5463 - 0.4751i	0.5462 - 0.4768i	
3	0		0.7842 - 0.0924i	0.7844 - 0.0924i	0.7844 - 0.0924i
					(<0.01% , <0.01%)
	1		0.7728 - 0.2791i	0.7732 - 0.2790i	0.7734 - 0.2790i
					(0.03% , <0.01%)
	2		0.7524 - 0.4700i	0.7522 - 0.4707i	0.7493 - 0.4775i
					(0.39% , 1.44%)
	3		0.7257 - 0.6652i	0.7237 - 0.6700i	